Some remarks on non-standard plastic behaviour with Coulomb's friction starting from an unconventional stone flat arch

Danila Aita[1], Valentina Beatini[2], Hugo Caruso[3], Elsa Garavaglia[1], Luca Sgambi[3]

[1]*Department of Civil and Environmental Engineering (DICA), Politecnico di Milano, Milan, Italy*

E-mail: danila.aita@polimi.it, elsa.garavaglia@polimi.it

[2] *Department of Civil and Architectural Engineering, Aarhus University, Aarhus, Denmark*

E-mail: vb@cae.au.dk

[3] *Louvain research institute for Landscape, Architecture, Built environment, Université Catholique de Louvain, Tournai, Belgium*

E-mail: hugo.caruso@uclouvain.be, luca.sgambi@uclouvain.be

Corresponding author: Danila Aita, *Department of Civil and Environmental Engineering (DICA), Politecnico di Milano, Milan, Italy; E-mail: danila.aita@polimi.it*

Supprimé: *valentina.beatini*

Mis en forme : Couleur de police : Rouge

Supprimé: *c*

Mis en forme : Italien (Italie)

Mis en forme : Couleur de police : Rouge, Italien (Italie)

Mis en forme : Italien (Italie)

Abstract

The present article aims to explore the non-standard plastic behaviour that occurs in masonry structures when considering a finite Coulomb friction, by starting from the equilibrium analysis of an interesting case study inspired by an unconventional architectural element, i.e., the flat arch crowning the transept portal in the Prato Cathedral, characterized by a 'wrong' shape of certain voussoirs.

Investigations using various methods are conducted to assess the equilibrium of such a non-traditional blocky structure.

At first a novel non-standard approach which couples static and kinematic analyses is proposed. The static method exploits the so-called 'stability area method', theoretically framed in the context of the lower bound theorem of Limit Analysis, assuming a limited friction coefficient. This procedure is capable of considering also the effects of a limited compression strength for masonry. By combining such method with kinematic analyses based on the virtual work theorem, the limit friction coefficient compatible with the safety of the

Supprimé: n

Supprimé: inedited

Mis en forme : Couleur de police : Rouge

structure is found. Following that, the results of these preliminary analyses are compared to those derived by other approaches - that is, a plastic limit state lower approach, finite element analyses, and a Non-Smooth Contact Dynamics approach.

Some reflections are provided on the difficulties related to the adoption of a lower bound approach to capture the actual mechanical behaviour of this flat arch, highlighting the need to integrate the equilibrium analyses with kinematic/dynamic investigations or Finite Element Analysis aimed at describing the behaviour of the structure near collapse.

It is observed that the anomalous mechanical behaviour is due not only to the presence of a finite Coulomb friction but also to the atypical stereotomy of the voussoirs, which could be subject to mutual detachment.

This research, starting from a specific, unconventional, case study demonstrates the need for a critical perspective in the analysis of the mechanical behaviour of masonry vaulted structures.

Keywords: masonry, stone, flat arch, finite friction, limit analysis, lower bound theorem, non-standard plastic behaviour, graphical statics, FEA, DEM

Commenté [EG1]: togliere

Mis en forme : Couleur de police : Rouge

Supprimé: n

Supprimé: s

Mis en forme : Couleur de police : Rouge

Mis en forme : Couleur de police : Rouge

Supprimé: c

Supprimé: d

Mis en forme : Couleur de police : Rouge

Supprimé: EA

Supprimé:

Mis en forme : Couleur de police : Rouge

Supprimé: unconventional

Mis en forme : Couleur de police : Rouge

Supprimé: ¶

1. Introduction

The current study is part of an ongoing research project on masonry structures featuring interlocking blocks (Pizzigoni, Beatini, and Paris, 2022; Aita et al., 2023a; 2024a), addressing the effects of an unconventional stereotomy of masonry blocks on the collapse behaviour. In this framework, the investigation here proposed focuses on the equilibrium of an interesting stone structure with unconventional voussoirs, inspired by the front layer (Fig. 1a) of the flat arch that crowns the transept portal in Prato Cathedral, whose apparent static absurdity already caught the interest of Ruskin (Ruskin, 1849), see Fig. 1b.

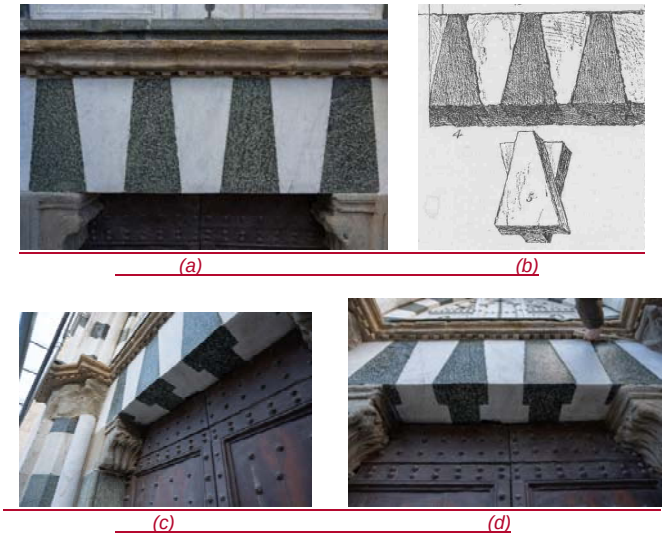


Figure 1. The front layer of the flat arch crowning the transept portal in the Prato Cathedral (*a*); sketch of the flat arch and detail of the interlocking blocks, drawn from (Ruskin, 1849) (*b*); the interlocking system (*c*, *d*) (Photo: courtesy of Piacenti S.p.a.).

The stability of the actual flat arch is ensured by the interlocking of the blocks (Figures 1c and 1d): their peculiar shape prevents the activation of any kinematically admissible mechanism. Such a structure could be analysed from the structural point of view by means of procedures aimed at capturing the interlocking behaviour (Mousavian et al., 2022), out of the scope of the current paper. It is briefly remarked that this type of flat arch has been described by Leonardo da Vinci in the *Codex Atlanticus* (Folio 91) (Lampariello, 2012). Real architectural examples of this type of flat arches are rare. In addition to the one in Prato

Mis en forme : Couleur de police : Rouge

Mis en forme : Couleur de police : Rouge

Supprimé: of the flat arch that crowns the transept portal in Prato Cathedral, whose apparent static absurdity already caught the interest of Ruskin (Ruskin, 1849), see Fig. 1

Mis en forme : Couleur de police : Rouge, Surlignage

Mis en forme : Non Surlignage

Commenté [EG2]: Nella didascalia mancava il riferimento (b), ma a parte quello io girerei il riferimento (b) così come l'ho messo e non lo lascerei alla fine, altrimenti non si capisce.

Mis en forme : Non Surlignage

Supprimé: ¶



Figure 1. The front layer of the flat arch crowning the transept portal in the Prato Cathedral, left; sketch of the flat arch and detail of the interlocking blocks, drawn from (Ruskin, 1849) (*b*); detail of the interlocking blocks*d* , right (Photo: courtesy of Piacenti S.p.a.).¶

¶

Supprimé: 1, right

Mis en forme : Police :(Par défaut) Arial, 10 pt, Italique

Mis en forme : Police :(Par défaut) Arial, 10 pt, Italique

Mis en forme : Couleur de police : Rouge

Mis en forme : Police :Italique

Mis en forme : Couleur de police : Rouge

Mis en forme : Couleur de police : Rouge

Mis en forme : Couleur de police : Rouge

Supprimé: z

Mis en forme : Non Surlignage

Mis en forme : Police :Italique

Mis en forme : Anglais (Royaume-Uni)

Cathedral, we could mention a flat arch in St. Michael's Cathedral in Alba Iulia (Romania) and another one in Esztergom Castle (Hungary) (Motro, 2009; Fantin, 2017).

The proposed research starts from a simple question: what might happen if the flat arch were instead composed of blocks cut according to the stereotomy of the frontal layer (Figure 1a)? From this question emerges a theoretical problem of great interest, which invites a reflection on the concept of "voussoir", posing challenges related to the use of limit analysis approaches to evaluate the collapse conditions.

As is well known, classical limit analysis of masonry structures is based on the fundamental work of Heyman (Heyman, 1966; 1969), who, revisiting historical contributions regarding the stability of masonry arches (Coulomb, 1776) and developing the research carried out by Kooharian (1952), proposed to apply the plastic theory to the "stone skeleton" rather than the "steel skeleton". Accordingly, the structure is discretized into its constituent blocks, and a rigid material with infinite friction and nil tensile strength at the interfaces is assumed: failures due to sliding are disregarded and compression capacity is infinite. In collapse conditions, macroblocks are formed which undergo mechanisms when the masonry structure is subjected to limit actions or settlements. To the aims of the current research, it is worth recalling that the limit analysis of masonry structures according to Heyman's hypotheses can be defined as standard, i.e., it can be regarded as a well-established linear complementarity problem with a unique solution, due to the normality law between statically admissible stress states and the corresponding flow rule for the displacement field. In this instance, it is irrelevant whether the collapse condition is ascertained by means of the kinematic or static theorem. In particular, under these hypotheses, the structure can be considered safe if a static solution is found for the given load condition contained within the yield limits (lower bound approach). For its simplicity, the methodology proposed by Heyman is commonly adopted also nowadays, as testified by a number of even recent contributions aimed at applying either kinematic or static methods to the limit analysis of masonry arches/structures. Without pretending to be complete, the contributions by Sinopoli, Corradi and Foce (1997), Block and Lachauer (2014), Angelillo (2014), Marmo and Rosati (2017), Grillanda et al. (2019), Montanino, De Gregorio, Olivieri, Iannuzzo (2022), Milani (*in press*) can be cited.

Supprimé: ; but investigating
Mis en forme : Couleur de police : Rouge
Supprimé: , left
Supprimé: is a theoretical problem of great interest, which allows for a reflection on the concept of 'voussoir',
Mis en forme : Couleur de police : Rouge
Supprimé: when a finite value of the friction coefficient is considered.
Mis en forme : Police :Gras, Couleur de police : Bleu
Mis en forme : Police :Gras, Couleur de police : Bleu
Supprimé: NON CHIARA
Mis en forme : Surlignage
Supprimé: shear
Mis en forme : Couleur de police : Rouge
Supprimé:
Mis en forme : Couleur de police : Rouge
Déplacé vers le bas [1]: It is remarked that, under Heyman's hypotheses, the structure can be considered safe if a static solution is found for the given load condition contained within the yield limits (lower bound approach).
Supprimé: Actually, high friction levels ensure that the static (or safe or lower bound) and kinematic (or unsafe or upper bound) theorems of Limit Analysis - derived from the normality law between statically admissible stress states ... [1]
Déplacé (insertion) [1]
Supprimé: It is remarked that,
Mis en forme : Couleur de police : Rouge
Supprimé: Heyman's
Supprimé: The
Supprimé: (
Supprimé: ,
Supprimé: ;
Supprimé: ,
Supprimé: ;
Supprimé: ,
Supprimé: ;
Supprimé: ,
Supprimé: ;
Supprimé: ,
Mis en forme : Italien (Italie)
Supprimé: ;
Supprimé: ,
Supprimé: ;
Supprimé: ,
Mis en forme : Italien (Italie)
Mis en forme : Italien (Italie)

Heyman's simplifying assumptions offer foundational insights and can capture fundamental features of the collapse behaviour of masonry structures. However, they do not describe the real material properties and may be inconvenient to address more complex situations.

Therefore, various approaches have been eventually developed to assess the safety of masonry structures by assuming finite non-associative friction (i.e., a non-standard plastic behaviour) and/or a limited compressive strength or considering the role of interlocking blocks.

In particular, as regards sliding failure, it is remarked that it can occur in practice in the case of finite friction, due to reaching a limit condition that relates the normal force and the shear force according to Coulomb's friction law. In the general case, to address finite shear capacity within a lower bound plastic formulation and preserving the validity of the dual formulation (uniqueness theorem), an associative friction model must be assumed. It implies that sliding occurs in a direction perpendicular to the yield surface, and such has a dilatancy component with respect to the direction of the associated frictional force. If, from the kinematic point of view, simple sliding is assumed - as in the case of Coulomb's friction with zero dilatancy - sliding occurs according to a non-associative friction model in the direction parallel to the shear force. Drucker (Drucker, 1954) firstly noted that in this scenario there can be a gap between the upper and lower bound. In such cases, limit state approaches (Livesley, 1978) shall consider either at once or successively (Gilbert and Melbourne, 1994; Gilbert et al., 2006) the two bounding criteria (Radenkovic, 1961; Palmer, 1966), by coupling both static and kinematic analyses. When the normality rule does not hold, the lower bound approach of limit analysis can be applied only to some classes of problems (Casapulla, 1999; Casapulla and Jossa, 2001; Casapulla and Lauro 2001). Without claiming completeness, the interest in frictional constraint and non-standard behaviour is testified by a number of contributions on masonry structures (Andreaus and Augusti, 1991; Ferris and Tin Loi, 2001; D'Ayala and Tomasoni, 2011; Cocchetti and Rizzi, 2020; Aita and Sinopoli, 2020; Pepe, Pingaro and Trovalusci, 2021; Hua and Milani, 2023).

The assumption of an infinite compressive strength may also be considered critically. While masonry material is most often not stressed to the yield limits, assuming infinite compressive strength may lead to the erroneous conclusion that any thrust line contained within the structure's profile and compatible with

Supprimé: ¶
Mis en forme : Couleur de police : Rouge
Mis en forme : Couleur de police : Automatique
Supprimé: ~~(i.e., when the material has a non-standard plastic behaviour)~~
Mis en forme : Couleur de police : Rouge
Mis en forme : Couleur de police : Rouge, Barré
Mis en forme : Couleur de police : Rouge
Supprimé: ,
Mis en forme : Couleur de police : Rouge
Supprimé: which
Mis en forme : Couleur de police : Rouge
Mis en forme : Non Surlignage
Mis en forme : Couleur de police : Rouge
Mis en forme : Couleur de police : Rouge
Supprimé: It is remarked that, w
Mis en forme : Couleur de police : Rouge
Supprimé: some recent
Mis en forme : Couleur de police : Rouge
Mis en forme : Couleur de police : Rouge
Mis en forme : Couleur de police : Rouge
Mis en forme : Couleur de police : Rouge
Supprimé: G.

the friction constraints imposed on each joint is statically admissible and then, that any value of compressive strength is admissible. It is remarked that, for some typologies of masonry vaults, the effects of a limited compressive strength cannot be neglected, and complementary constraints shall be set to ensure that compressive strength is activated only if the blocks are in contact. Moreover, it is interesting to observe that knowledge of the compression requirements may suggest proportions within the shape of the blocks that favor stability, as envisioned in (Beatini et al., 2019) with reference to the Brunelleschi dome and its herringbone bricks. Other contributions introduce a limited compressive strength in the limit analysis of masonry blocky structures, see for example Clemente, Occhiuzzi and Raithel (1995), Rossi et al. (2020), Clemente et al. (2023). Static methods based on an updated version of thrust line approaches are proposed for example by (Fantin and Ciblac, 2016), who perform static deterministic analyses, and (Aita, Bruggi and Garavaglia, 2024), where the topic of collapse of masonry arches and domes with uncertain finite compressive strength and finite friction is discussed.

Finally, when tackling unconventional shapes of the voussoirs, attention must be paid to the effective activation of the unilateral constraints. If they are able to transmit sufficient compressive force for the structure to be stable - i.e., if it can be assumed that the normal reactive force is actually present and not due to precompression - the safety of a masonry structure can be assessed by means of static methods. In particular, it should be observed that the shape of the voussoirs is crucial when introducing a finite friction coefficient. With regards to this, Smars and D'Ayala examine interesting case studies of non-standard plastic behaviour by considering the relationship between stability and the rules of the art, by emphasizing the role of kinematic analysis (Smars, 2000; 2023; D'Ayala and Smars, 2003). In this line of research, by simulating the symmetric masonry arch as a system of rigid plastic blocks with frictional sliding, Trentadue et al. (2024) examine the impact of a support settlement, while (Ting-Chun Kao et al., 2022) consider the effects of an unconventional shape on the stability of an assemblage of blocks, by referring to some possible critical cases.

The issue relating to the shape of the blocks is also very important from a design point of view. In the recent scientific literature, some contributions are aimed at studying how to increase the stability of a structure

Supprimé:
Mis en forme : Non Surlignage
Supprimé: ,
Supprimé: by developing s
Mis en forme : Couleur de police : Rouge
Supprimé: .
Supprimé:
Mis en forme : Couleur de police : Rouge
Mis en forme : Couleur de police : Rouge
Supprimé: ,
Supprimé: see
Mis en forme : Couleur de police : Rouge
Supprimé: See
Mis en forme : Couleur de police : Rouge
Supprimé: with
Mis en forme : Couleur de police : Rouge
Mis en forme : Couleur de police : Rouge
Supprimé: s
Mis en forme : Couleur de police : Rouge
Mis en forme : Couleur de police : Rouge
Supprimé: 2003;
Supprimé: 2024
Mis en forme : Couleur de police : Rouge
Supprimé: (
Mis en forme : Couleur de police : Rouge
Supprimé: ,
Mis en forme : Couleur de police : Rouge

composed of blocks while avoiding the use of mortar, by proposing interlocking designs. The blocks are characterized by unusual shapes of the contact surfaces, which create kinematic incompatibilities aimed to prevent mutual displacement between the voussoirs (Pizzigoni et al., 2024).

All the above problems become relevant even for the simple stone structure with unusual shape - inspired by the front layer of that of the Prato Cathedral -, object of the current investigation. A model of this theoretical flat arch structure has been 3D printed in PLA and is depicted in Figure 2a. The dimensions of the model correspond to those described in Section 2, scaled 1:10. As the picture shows, a compression force at supports is exerted by the tester to keep the blocks in position. In fact, if the precompression is released, mutual sliding/detachment between the blocks will be activated, and the model will fail. The flat arch typology has been chosen due to its interest as regards design of blocky structures (Ting-Chun Kao et al., 2022), with reference to its susceptibility to instability under suboptimal orientations of the contact interfaces for the given resultant forces (Beatini et al., 2018) which makes it sensitive to precompression requirements.

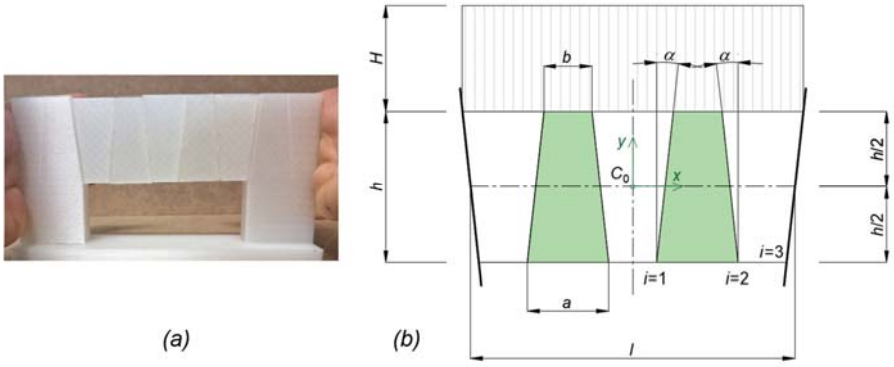


Figure 2. A PLA model of the flat arch used as a case study, kept in place by the application of a restraining force at supports (*a*). Front layer of the flat arch of the Prato Cathedral: geometric parameters (*b*).

The investigation of the mechanical behaviour of this atypical flat arch focuses on the five central voussoirs (Fig. 2b), while the lateral blocks, denoted by (*C*) in Fig. 3, are assumed to be embedded between the wall and the portal jambs. The inclination of joint $i = 2$ (and that of its symmetrical joint with respect to the *y*-axis) is "wrong" because it deviates downward from the *y*-axis; this contrasts with the ordinary arrangement

Mis en forme : Non Surlignage
Supprimé:
Mis en forme : Couleur de police : Rouge
Supprimé: the
Mis en forme : Non Surlignage
Mis en forme : Couleur de police : Rouge
Supprimé:
Mis en forme : Couleur de police : Rouge
Mis en forme : Couleur de police : Rouge
Mis en forme : Non Surlignage
Supprimé: .
Mis en forme : Couleur de police : Rouge
Mis en forme : Non Surlignage
Mis en forme : Couleur de police : Rouge
Mis en forme : Couleur de police : Rouge
Mis en forme : Couleur de police : Rouge
Mis en forme : Couleur de police : Rouge
Mis en forme : Centré
Mis en forme : Police :Italique
Commenté [EG3]: La sposterei qui come figura ancora n.2
Mis en forme : Anglais (Royaume-Uni)
Mis en forme : Normal, Paragraphes solidaires
Mis en forme : Police :Italique, Non Surlignage
Mis en forme : Police :Italique, Non Surlignage
Mis en forme : Non Surlignage
Mis en forme : Non Surlignage
Mis en forme : Non Surlignage
Mis en forme : Non Surlignage
Mis en forme : Police :Italique, Non Surlignage
Mis en forme : Non Surlignage

of voussoirs, which is characteristic of conventional vaulted masonry construction and guarantees compression between the blocks.

To qualitatively clarify the critical aspects related to the collapse response of the investigated flat arch, it is interesting to observe that - assuming non-smooth unilateral constraints at the blocks' interfaces - the voussoirs denoted by (*B*) in Fig. 3a can slide with frictional dissipation along the inclined planes of the interfaces between blocks (*B*) and (*C*) (marked with thick black lines), while simultaneously maintaining contact with the macroblock (*A*) (delimited by the "wrong" joints); thus, the sliding mechanism of blocks (*B*) allows for stabilizing the system, generating a horizontal thrust. Another peculiarity is that the purely sliding collapse mode just identified implies that both macroblock (*A*) and blocks (*B*) slide downwards. This situation differs from the kinematically admissible sliding mechanisms found in flat arches and vaults with regular voussoirs, which are characterized by reciprocal sliding both inwards and outward, see for example Aita, Barsotti and Bennati (2019); Aita and Sinopoli (2020).

Imagining that blocks (*B*), are perfectly fastened to the blocks (*C*) (by mortar or other type of constraint), see Fig. 3b, it is apparent that the macroblock (*A*) would move downwards with a detachment from blocks (*B*), i.e., without a frictional dissipation at the interfaces, unless the structure is subjected to precompression. Indeed, the constraints at joints separating (*A*) and (*B*) are non-conventional and the presence of a thrust might not be guaranteed. Concerns regarding the stability of the flat arch are raised by macroblock (*A*)'s unusual shape.

The above observations are an important point to remember when using static methods on block assemblages. The case study under consideration can be linked to a few of the instances put forth by Bagi (2014), who focuses on "non-Heymanian" collapse modes of masonry structures, that is, on the onset of collapse conditions even in situations where statically admissible solutions are found in the hypothesis of an infinite friction. Moreover, it seems interesting to examine this case study in the light of the analysis performed by Ting-Chun Kao et al. (2022). They point out the need of combining both equilibrium and kinematics to assess the stability of rigid blocks assemblages when the shape of the voussoirs is

Commenté [EG4]: Al revisore non è chiaro perché questo blocco non è fisso, e a cosa si aggancia se non è fisso. In effetti dobbiamo chiarirlo.

Supprimé: (Fig 3a)

Mis en forme ... [2]

Mis en forme : Police :(Par défaut) Times New Roman, 12 pt, Couleur de police : Rouge

Mis en forme ... [3]

Mis en forme ... [4]

Mis en forme

Mis en forme ... [5]

Mis en forme ... [6]

Mis en forme ... [7]

Mis en forme ... [8]

Mis en forme ... [9]

Supprimé: ,

Mis en forme : Couleur de police : Rouge

Supprimé: who

Mis en forme : Couleur de police : Rouge

unconventional, and highlight some aspects related both to frictional constraints and to detachment between the blocks.

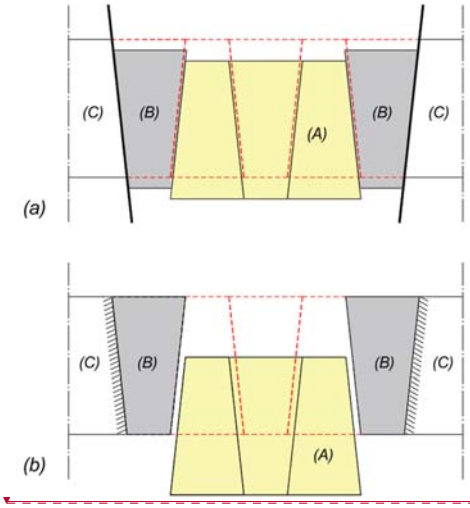


Figure 3. Pure sliding collapse mechanism (*a*); collapse mechanism when blocks (*B*) are fixed (*b*).

The question this paper seeks to answer is to what extent can different masonry analysis approaches accurately predict the structural behaviour of such a structure, characterized by a non-traditional block design, under the hypothesis of finite non-associative friction. To this end, a comparative study is here proposed to provide information on the failure mode, loading conditions and relevant mechanic parameters affecting the collapse behaviour. It is recalled that in the scientific literature there are several structural analysis methods tailored to discrete block modelling. Just to name a few, Petracca et al. (2017) propose block-based continuum models aimed at modelling joints and blocks independently of one another in a Finite Element (FE) framework with nonlinear elements; Lemos (2007), Simon and Bagi (2016), Sarhosis, Lemos and Bagi (2019) propose Discrete Element Modelling (DEM). For the purpose of this work, the selection of the different techniques adopted in the analyses is driven by the need to understand the collapse response of the unusual flat arch, by considering both a limited friction coefficient and the unconventional stereotomy of the voussoirs. A first investigation performed via a modern version of Durand-Claye method (Durand-Claye A.,1867; 1868; Aita, Barsotti and Bennati, 2019; Aita, Milani and Taliercio, 2023), based

Mis en forme : Couleur de police : Rouge
Supprimé: <*objet*><*objet*>
Supprimé: (a) . (b)
Mis en forme : Police :Italique
Supprimé: (left)
Mis en forme : Couleur de police : Rouge, Non Surlignage
Supprimé: (right).
Mis en forme : Surlignage
Mis en forme : Taquets de tabulation : 5,75 cm,Gauche + 14,25 cm,Gauche
Mis en forme : Couleur de police : Rouge, Non Surlignage
Supprimé: (a)
Mis en forme : Couleur de police : Rouge, Non Surlignage
Mis en forme : Couleur de police : Rouge, Surlignage
Mis en forme : Couleur de police : Rouge, Non Surlignage
Supprimé: (b)
Mis en forme : Couleur de police : Rouge, Non Surlignage
Mis en forme : Couleur de police : Rouge, Non Surlignage
Mis en forme : Police :Italique
Mis en forme : Couleur de police : Rouge, Non Surlignage
Mis en forme : Couleur de police : Rouge, Surlignage
Mis en forme : Couleur de police : Rouge, Non Surlignage
Mis en forme : Couleur de police : Rouge
Supprimé: ¶
Mis en forme : Espacement automatique entre les caractères asiatiques et latins, Espacement automatique entre les caractères asiatiques et les chiffres
Mis en forme : Couleur de police : Rouge
Commenté [EG5]: manac citazione in biblio
Mis en forme : Couleur de police : Rouge
Mis en forme : Couleur de police : Rouge
Supprimé: ,
Supprimé: To the aims of this paper,
Supprimé: focus will be made on some techniques based on different approaches, i.e., static methods exploiting gr... [10]
Mis en forme : Couleur de police : Rouge
Mis en forme : Couleur de police : Rouge

on the lower bound theorem of limit analysis, shows that a purely static approach is not suitable for obtaining plausible results (this is confirmed by the investigation conducted by means of multi-objective optimization procedure based on the static method). For this reason, a novel non-standard analytical procedure is here proposed, which integrates the classical stability area graphic approach with kinematic analyses based on the virtual work theorem. Moreover, to validate such a procedure, both a Finite Element micro-modelling and DEM within a Non-Smooth Contact Dynamics (NSCD) formulation are adopted. Also, for the finite elements, a new procedure, specifically developed, is implemented to overcome some difficulties related to the "wrong" shape of the voussoirs.

The paper is structured as follows. In Section 2 the geometric and mechanical parameters describing the flat arch are provided. Then, the problem is explored parametrically using the novel procedure based on static (Durand-Claye's method) and kinematic (virtual work theorem) analyses aimed at finding the conditions compatible with the safety of the structure and allowing for preliminary insights into the structural responses (Section 3). Each method requiring specific assumptions, the findings from the preliminary analyses are then compared for what relevant with results from the other methods. Finite Element Analyses are presented in Section 4 and compared with the analytical method. Then, the results obtained by means of a plastic limit state lower bound approach is presented and commented in Section 5. Section 6 describes the collapse modes derived by Non-Smooth Contact Dynamics. The Concluding remarks (Section 7) provide a critical review of the comparative analysis, focusing on the capability of the different methods in correctly describing the collapse behaviour of the structure, on the related setting and assumptions, and on the role of the different influencing parameters.

2. Geometric and mechanical parameters describing the front layer of the flat arch

As introduced above, the object of the mechanical investigations reported in the following sections refer to a flat arch inspired by the front layer of Prato Cathedral (Figure 1a).

The stone is assumed to have a limited value of the ultimate compressive strength, σ_c, while the interfaces between the joints are characterized by no-tension behaviour and a limited Coulomb's friction, $\mu = \tan\psi$.

Mis en forme : Police :(Par défaut) Times New Roman, 12 pt, Couleur de police : Rouge

Mis en forme : Couleur de police : Rouge

Mis en forme : Non Barré

Supprimé: focus will be made on some techniques based on different approaches, i.e., static methods exploiting graphic statics coupled with kinematic approaches based on the virtual work theorem,

Mis en forme : Couleur de police : Rouge

Mis en forme : Couleur de police : Rouge

Supprimé: ,

Mis en forme : Couleur de police : Rouge

Mis en forme : Couleur de police : Rouge

Supprimé: ¶ ... [11]

Mis en forme : Anglais (Royaume-Uni)

Mis en forme : Couleur de police : Rouge

Supprimé: an unedited non-standard analytical approach. By starting from the modified Durand-Claye graphic m ... [12]

Mis en forme : Couleur de police : Rouge

Supprimé: approach is integrated with

Supprimé: ¶

Supprimé: ¶

Supprimé: , left

Mis en forme : Couleur de police : Rouge

According to (Coli et al, 2022), the actual flat arch is composed of two different types of stone: *Verde Prato*, characterized by a compressive strength $\sigma_c = 45$ MPa, and a weight density $\gamma = 26\,{}^{\mathrm{kN}}/_{\mathrm{m}^3}$, and marble, with an higher compressive strength, around 120MPa, and almost the same weight density as *Verde Prato*. For simplicity, and in favour of safety, the mechanical properties of *Verde Prato* are assumed for all the stones making up the theoretical flat arch object of the current study. As will be shown later, although the compressive strength of *Verde Prato* is lower than that of marble, its influence on the collapse behaviour is not evident with respect to the hypothesis of an infinite compressive strength.

The portion of the flat arch of structural interest (Fig. 2a) is composed of five voussoirs of trapezoidal shape (Fig. 2b). In the analyses, the flat arch is subjected to gravitational loads, i.e., its self-weight and the weight of a wall above, modelled by considering a uniformly distributed load, $q = \gamma H t$, where γ is the weight density of the stone, $t = 0.135$ m is the constant out-of-plane thickness of the flat arch (corresponding to that of the front layer of the Prato flat arch), H is the height of the wall. The depth of the flat arch is denoted as $h = 0.505$ m, while the middle span is $l = 1.075$ m. The inclination of the joints is defined by angle $\alpha = 6.216°$.

By assuming the planar coordinate reference system $(O; x, y)$ plotted in Figure 2b, with $O \equiv C_0$, the x-coordinates of the intrados and extrados points of the i-th joint, I_i and E_i, respectively (see Figures 2b and 4a), are specified as follows:

$x_{I_1} = b/2; x_{E_1} = a/2; x_{I_2} = b/2 + a; x_{E_2} = a/2 + b; x_{I_3} = 3\,b/2 + a;\ x_{E_3} = 3\,a/2 + b.$

3. Search for the minimum friction coefficient compatible with equilibrium: a semi-analytical procedure

3.1 A revised version of the stability area method

In this section, a revised version of the stability area method, first introduced by Alfred Durand-Claye (Durand-Claye, 1867; 1868), and re-worked by (Aita, Barsotti and Bennati, 2019; Aita, Milani and Taliercio, 2023), is presented to assess the existence of statically admissible solutions compatible with strength and friction requirements.

Mis en forme : Couleur de police : Rouge
Mis en forme : Police :Italique
Mis en forme : Non Surlignage
Supprimé: As will be shown later, although this is the lowest value between that of marble and *Verde Prato*, the influence of this value of the limited compressive strength is not evident in the analyses compared to the assumption of an infinite compressive strength.
Mis en forme : Police :Italique
Mis en forme : Espacement automatique entre les caractères asiatiques et latins, Espacement automatique entre les caractères asiatiques et les chiffres
Supprimé: ¶
Mis en forme : Couleur de police : Rouge
Mis en forme : Couleur de police : Rouge
Mis en forme : Couleur de police : Rouge
Mis en forme : Couleur de police : Rouge
Supprimé: ¶
With reference to Figure 2, right, the portion of the flat arch of structural interest is that comprised between the lateral fixed voussoirs (Fig. 2, left). It is composed of five voussoirs of trapezoidal shape.
Mis en forme : Couleur de police : Rouge
Mis en forme : Couleur de police : Rouge
Supprimé: , right
Mis en forme : Couleur de police : Rouge
Mis en forme : Non Surlignage
Mis en forme : Couleur de police : Rouge
Supprimé: 4, left, and Figure
Mis en forme : Non Surlignage
Supprimé: 5
Mis en forme : Couleur de police : Rouge
Supprimé: ¶
¶
Mis en forme : Couleur de police : Rouge
Supprimé: of
Mis en forme : Couleur de police : Rouge
Supprimé: the
Supprimé: of the flat arch
Supprimé: using a modern version of Durand-Claye's method combined with kinematic analysis

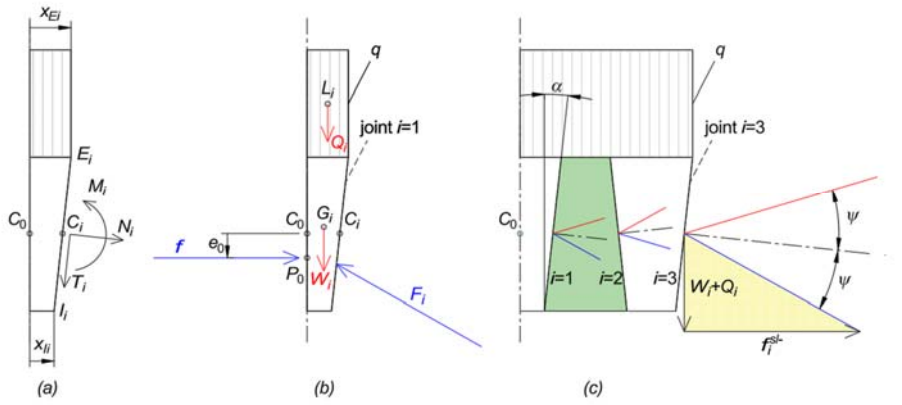
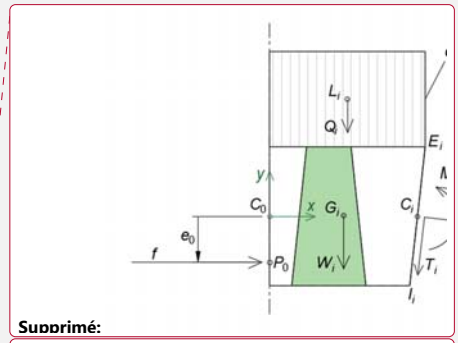


Figure 4. Portion of the flat arch comprised between the midspan vertical joint and any joint *i*: notation adopted and positive convention for the stress resultants (*a*); internal forces (in blue) and applied loads (in red); friction cone of amplitude ψ (*c*).

The stability area method exploits the static theorem of Limit Analysis; the so-called lower bound consists in any stress system in which the applied forces are just sufficient to cause yielding; the internal stress fields must balance the externally applied forces. To the aims of this research, stress resultants (i.e., the normal compressive force N_i, the bending moment M_i, and the shear force T_i, see Fig. 4a) instead of stress states are considered at any contact joint *i*. Masonry is defined as a no-tension rigid-perfectly plastic material with a finite compressive strength, σ_c, and finite Coulomb's friction, $\mu = \tan\psi$, where ψ is the friction angle. The collapse condition is sought by progressively decreasing μ, assumed as a stability parameter.

As will be shown below, this static, semi-analytical graphical method can be used to draw the so-called "stability area". The method is usually applied to symmetric arches subjected to symmetric gravitational loads but can be extended to the assessment of other types of symmetric structures. The statically admissible solutions are determined by taking into account strength and friction requirements pertaining to any cross-section *i*, as well as the equilibrium conditions related to the portion of the structure between the ideal vertical midspan section, belonging to the *y*-axis (see Fig. 2b), and generic joint *i*.

Looking at Figure 4b, where the applied loads are shown in red and the internal forces in blue, an eccentric horizontal thrust *f* operates on the midspan cross-section due to symmetry hypotheses. The measurement of



Supprimé:
Supprimé: ¶
Supprimé: 3
Supprimé: Equilibrium of the portion…ortion of the ... [14]
Supprimé: at the midspan
Mis en forme : Couleur de police : Rouge
Mis en forme ... [13]
Mis en forme ... [15]
Mis en forme ... [16]
Supprimé: stress resultants
Mis en forme ... [17]
Supprimé: (*left*);
Mis en forme ... [18]
Supprimé: *right*
Mis en forme ... [19]
Mis en forme : Couleur de police : Rouge
Supprimé: ¶
Mis en forme ... [20]
Mis en forme ... [21]
Mis en forme ... [22]
Mis en forme ... [23]
Mis en forme ... [24]
Mis en forme ... [25]
Mis en forme : Non Surlignage
Mis en forme ... [26]
Supprimé: As will be shown below, this static, semi- ... [27]
Mis en forme : Couleur de police : Rouge, Surlignage
Mis en forme : Couleur de police : Rouge
Mis en forme ... [28]
Supprimé: ¶ ... [29]
Mis en forme : Couleur de police : Rouge
Supprimé: this
Mis en forme : Couleur de police : Rouge
Supprimé: vertical
Mis en forme : Couleur de police : Rouge
Supprimé: (Figure 3, left)

f's eccentricity, denoted by e_0, is made in relation to the centroid of the vertical cross-section, or C_0, being P_0 the pressure centre of f. As regards the sign convention, the eccentricity e_0 is positive if P_0 falls below C_0 (as happens in Figure 4b).

The stability area can be determined while fixing a value of the uniformly distributed load, q (depending on the height, H, of the wall above the flat arch), reinterpreting Durand Claye's graphical constructions in terms of stress resultants. The weight of the portion of the flat arch comprised between the vertical axis of symmetry and joint i is given by: $W_i = \gamma t h \left(x_{I_i} + x_{E_i}\right)/2$, while the x-coordinate of the centre of gravity, G_i, of such portion is: $x_{G_i} = \frac{x_{E_i}{}^2 + x_{I_i}{}^2 + x_{E_i} x_{I_i}}{3\left(x_{I_i} + x_{E_i}\right)}$. The formal expressions of the bending moment, M_i, and normal force, N_i, can be easily determined by means of equilibrium relations (by considering the positive sign convention in Fig. 4a):

$$M_i(f, e_0, \theta_i) = -f e_0 - W_i\left[\left(x_{I_i} + x_{E_i}\right)/2 - x_{G_i}\right] - Q_i\left[\left(x_{I_i} + x_{E_i}\right)/2 - x_{L_i}\right] \quad (1)$$

$$N_i(f, \theta_i) = -f \cos\theta_i - (W_i + Q_i) \sin\theta_i, \quad (2)$$

where $Q_i = q\, x_{E_i}$; $x_{L_i} = x_{E_i}/2$; $\theta_1 = \theta_3 = \alpha$; $\theta_2 = -\alpha$.

In order to define the domain of the statically admissible solutions, the problem is decomposed in normal and tangential sub-problems for which collapse conditions can be defined. As regards the normal problem, the limit condition at the cross section here assumed relates to a rectangular distribution of the normal stresses over the joint, attaining the limit value, σ_c, with the possibility of partialization of the section. According to this stress distribution, by static equivalence the limiting value of the bending moment, $M_i = M_i^{lim}$, is linked to the normal force, N_i, according to the following relationship:

$$M_i^{lim} = -\frac{N_i(N_i + t\, s\, \sigma_c)}{2\, t\, \sigma_c}, \quad (3)$$

where s is the depth of the joint, see Fig. 5a.

More in detail, by assuming that the partialized region is a rectangle of dimensions $t \times p$ (see the grey rectangle in Figure 5b), the normal force N_i corresponding to the stress distribution of Fig. 5c can be expressed as $N_i = -\sigma_c t(s - p)$, therefore $p = \frac{(N_i + t\, s\, \sigma_c)}{t \sigma_c}$.

Supprimé: 3, left
Mis en forme : Couleur de police : Rouge
Supprimé: (Fig. 3, left)
Mis en forme : Couleur de police : Rouge
Mis en forme ... [30]
Mis en forme : Couleur de police : Rouge
Mis en forme ... [31]
Mis en forme ... [32]
Mis en forme ... [33]
Mis en forme ... [34]
Supprimé: For this static analysis, masonry is defined as a no-tension material with a finite compressive strength, σ_c
Supprimé: . T
Mis en forme : Couleur de police : Rouge
Supprimé:
Supprimé: stress
Mis en forme ... [35]
Supprimé: , see for example (Aita, Bruggi and Garavaglia, 2024)
Mis en forme ... [36]
Mis en forme : Couleur de police : Rouge
Mis en forme : Espacement automatique entre les caractères asiatiques et latins, Espacement automatique entre les caractères asiatiques et les chiffres, Taquets de tabulation : 17 cm, Droite
Mis en forme : Couleur de police : Rouge
Mis en forme ... [37]
Mis en forme ... [38]
Mis en forme ... [39]

The limit bending moment is $M_i^{lim} = -N_i(s/2 - (s-p)/2) = -N_i\,p/2$, from which, considering the expression for p just obtained, Eq. (3) is retrieved.

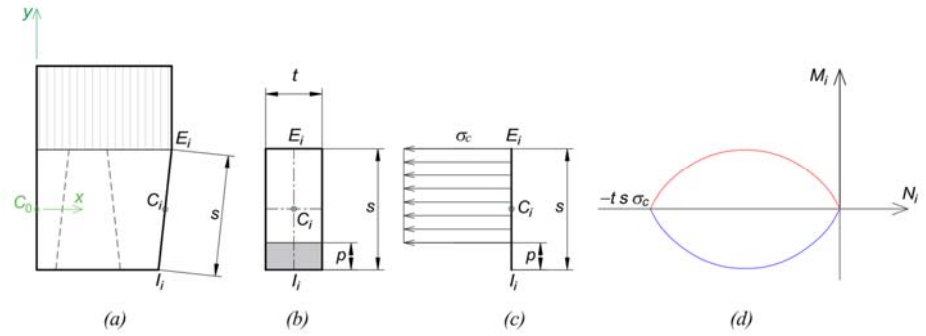


Figure 5. Geometry of the joint (*a*) and generic cross-section I_iE_i (*b*); limit condition by assuming a no-tension material with a compressive strength σ_c (*c*); rotational domain in the (N_i, M_i) plane (*d*).

When $\sigma_c \to \infty$, the limit moment (3) becomes $M_i^{lim} = -\frac{N_i\,s}{2}$, which corresponds to that provided by Heyman's hypotheses: the limit condition at any *i*-th joint is attained when the centre of pressure of the normal force coincides with the intrados or extrados points (I_i or E_i).

By adopting notation and definitions used for example in (Aita, Bruggi and Garavaglia, 2024), the so-called rotational domain, A_i^{rot}, related to generic *i*-th joint, is obtained by drawing the $-M_i^{lim}$ and M_i^{lim} curves in the (f, e_0) plane, and considering the inequalities

$$-M_i^{lim} \le M_i \le +M_i^{lim}. \qquad (4)$$

As an example, in Fig. 6a, obtained by setting $H = 1$ m, and $\mu = 1.7772$, the $-M_i^{lim}$ and $+M_i^{lim}$ curves are represented by the blue and red curves, respectively.

It is recalled that the rotational domain A_i^{rot} corresponds to the domain plotted in the (N_i, M_i) plane plotted in Fig. 5d, where the blue and red parabolas correspond to $-M_i^{lim}$ and $+M_i^{lim}$, respectively; for further insights, see for example (Andreaus and Augusti, 1991; Rossi et al., 2020; Clemente et al. 2023).

Mis en forme ... [40]
Mis en forme : Couleur de police : Rouge
Mis en forme : Couleur de police : Rouge
Mis en forme ... [41]
Mis en forme : Couleur de police : Rouge
Mis en forme ... [42]
Mis en forme : Couleur de police : Rouge
Mis en forme : Justifié, Taquets de tabulation : Pas à 17 cm
Mis en forme ... [43]
Mis en forme ... [44]
Mis en forme ... [45]
Mis en forme ... [46]
Supprimé: T
Mis en forme : Couleur de police : Rouge
Mis en forme : Justifié
Mis en forme : Couleur de police : Rouge
Mis en forme : Couleur de police : Rouge
Supprimé: , … rr
Mis en forme ... [47]
Mis en forme : Couleur de police : Rouge
Supprimé: curves
Mis en forme ... [48]
Mis en forme ... [49]
Supprimé: ¶
Mis en forme ... [50]
Mis en forme ... [51]

(a)

(b)

(c)

(d)

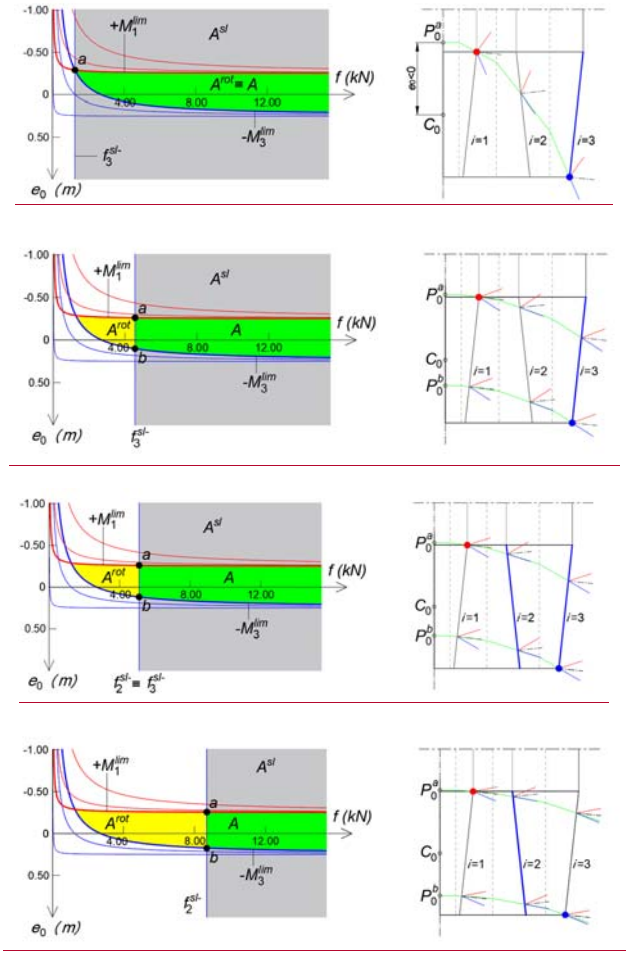


Figure 6. Stability area (left) and thrust line (right) for H = 1 m, and: μ = 1.7772 (*a*); μ = 0.5 (*b*); μ = 0.4389 (*c*); μ = 0.3 (*d*). Joints where the limit sliding condition is attained are coloured blue.

As regards the tangential problem, an internal Coulomb's friction is considered. The sliding domain related to any joint i is plotted both in the (N_i, T_i) plane of Fig. 7a (considering the stress resultants) and in the $(R_{i,n}, R_{i,t})$ plane of Fig. 7b (with reference to the components of the reaction force $\boldsymbol{R}_i = -\boldsymbol{F}_i$ at joint i along the directions n_i and t_i, see Fig. 7c, right). With reference to Fig. 4a, it is bounded by the blue and red

Mis en forme : Couleur de police : Rouge

Supprimé: 4

Mis en forme : Couleur de police : Rouge

Mis en forme : Couleur de police : Rouge

Supprimé:

Supprimé: . (4)¶

Mis en forme : Couleur de police : Rouge

Supprimé: In order to account for the existence of

Mis en forme : Couleur de police : Rouge

Mis en forme : Non Surlignage

Mis en forme : Non Surlignage

Mis en forme : Non Surlignage

Mis en forme : Non Surlignage

Mis en forme : Non Surlignage

Mis en forme : Non Surlignage

Mis en forme : Non Surlignage

Mis en forme : Non Surlignage

Mis en forme : Non Surlignage

Mis en forme : Non Surlignage

Mis en forme : Non Surlignage

Mis en forme : Non Surlignage

Mis en forme : Non Surlignage

Mis en forme : Non Surlignage

Mis en forme : Non Surlignage

Mis en forme : Non Surlignage

Mis en forme : Non Surlignage

Mis en forme : Non Surlignage

Mis en forme : Non Surlignage

Mis en forme : Non Surlignage

Mis en forme : Non Surlignage

Mis en forme : Non Surlignage

straight lines identified by the equations $N_i \tan(\psi) - T_i = 0$ and $N_i \tan(\psi) + T_i = 0$, with $N_i \leq 0$, respectively.

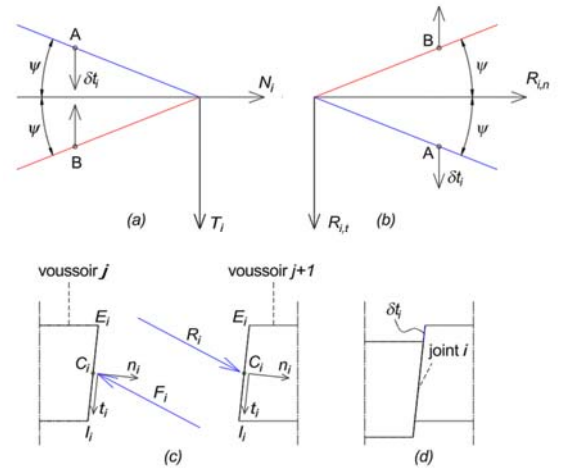


Figure 7. The sliding domain related to any joint i in the plane (N_i, T_i) (*a*) and in the plane $(R_{i,n}, R_{i,t})$ (*b*). Internal force at joint i and notation adopted (*c*); mutual sliding at joint i (*d*).

In order to draw the stability area in the plane (f, e_0), the so-called sliding domain, A_i^{sl} corresponding to any i-th joint, independent on e_0, is defined by the inequalities

$$f_i^{sl-} \leq f \leq f_i^{sl+} \qquad (5)$$

where f_i^{sl-}, and f_i^{sl+}, are the minimum and maximum thrusts compatible with the friction cone of amplitude ψ. To better visualize the limit condition imposed by Coulomb's friction, in Fig. 4c and in Fig. 6, right, the sliding domain in the plane $(R_{i,n}, R_{i,t})$ is plotted for each joint i. The blue (resp. red) straight lines correspond to those of Fig. 7b. As an example, with reference to joint $i = 3$ in Fig. 4c, the triangle of forces involved in the determination of f_3^{sl-} is highlighted in yellow: the limit reaction at the i-th joint, corresponding to the horizontal thrust f_3^{sl-}, is tangent to the blue straight line of the friction cone. By writing the translational equilibrium relation, f_i^{sl-}, and f_i^{sl+} can be determined for any joint i:

$$f_i^{sl\pm} = (W_i + Q_i) \tan\left(\frac{\pi}{2} - \theta_i \pm \psi\right). \qquad (6)$$

In Fig. 6a, the blue straight line parallel to the e_0-axis corresponds to f_3^{sl-} in the (f, e_0) plane.

Mis en forme ... [52]
Mis en forme ... [53]
Mis en forme ... [54]
Mis en forme ... [55]
Mis en forme ... [56]
Mis en forme ... [57]
Mis en forme ... [58]
Mis en forme ... [59]
Mis en forme ... [60]
Mis en forme ... [61]
Supprimé: ,
Mis en forme ... [62]
Supprimé: ,
Supprimé: , is define
Mis en forme ... [65]
Supprimé: d
Mis en forme ... [63]
Mis en forme ... [64]
Supprimé: e
Supprimé: (Fig. 3, right),
Mis en forme ... [66]
Mis en forme ... [67]
Supprimé: according to the equilibrium relation:¶
Mis en forme ... [68]
Mis en forme ... [69]
Mis en forme ... [70]
Supprimé: related to
Mis en forme ... [71]
Mis en forme ... [72]
Supprimé: *i*
Mis en forme ... [73]
Supprimé: (at joint $i = 3$)
Mis en forme ... [74]
Supprimé: *i*
Mis en forme ... [75]
Supprimé: according to the
Mis en forme ... [76]
Mis en forme ... [77]
Mis en forme ... [78]
Mis en forme ... [79]
Mis en forme ... [80]
Supprimé: equilibrium relation:
Mis en forme ... [81]
Mis en forme ... [82]
Mis en forme ... [83]
Mis en forme ... [84]
Mis en forme ... [85]

If the previously stated procedure is performed for each joint i, taking into account the intersections between all the A_i^{rot}, A_i^{sl} domains, one may obtain both the rotational domain and the sliding domain related to the complete flat arch, denoted by A^{rot}, A^{sl} respectively (see for example Fig. 6a, left, where the rotational domain A^{rot} is the green solid area, while the sliding domain A^{sl} is the grey region delimited by the straight line f_3^{sl-}). The stability area is the intersection between A^{rot} and A^{sl} (in Fig. 6a, A coincides with A^{rot}; in Fig. 6b, it is coloured green).

It is interesting to observe that the flat arch is characterized by a small inclination of the joints ($\alpha = 6.216°$, which turns to be unconventional at joint $i = 2$ ($\theta_2 = -\alpha$), as already observed in the Introduction, with reference to Fig. 3. By drawing the friction cone of amplitude ψ at $i = 1$, $i = 3$ (Fig. 4c) the sliding domains related to joints $i = 1$ and $i = 3$, i.e., A_1^{sl}, A_3^{sl} are defined by the inequalities (5) for a low value of the friction angle, i.e., for $\psi < \alpha$; on the contrary, A_1^{sl}, A_3^{sl} are delimited only by the condition $f_i^{sl-} \leq f$ for $\psi \geq \alpha$ (in Fig. 4c, only f_i^{sl-} has a finite value, see the blue straight line of the friction cone, while f_i^{sl+} is unbounded, see the red straight line). The inclination of joint $i = 2$ requires that the condition $\psi > \alpha$ is respected in order to comply equilibrium. If $\psi \leq \alpha$, both f_i^{sl-} and f_i^{sl+} are unbounded, and no statically admissible solution can be found: the sliding domain A^{sl} would coincide with the empty set, and therefore the stability area A would not provide statically admissible solutions in the plane (f, e_0). Given the above, the minimum friction angle compatible with sliding equilibrium is $\psi = \alpha = 6.216°$, corresponding to $\mu = 0.1089$; considering a limited compressive strength, i.e., for $\sigma_c = 45$ MPa, the static method would provide a slightly higher limit value ($\mu = 0.1094$). In the analyses that will be described below, it will be demonstrated that this result is not acceptable, since an incipient collapse mechanism is found for a higher value of the friction coefficient.

3.2. Some non-standard investigations on the purely sliding collapse mode

In this Section, non-standard investigations are proposed to clarify the unconventional behaviour of the flat arch. When the stress state is represented by point A (resp. point B) of the boundary of the sliding domain (see Figures 7a and 7b) and dilatancy is zero, an incipient mutual sliding δt_i occurs between the blocks j

Supprimé: ¶

Supprimé: 4a

Mis en forme : Couleur de police : Rouge

Mis en forme : Anglais (Royaume-Uni)

Supprimé: 4a

Mis en forme : Couleur de police : Rouge

Mis en forme ... [86]

Supprimé:)

Mis en forme ... [87]

Supprimé: .

Mis en forme : Couleur de police : Rouge

Supprimé: 3, right

Mis en forme : Couleur de police : Rouge

Supprimé: 3, right

Mis en forme : Couleur de police : Rouge

Supprimé: the equilibrium conditions

Mis en forme : Couleur de police : Rouge

Mis en forme : Non Surlignage

Mis en forme ... [88]

Mis en forme ... [89]

Supprimé:

Mis en forme ... [90]

Mis en forme : Non Surlignage

Mis en forme ... [91]

Mis en forme : Police :(Par défaut) Times New Roman, Non Italique

Supprimé: ¶

Mis en forme : Couleur de police : Rouge

Mis en forme : Couleur de police : Rouge

Supprimé: The static method described in Section 3.1 is coupled with a kinematic analysis, by extending the approach proposed in (Sinopoli, Aita and Foce, 2007) to a structure with non-conventional voussoirs in order to determine which condition divides equilibrium from incipient collapse.

Mis en forme ... [92]

Mis en forme ... [93]

and j+1, with the voussoir j sliding downwards (resp. upwards) with respect to the voussoir j+1 (Fig. 7d). The flow rule just described implies that this mutual displacement between the voussoirs is not normal to the yield surface, and a non-standard behaviour can arise.

For this reason, the static method described in Section 3.1 is coupled with a kinematic analysis, extending the approach proposed in (Sinopoli, Aita and Foce, 2007) to a structure with non-conventional voussoirs to determine which condition divides equilibrium from incipient collapse.

Let consider the front layer of the flat arch, by assuming the geometric parameters described in Section 2. The mechanical behaviour of this structure under gravitational loads is studied while varying the friction coefficient. The self-weight and the weight of the wall above, with H = 1 m, are considered; additionally, in the numerical investigations, the mechanical parameters described in Section 2 are applied.

The investigations performed by means of the stability area method assume a finite value of the compressive strength, $\sigma_c = 45$ MPa. As will be clarified in the following, for the case studies here examined, the influence of this limited value of σ_c on the structural response is not apparent with respect to the assumption of an infinite value of σ_c.

The first investigation aims at finding the minimum friction coefficient $\mu = \tan\psi$ according to which the rotational domain is completely included in the sliding domain (Heyman, 1966; 1969). From now on the friction coefficient corresponding to this situation will be denoted by μ_0. The black point a in the (f, e_0) plane (Fig. 6a, left) corresponds to the minimum value of the thrust f belonging to the rotational domain, A^{rot}. This point, of eccentricity e_0, identifies the attainment of the limit bending moment at joints $i = 1$ (positive bending moment, see the red curve $+M_1^{lim}$) and $i = 3$ (negative bending moment, see the blue curve $-M_3^{lim}$). For a friction coefficient $\mu = 1.7772$, the straight line related to the maximum value of f_i^{sl-}, i.e., $\max f_i^{sl-} = f_3^{sl-} = 4.56$ kN, passes through point a, i.e., $\mu = \mu_0$. The line of pressure corresponding to point a of the stability area is plotted in Figure 6a, right: the green piecewise linear curve is the funicular polygon obtained by starting from point P_0^a, matching the eccentricity defined by point a; the segments have the direction of the compressive force acting on each joint: the red and blue dots are the centres of pressure of the thrust at joints $i = 1$ and $i = 3$, and correspond to the attainment of a limit positive or

Mis en forme : Non Surlignage
Mis en forme : Non Surlignage
Supprimé: The
Mis en forme : Couleur de police : Rouge
Mis en forme : Couleur de police : Rouge
Supprimé: ¶
Mis en forme : Couleur de police : Rouge
Mis en forme : Couleur de police : Rouge
Supprimé: ¶
Mis en forme : Couleur de police : Rouge
Supprimé: F
Supprimé: a
Mis en forme : Couleur de police : Rouge
Supprimé: the compressive strength
Mis en forme : Couleur de police : Rouge
Supprimé:
Mis en forme : Couleur de police : Rouge
Mis en forme : Couleur de police : Rouge
Mis en forme : Couleur de police : Rouge
Mis en forme : Couleur de police : Rouge
Mis en forme : Couleur de police : Rouge
Supprimé: 4a
Mis en forme : Couleur de police : Rouge
Mis en forme : Couleur de police : Rouge
Supprimé: .
Supprimé:
Supprimé: 4a
Mis en forme : Couleur de police : Rouge
Mis en forme : Couleur de police : Rouge
Mis en forme : Non Surlignage
Mis en forme : Couleur de police : Rouge
Mis en forme : Non Surlignage
Mis en forme : Couleur de police : Rouge

negative bending moment, respectively; moreover, the blue joint ($i = 3$) indicates the attainment of the limit condition provided by the friction cone. The condition identified by point *a* of the stability area (Fig. 6a, left) is investigated from the kinematic point of view to evaluate whether this statically admissible solution, lying at the boundary of the stability area, can correspond to a kinematically admissible mechanism. The kinematic compatibility is sought starting from the thrust line corresponding to point *a* in Fig. 6a, right, and considering joints $i = 1$ and $i = 3$, where the limit value of the bending moment is attained (see the $+M_1^{lim}$ and $-M_3^{lim}$ curves) and the flow rule respects the normality low - as discussed, for example, in (Andreaus and Augusti, 1991). If the normal force acts at a distance $(s - p)/2$ from the extrados (resp. intrados) of the joint (Fig. 5c), the plastic hinge will be at a distance $s - p$ from the extrados (resp. intrados). In the case in question (Fig. 6a), the effects of a limited compressive strength are not evident, since the hinge lies close to the extrados (resp. intrados); the reciprocal rotation between the voussoirs according to a kinematically admissible mechanism would imply an interpenetration between the blocks that is not consistent with the position of the hinges identified by the static method. Furthermore, even the downward sliding at joint $i = 3$ (see the straight line corresponding to f_3^{sl-} in Fig. 6a) would be incompatible with a mixed (rotational + sliding) collapse mode, since it would imply a wider interpretation region, again not consistent with the static solution. Therefore, the stress state identified by point *a* does not correspond to a kinematically admissible mechanism for the flat arch. Even more so, the same applies to all the stress states identified by the points belonging to the $+M_3^{lim}$ and $-M_3^{lim}$ curves delimiting the stability area A in Fig. 6a. It can be concluded that none of the solutions corresponding to (f, e_0) points contained within the stability area A is compatible with a collapse mechanism.

By the way, it should be noted that $\mu = 1.7772$ is unrealistic for masonry structures: according to Lourenço and Ramos (2004), for dry masonry joints the Coulomb friction coefficient varies in the range $0.20 \leq \tan\psi \leq 0.60$, depending on the surface roughness. The high value just retrieved, however, is theoretically significant when compared with Heyman's assumption related to friction ($\mu \to \infty$).

By decreasing the friction coefficient, the sliding domain A^{sl} shrinks, so that the rotational domain A^{rot} is not entirely included in A^{sl}. Let us now focus on Figure 6b, obtained by setting $\mu = 0.5 < 1.7772$. The

Supprimé: ;

Supprimé: The condition identified by point *a* of the stability area (Fig. 4a, left) does not correspond to a kinematically admissible mechanism for the flat arch

Mis en forme ... [94]

Supprimé: .

Mis en forme : Couleur de police : Rouge

Mis en forme ... [95]

Mis en forme ... [96]

Mis en forme ... [97]

Supprimé: T

Mis en forme : Couleur de police : Rouge, Non Surlignage

Supprimé: condition identified…tress state identified by point *a* of the stability area (Fig. 4a, left) ... [98]

Mis en forme ... [99]

Mis en forme ... [100]

Mis en forme ... [101]

Supprimé: Even more so,

Mis en forme ... [102]

Mis en forme ... [103]

Mis en forme ... [104]

Mis en forme : Couleur de police : Rouge

Mis en forme : Justifié

Supprimé: 4b

Mis en forme : Couleur de police : Rouge

straight line delimiting the sliding domain corresponds again to max $f_i^{sl-} = f_3^{sl-}$. The existence of statically admissible solutions in the (f, e_0) plane is assured by the stability area A (see the green region), but some investigations must be performed by examining the boundaries of this area, in particular the points belonging to segment ab. By plotting the lines of thrusts corresponding to points a and b, the internal reaction at joint $i = 3$ touches the blue straight line of the friction cone (Fig. 6b, right). This local limit condition is incompatible with a purely sliding mechanism for the entire flat arch. Moreover, repeating the same reasoning made with reference to Fig. 6a, it is incompatible also with a mixed collapse mode.

By further reducing μ, the response of the flat arch remains analogous to that just described (i.e., the friction limit condition is attained at joint $i = 3$) until the value $\mu = 0.4389$, corresponding to max $f_i^{sl-} = f_3^{sl-} = f_2^{sl-} = 5.103$ kN. In this case, although the existence of statically admissible solutions is found (see the green stability area of Fig. 6c, left), the solutions represented by points (f, e_0) belonging to the segment ab are compatible with a purely sliding mechanism: in both $i = 2$ and $i = 3$ joints, the internal reaction touches the blue straight line of the friction cone (Fig. 6c, right), and downward sliding occurs according to the flow rule described with reference to Figures 7a and 7b.

The mechanism thus identified corresponds to the one introduced qualitatively with reference to Fig. 3a. It can be described by assuming an independent virtual displacement parameter, for example the downward translation along joint $i = 3$, denoted by δt_3. The vertical displacement of block (B) (with the wall above) can be expressed as follows: $\delta y_b = \delta t_3 \cos\alpha$, positive if downwards.

Supprimé: 4b

Supprimé: T

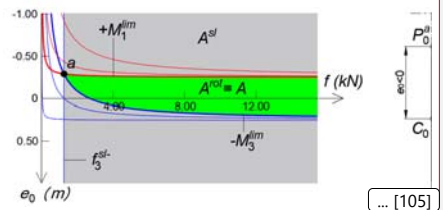
Mis en forme : Couleur de police : Rouge

Mis en forme : Surlignage

Mis en forme : Couleur de police : Automatique

Mis en forme : Non Surlignage

Supprimé: ¶
<objet>



... [105]

Supprimé: decreasing

Mis en forme : Couleur de police : Rouge

Supprimé: 4c

Mis en forme : Couleur de police : Rouge

Supprimé: an unconventional

Mis en forme : Couleur de police : Rouge

Supprimé: 4c

Mis en forme : Couleur de police : Rouge

Mis en forme : Couleur de police : Rouge

Mis en forme : Non Surlignage

Mis en forme : Non Surlignage

Mis en forme : Non Surlignage

Mis en forme : Couleur de police : Rouge

Supprimé: .

Supprimé: is plotted in Fig. 5, and

Mis en forme : Couleur de police : Rouge

Supprimé:

Supprimé: *b*.

Supprimé: .

Mis en forme : Couleur de police : Rouge

Supprimé: With reference to a half of the flat arch, t

Supprimé: b

Mis en forme : Police :Non Italique

Mis en forme : Police :Non Italique

Mis en forme : Police :Non Italique

Supprimé: *b*

Supprimé: (see the grey block in Fig. 5, left)

Mis en forme : Couleur de police : Rouge

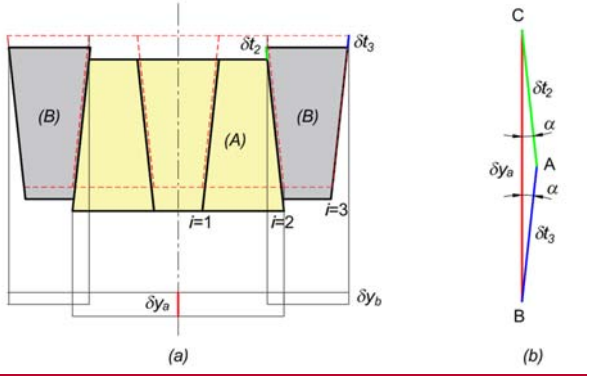


Figure 8. Pure sliding collapse mechanism retrieved for $\mu = 0.4389$ (*a*); geometric construction to determine the virtual displacements (*b*).

Considering the geometric construction plotted in Fig. 8b (see triangle ABC), the law of sines provides: $\frac{\delta t_3}{\sin\alpha} = \frac{\delta y_a}{\sin 2\alpha} = \frac{\delta t_2}{\sin\alpha}$, from which the vertical displacement δy_a of macroblock (*A*) (with the wall above), is given by $\delta y_a = \frac{\sin 2\alpha}{\sin\alpha}\delta t_3$, while the mutual translation δt_2 between blocks a and b along joint $i = 2$ is: $\delta t_2 = \delta t_3$. By substituting the numerical values of the quantities corresponding to the case study just examined, the virtual work of the external loads, δL^a, minus the dissipation at the frictional constraints, δL^ψ, is equal to zero for $\mu = 0.4389$ (see Eq. (7) referred, for simplicity, to the right half of the flat arch):

$$\delta L^a - \delta L^\psi = (W_a + Q_a)\delta y_a + (W_b + Q_b)\delta y_b + \\ -\mu\left|\left((W_3 + Q_3)\sin\alpha + f_3^{sl-}\cos\alpha\right)\delta t_3\right| + \\ -\mu\left|\left(-(W_2 + Q_2)\sin\alpha + f_3^{sl-}\cos\alpha\right)\delta t_2\right| \qquad (7)$$

where $W_a = W_2$; $Q_a = Q_2$; $W_b = W_3 - W_2$; $Q_b = Q_3 - Q_2$.

As for the horizontal thrust that compresses the flat arch, it is observed that it must correspond to f_3^{sl-}, uniquely determined by the friction law at the unilateral constraint $i = 3$. Actually, unless the flat arch is pre-compressed, the unconventional inclination of the joint $i = 2$ might not ensure that a thrust equal to f_2^{sl-} is transmitted to the adjacent voussoirs.

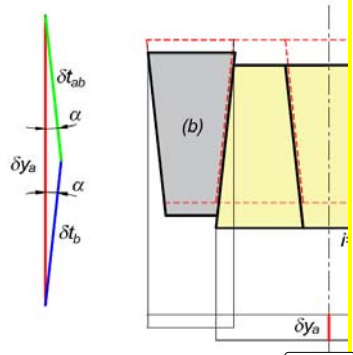
Mis en forme : Centré
Mis en forme : Non Surlignage
Mis en forme : Police :10 pt, Couleur de police : Rouge
Mis en forme : Police :10 pt, Italique, Couleur de police : Rouge
Mis en forme : Police :10 pt, Couleur de police : Rouge
Mis en forme : Police :10 pt, Couleur de police : Rouge
Mis en forme : Police :Italique
Supprimé: By considering
Mis en forme : Couleur de police : Rouge
Mis en forme : Couleur de police : Rouge
Supprimé: triangle
Supprimé: 5
Supprimé: , left,
Mis en forme : Couleur de police : Rouge
Mis en forme : Couleur de police : Rouge
Supprimé: *b*
Supprimé: *ab*
Mis en forme : Couleur de police : Rouge
Supprimé: *a*
Mis en forme : Police :Non Italique, Couleur de police : Rouge
Mis en forme : Couleur de police : Rouge
Supprimé: ; see the yellow block
Supprimé: *b*
Supprimé: *ab*
Supprimé: *ab*
Supprimé: *b*
Supprimé: see Eq. (7),
Supprimé: :
Supprimé: ¶
Mis en forme : Anglais (Royaume-Uni)
Supprimé: .
Mis en forme : Couleur de police : Rouge

By further decreasing the friction coefficient, the static method identifies a limit friction condition only at joint $i = 2$. In figure 6d, left, obtained by assuming $\mu = 0.3 < 0.4389$, the value of the minimum thrust, $f_2^{sl-} = 8.69$ kN, is considerably greater than that obtained in the previous cases. The stability area is always present (see the green area A in Fig. 6d, left), and corresponds to statically admissible solutions, but the points belonging to the segment ab identifies a collapse condition, as can be shown by the kinematic analysis and by Eq. 7.

In the situation relating to the purely sliding collapse mode represented in Fig. 8a, defined when $\mu = 0.4389$, for the minimum value of the crown thrust f compatible with the equilibrium, i.e., $f = \max f_i^{sl-} = f_3^{sl-} = f_2^{sl-}$, both block ($A$) and block ($B$) can slide downwards, and sliding can occur due to contact between the blocks. As observed before, the expression (7), providing $\delta L^a - \delta L^\psi$, is equal to zero when the virtual work of the external loads and the internal dissipation due to the finite friction are computed. When $\mu \neq 0.4389$, the expression (7) has to be calculated by considering the horizontal thrust actually transmitted through the structure, corresponding to f_3^{sl-} as defined by the unilateral frictional constraint at joint $i = 3$. When $\mu > 0.4389$, $\max f_i^{sl-} = f_3^{sl-}$, and formula (7) provides a negative value for the virtual work minus the internal dissipation, by identifying an equilibrium condition. When $\mu < 0.4389$, i.e., when $\max f_i^{sl-} = f_2^{sl-}$, relation (7) provides a positive value, by confirming the occurring of a collapse condition.

From this procedure, the limit value of the friction coefficient compatible with the system's equilibrium is $\mu = 0.4389$, denoted below by μ_1. The value of μ_1 is higher than the one determined at the end of Section 3.1 ($\mu = 0.1094$) using static considerations alone. This clarifies why the stability area method cannot be conventionally applied to evaluate the structural response of this flat arch: the existence of statically admissible solutions does not guarantee the equilibrium of this structure.

The procedure just proposed, which combines statics and kinematics, allows parametric investigations. A first set of analyses aims at determining the friction coefficient μ_0, above which the rotational domain is fully contained in the sliding domain (see Fig. 6a), by varying the height of the wall, H. By fixing the value



Supprimé: ... [106]

Mis en forme : Couleur de police : Rouge, Surlignage

Mis en forme : Couleur de police : Rouge, Surlignage

Mis en forme : Couleur de police : Rouge

Supprimé: 4d

Mis en forme : Couleur de police : Rouge

Mis en forme : Couleur de police : Rouge

Mis en forme : Couleur de police : Rouge

Supprimé: 4d

Mis en forme : Couleur de police : Rouge

Supprimé: correspond to

Mis en forme : Couleur de police : Rouge

Mis en forme : Couleur de police : Rouge

Supprimé: , see

Supprimé: If we now consider for a moment a sligh ... [107]

Mis en forme : Couleur de police : Rouge

Mis en forme : Couleur de police : Rouge

Supprimé: 5, left

Supprimé: *a*

Supprimé: *b*

Mis en forme : Couleur de police : Rouge

Mis en forme : Couleur de police : Rouge

Supprimé: is

Mis en forme : Couleur de police : Rouge

Supprimé: .

Mis en forme : Couleur de police : Rouge

Mis en forme : Non Surlignage

Mis en forme : Couleur de police : Rouge

Mis en forme : Couleur de police : Rouge

Mis en forme : Couleur de police : Rouge

Mis en forme : Couleur de police : Rouge

of the compressive strength, $\sigma_c = 45$MPa (see Section 2), for $0 \leq H \leq 10$ m, the friction coefficient μ_0 ranges from 1.7158 ($H = 0$) to 1.7991 ($H = 10$ m), while the minimum crown thrust corresponding to a statically admissible solution, i.e., $\max f_i^{sl-}$, increases with H from 0.42456 kN to 8.75852 kN. It is interesting to observe that the value of the friction coefficient μ_0 is affected by the compressive strength σ_c. By fixing now the value of the wall's height, $H = 10$ m, μ_0 increases with σ_c, while the minimum horizontal thrust decreases as the stability area widens. For example, when $\sigma_c = 2.5$ MPa, $\mu_0 = 1.6932$, while $\mu_0 = 1.8049$ is retrieved when the compressive strength is infinite.

A second set of analyses aims at assessing the influence of the compressive strength on the collapse condition. The friction coefficient μ_1 - corresponding to the purely sliding collapse mode of Fig. 8a - is determined by fixing the height of the wall, $H = 1$ m, and varying the compressive strength. The study of the stability area allows for concluding that the values of μ_1 are not affected by the compressive strength for $\sigma_c \geq 0.106$ MPa. By fixing now the mechanical parameters related to the compressive strength as well as the weight density consistently with the parameters described in Section 2 ($\sigma_c = 45$ MPa, $\gamma = 26$ kN/m^3), while varying H, the value of μ_1 increases while decreasing H (and q), ranging from $\mu_1 = 0.4023$ (for $H = 10$ m) to $\mu_1 = 0.5709$ (for $H = 0$). For all these values of H the collapse behaviour involves a purely sliding collapse mode analogous to that plotted in Fig. 8a. The same numerical results are obtained by assuming $\sigma_c \to \infty$, confirming that the assumption of a limited compressive strength does not affect the collapse response of the flat arch for loading conditions and material properties compatible with the architectural features of the Prato Cathedral. This allows to justify the choice to assume the simplified hypothesis of infinite compressive strength in some of the analyses that will be performed with other methods, see Sections 4 and 6.

4. Non-linear elastic analysis by means of a FEA model with Abaqus, accounting for finite friction

The non-standard analyses carried out in Section 3 require validation due to their peculiarity. To help understand the collapse behaviour of the unconventional flat arch under study, a comparison with the results of numerical analyses is provided in this section along with commentary.

Mis en forme : Couleur de police : Rouge

Supprimé: The analytical method just proposed allows for determining the friction coefficient μ_0, above which the rotational domain is fully contained in the sliding domain, by varying the height of the wall, H. By fixing the value of the compressive strength, $\sigma_c = 45$MPa (see Section 2), for $0 \leq H \leq 10$ m, the friction coefficient μ_0 ranges from 1.7158 ($H = 0$) to 1.7991 ($H = 10$ m), while the minimum crown thrust corresponding to a statically admissible solution, i.e., $\max f_i^{sl-}$, increases with H from 0.42456 kN to 8.75852 kN. It is interesting to observe that the value of the friction coefficient μ_0 is affected by the compressive strength σ_c. By fixing now the value of the wall's height, $H = 10$ m, μ_0 increases with σ_c, while the minimum horizontal thru ... [108]

Mis en forme : Couleur de police : Rouge

Mis en forme ... [109]

Mis en forme ... [110]

Mis en forme ... [111]

Mis en forme ... [112]

Mis en forme ... [113]

Mis en forme ... [114]

Mis en forme ... [115]

Mis en forme ... [116]

Mis en forme ... [117]

Mis en forme ... [118]

Mis en forme ... [119]

Mis en forme ... [120]

Mis en forme ... [121]

Mis en forme ... [122]

Mis en forme ... [123]

Mis en forme ... [124]

Mis en forme ... [125]

Mis en forme ... [126]

Mis en forme ... [127]

Mis en forme ... [128]

Mis en forme ... [129]

Mis en forme ... [130]

Commenté [EG6]: Perché?

Mis en forme ... [131]

Mis en forme : Non Surlignage

Mis en forme ... [132]

Mis en forme ... [133]

Mis en forme ... [134]

Mis en forme ... [135]

Commenté [EG8]: Non è chiaro perché

Supprimé: ¶ ... [136]

4.1 Some general remarks

The numerical analysis is carried out employing the ABAQUS/CAE code, ver. 2023, in the non-linear context of contact (to represent the sliding of the blocks against each other) and geometry (to enforce equilibrium in a deformed position, considering the past load history).

From a geometric point of view, the 3D Finite Element Analysis (FEA) modelling of half a flat arch was implemented, employing a central symmetry constraint to simulate the entire flat arch's behaviour. In the numerical model, 4752 nodes and 2587 C3D10 elements (10-node tetrahedral element) were used.

The voussoirs are modelled separately, and their assembly is obtained through a contact interaction. More precisely, in the direction normal to the contact surfaces, a "hard" contact is considered with the possibility that the surfaces may separate during the loading history. In the tangential direction, the occurring of sliding is admitted by assuming a contact with friction, by suitably setting a friction coefficient, μ.

The material is defined as isotropic and in the linear elastic range, with a modulus of elasticity E equal to 54000 MPa, a Poisson's ratio equal to 0.2 and a specific weight equal to $\gamma = 26$ kN/m^3. A uniformly distributed load γH of 0.026 MPa on the upper surface of the model is set. This load is equivalent to the uniformly distributed load q considered in the examples of Section 3.2. It is emphasized that the FE analyses aim at a comparison with the semi-analytical procedure presented in Section 3, in search of the limit friction coefficient compatible with the flat arch equilibrium. The choice of the linear elastic model is dictated by simplicity. The mechanical parameters of a rock possess great variability depending on the type of rock and its internal structure. In this research, given the impossibility of conducting in situ experimental tests, the mechanical parameters are selected for the modelling of a rather rigid stone material (see for example You, 2011). The authors also performed a sensitivity analysis of the presented results that shows their little dependance on a change in the assumed mechanical parameters. Moreover, recalling the results obtained in Section 3, the influence of a limited value of compressive strength on the collapse response of the flat arch is not evident for the assigned loading conditions. For this reason, and for simplicity, an infinite compressive strength will be assumed in the FEA.

Supprimé: FEM

Mis en forme : Couleur de police : Rouge

Déplacé (insertion) [2]

Supprimé: a

Mis en forme : Couleur de police : Rouge

Mis en forme : Non Surlignage

Mis en forme : Non Surlignage

Supprimé: To compare the results obtained by means of the numerical analyses with those derived by the analytical approach previously exposed,

Déplacé vers le haut [2]: a uniformly distributed load γH of 0.026 MPa on the upper surface of the model is set. This load is equivalent to the uniformly distributed load q considered in the examples of Section 3.2.

4.2 Constraints and loading history

Supprimé: ¶

Mis en forme : Couleur de police : Rouge

Particular attention was given to two main aspects: 1) the arrangement of the contact constraints between the voussoirs and on the part of the flat arch adjacent to the lateral wall support, and 2) the load history. In fact, a modelling of the structure that only involves such type of constraints with the direct application of gravitational and distributed loads would not lead to any results, as the central voussoirs would not be connected to the remaining part of the structure. In this case, the numerical analysis would immediately stop and find a matrix of zero stiffness (which would mean a rigid movement of the central blocks).

A difficulty of FEM-type numerical analyses, compared to analytical investigations conducted in the context of limit analysis (see Section 3), emerges. In approaches based on the lower bound theorem, simple equilibrium equations provide a range of values for the horizontal thrust, each corresponding to a different thrust line. It must then be assessed through non-standard analyses (see Section 3.2) whether the statically admissible solutions obtained may identify collapse kinematics. Differently, in the FEM numerical analysis, a unique thrust line is obtained as the result of the procedure involving equilibrium, deformation and material properties, while thrust (and eccentricity) ranges cannot be established *a priori*. Therefore, to prevent the analysis from immediately stopping due to the rigid movement of the central blocks, the possible application of a stabilizing pre-compression force must be considered through the introduction of appropriate constraint devices (representing, for example, tie rods). Given the above, the procedure aims at simulating the construction and loading of the flat arch; stability is then assessed by checking if equilibrium is possible even removing the pre-compression force.

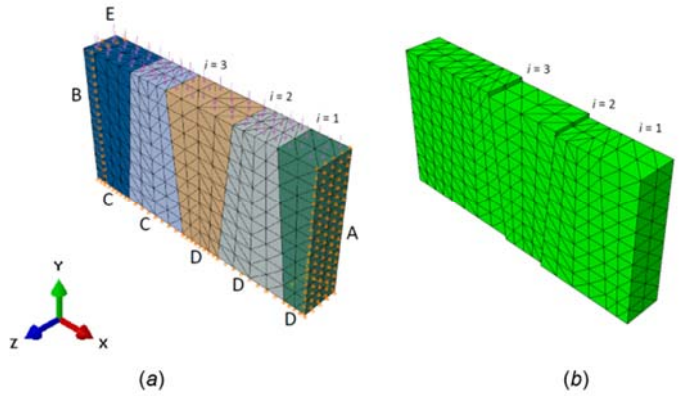


Figure 9. Geometry of the flat arch with highlighting the joints between the parts and the constraints (*a*); deformed configuration in the equilibrium situation after all precompression action has been removed (*b*).

In Figure 9a, the A constraints reproduce the symmetry of the structure. Based on the degrees of freedom of the C3D10 finite element, these constraints predict that the translation in the *x* direction is equal to zero. At the opposite extreme, there are similar B constraints, which however are associated with a non-zero translation history capable of providing pre-compression to the structure. The lower support constraints are distributed over the entire lower surface of the flat arch. Such constraints, both in the real support region (C constraints) and in the central region (D constraints), prevent only the translation in the *y* direction. To prevent the movement in the *z* direction, only the E constraint is inserted, the reaction of which will always be zero as it is the only force in the *z* direction.

The analyses are performed in geometric nonlinearity, so that the coordinates of the nodes are updated at each step and can model a variation of the constraints during the loading history.

The loading history involves several phases (Figure 9a). In the first step, a precompression is gradually inserted by means of an inward displacement of 1 mm in the axial direction of the constraints B and, at the same time, the distributed load q is gradually imposed. In the second step the type D constraints are removed; the flat arch therefore remains vertically supported only by the type C constraints. In the third step the displacement imposed in step 1 to simulate a pre-compression action is gradually removed. In the

Supprimé: ¶ ... [137]
Mis en forme : Police :(Par défaut) Arial
Mis en forme : Police :(Par défaut) Arial
Mis en forme : Police :(Par défaut) Arial
Mis en forme : Police :(Par défaut) Arial, 12 pt, Ne pas vérifier l'orthographe ou la grammaire
Supprimé: 6
Supprimé: *left*
Mis en forme : Couleur de police : Rouge
Mis en forme : Police :Italique, Couleur de police : Rouge
Supprimé: *right*
Mis en forme : Police :Italique, Couleur de police : Rouge
Supprimé: ¶
Supprimé: 6
Mis en forme : Couleur de police : Rouge
Supprimé: (left)
Supprimé: 6
Mis en forme : Couleur de police : Rouge
Supprimé: , left
Mis en forme : Couleur de police : Rouge
Supprimé: a 1 mm displacement in the axial direction of the constraints
Mis en forme : Couleur de police : Rouge

fourth step the load q is increased until the flat arch collapses or it reaches the limit value of 1000 times the load value present at the end of the third step.

4.3 Numerical results of the FEA

Some preliminary analyses show that for a very low friction coefficient ($\mu = 0.1$) the FEA method is unable to find a final equilibrium configuration without the precompression action (the analyses stop during load step 3). For very high friction coefficients ($\mu = 2$), - which are unrealistic but comparable to Heyman's hypotheses (Heyman, 1966) - the analyses lead to an equilibrium situation. An iterative bisection procedure in the framework of numerical analysis was employed to search for the minimum μ value capable of guaranteeing an equilibrium situation at the end of load step 3. This analysis shows that equilibrium at the end of load step 3 can be guaranteed starting from a value of $\mu = 0.4389$ while removing all the precompression action.

Figure 9b shows the deformed configuration at the beginning of load step 4 when all the precompression action has been removed. The flat arch finds an equilibrium configuration thanks to the sliding of the voussoirs which generates a stabilizing compression action along the sliding surfaces. The results thus obtained are in excellent agreement with the outcome of the analytical procedure described in Section 3.2, both in terms of the value of the limit friction coefficient and of kinematics.

Figure 10 shows the contour plot of the contact normal stresses that are exchanged along the separating surfaces of the voussoirs. Qualitatively, the state of equilibrium is characterized by a thrust line which is higher in the central area of the flat arch (Figure 10 on the left) while lowers towards the support points (Figure 10 on the right).

To obtain a more quantitative result, the reactions occurring at the section where the symmetry constraints are imposed were integrated (region A in Figure 9a). This operation provided a mid-span thrust value of 5.103 kN positioned 349 mm from the lower end of the flat arch (which approximately corresponds to the upper limit point of the central inertia core of the section, 337 mm). This value of the horizontal thrust is, again, in excellent agreement with the value of $f_3^{sl-} = f_2^{sl-}$ obtained via the analytical approach (Section 3.2) for $\mu = 0.4389$, see Fig. 6c. As regards the eccentricity of the thrust with respect to the center of gravity

Mis en forme : Couleur de police : Rouge
Mis en forme : Couleur de police : Rouge
Mis en forme : Couleur de police : Rouge
Mis en forme : Couleur de police : Rouge
Mis en forme : Couleur de police : Rouge
Supprimé:
Mis en forme : Couleur de police : Rouge, Non Surlignage
Mis en forme : Couleur de police : Rouge
Mis en forme : Couleur de police : Rouge, Non Surlignage
Mis en forme : Couleur de police : Rouge
Mis en forme : Couleur de police : Rouge, Non Surlignage
Mis en forme : Couleur de police : Rouge
Mis en forme : Couleur de police : Rouge, Non Surlignage
Mis en forme : Couleur de police : Rouge
Supprimé: We then proceeded, through an iterative bisection procedure in the framework of numerical analysis, to search for the minimum μ value capable of guaranteeing an equilibrium situation at the end of load step 3. This analysis shows that starting from a value of $\mu = 0.4389$ it is possible to remove all the precompression action, guaranteeing equilibrium at the end of load step 3. ¶
Mis en forme : Couleur de police : Rouge
Mis en forme : Couleur de police : Rouge
Supprimé: 6
Mis en forme : Couleur de police : Rouge
Supprimé: (right)
Supprimé: 7
Mis en forme : Couleur de police : Rouge
Supprimé: 7
Mis en forme : Surlignage
Supprimé: 7
Mis en forme : Couleur de police : Rouge
Supprimé: 6
Mis en forme : Couleur de police : Rouge
Supprimé: , left
Supprimé: 4c
Mis en forme : Couleur de police : Rouge

of the central section, the analytical approach provides a range of values ($-261\text{mm} \leq e_0 \leq 119$ mm), including that identified by the FEA ($e_0 = -96.5$ mm). This confirms that the collapse condition is governed by the translational equilibrium.

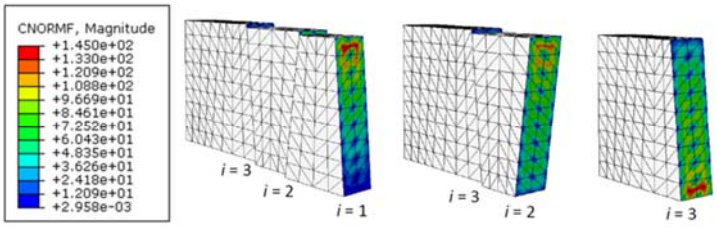
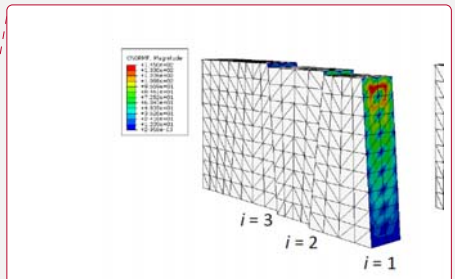


Figure 10. Contour plot of contact force values (CNORMF variable).

Figure 11 shows the vertical displacement of the upper part of the flat arch in its final equilibrium configuration. To show the influence of the friction coefficient on the final equilibrium position, several analyses are carried out with the four different friction coefficients shown in the figure. It can be observed that, as the friction coefficient decreases from the value 1 to 0.4389 (the minimum value required to ensure equilibrium under dead load), the vertical displacement of the flat arch increases. This displacement appears to be almost entirely caused by sliding at joints $j = 2$ and $j = 3$, while the central part remains essentially a macroblock (similarly to the situation plotted in Figure 9b), in good agreement with the graph in Fig. 8a. The loss of stiffness (defined as the ratio between the weight of the flat arch and the final displacement in the equilibrium position) is significantly influenced by the value of the friction coefficient. Taking as a reference the stiffness of the structure with a friction coefficient $\mu = 1$, the flat arch with $\mu = 0.4389$ seems to be 78% less stiff.



Supprimé:

Supprimé: 7

Mis en forme : Couleur de police : Rouge

Mis en forme : Couleur de police : Rouge, Anglais (Royaume-Uni)

Mis en forme : Couleur de police : Rouge

Mis en forme : Couleur de police : Rouge, Anglais (Royaume-Uni)

Mis en forme : Couleur de police : Rouge, Anglais (Royaume-Uni)

Mis en forme : Police :Italique

Mis en forme : Police :Italique

Mis en forme : Couleur de police : Rouge, Anglais (Royaume-Uni)

Mis en forme : Couleur de police : Rouge, Anglais (Royaume-Uni)

Mis en forme : Couleur de police : Rouge, Anglais (Royaume-Uni)

Mis en forme : Couleur de police : Rouge, Anglais (Royaume-Uni)

Mis en forme : Couleur de police : Rouge, Anglais (Royaume-Uni)

Mis en forme : Couleur de police : Rouge

Mis en forme : Couleur de police : Rouge, Anglais (Royaume-Uni)

Mis en forme : Couleur de police : Rouge, Anglais (Royaume-Uni)

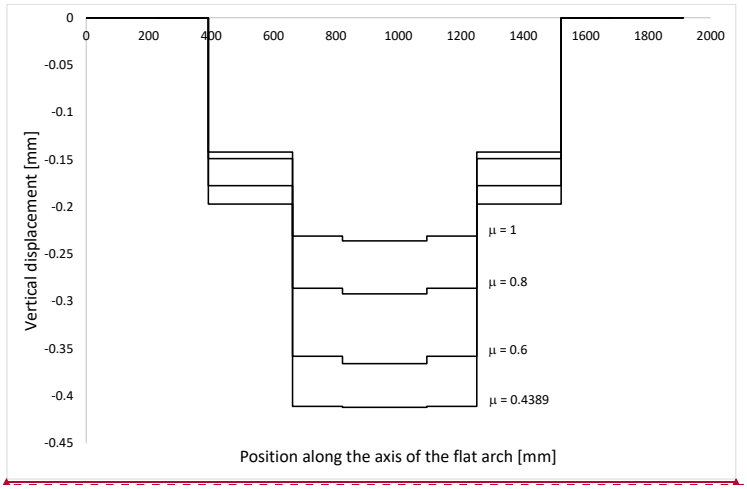


Figure 11. Influence of the friction coefficient on the vertical displacement.

In Figure 12, four equilibrium configurations are shown, depending on the load. 1 is the undeformed configuration. 2 is the equilibrium configuration with a distributed load equal to 0.026 MPa (reference load). 3 is an equilibrium configuration obtained in load step 4 with a load higher than the reference load. 4 is the equilibrium configuration of incipient collapse.

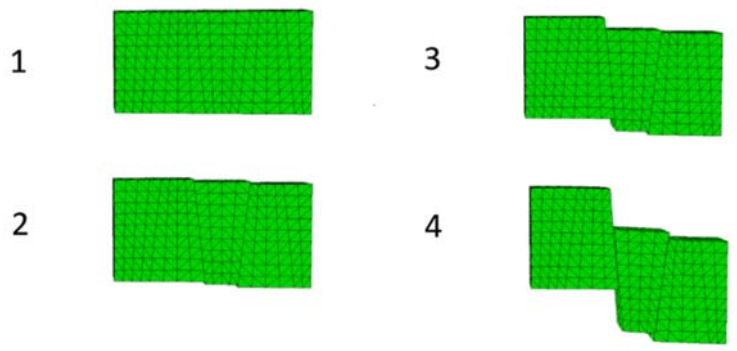


Figure 12. Equilibrium configurations depending on the load (1-3). Collapse mechanism that occurs during load step 4 for a load higher than the reference load (4).

Mis en forme : Police :10 pt
Mis en forme : Centré
Mis en forme : Police :10 pt, Couleur de police : Rouge, Anglais (Royaume-Uni)
Mis en forme : Police :10 pt
Mis en forme : Police :10 pt, Couleur de police : Rouge, Anglais (Royaume-Uni)
Supprimé: ¶
Supprimé: 8
Mis en forme : Couleur de police : Rouge
Supprimé: 8
Mis en forme : Couleur de police : Rouge

5. A multi-objective optimization procedure based on the static method: mathematical formulation of the equilibrium conditions

As mentioned in the Introduction, advances in computational capabilities, have led to the development of various approaches to address equilibrium conditions of blocky structures (Baggio and Trovalusci, 2000; Orduña and Lourenço, 2005; Portioli et al., 2014) through mathematical programming. The results presented here aim to clarify the meaning of limit solutions obtained by means of the lower bound approach for the flat arch with non-conventional voussoirs. A multi-objective optimization procedure is adopted to find the minimum friction coefficient compatible with the equilibrium of the flat arch. As will be clarified below, the non-standard behaviour of the system strongly affects the limit analysis of such type of structure, showing that static methods must be used with caution when assessing the stability of unconventional block structures.

To visualize the interaction between the values of the friction coefficient and internal forces, a verification is conducted limited to the equilibrium conditions. Following the original proposal by Livesley (1978), the method imposes the equilibrium of each block against translations and rotation, and the related equations, expressed in matrix formulation, are then composed for the whole structure as: $[A][X] = [B]$, where $[A]$ is the coefficient matrix of the vector of unknown internal force components $[X]$, and $[B]$ is the vector of external forces. Due to the indeterminacy of the problem, the matrix $[A]$ is vertically rectangular. This, along with the linearity of the equations, categorizes the problem as a linear programming or linear optimization problem.

The contact surface can be modelled either with a convex model, in which all forces and moments are assumed concentrated at the centre of convexity of the contact surface, or in a non-convex formulation, where they spread across the contact interface (Livesley, 1992). The latter approach is followed here due to its more straightforward implementation when limit strengths are assumed. With reference to Figure 12a, being the problem 2*D*, three forces are sufficient to describe each contact interface (joint *i*). Two normal forces, $f^{+}_{n(i)}$ and $f^{-}_{n(i)}$, account for non-uniform axial stress distribution and related bending/crushing failure, whereas a tangential force $f_{t(i)}$ accounts for possible deviations of the thrust line from normal to the contact

Supprimé: ¶
¶
5. A multi-objective optimization procedure based on the static method: mathematical formulation of the equilibrium conditions

Mis en forme : Couleur de police : Rouge, Non Surlignage

Mis en forme : Couleur de police : Rouge

Mis en forme : Couleur de police : Rouge, Non Surlignage

interface and allows for consideration of potential sliding failure. The external actions Y_j applied at any j-th blocks are the self-weight and the weight of an upper wall of height 1 m, as done in Section 3.2 and in Section 4, see Fig. 12, where $Y_1 = W_1 + Q_1$; $Y_2 = W_2 + Q_2 - (W_1 + Q_1)$; $Y_3 = W_3 + Q_3 - (W_2 + Q_2)$. Considering half a structure due to symmetry, the resulting matrix $[A]$ is a [9,11] matrix. The problem is formulated as a multi-objective optimization aimed at minimizing the friction coefficient μ:

Objective Function:

Minimize μ

$$\text{subject to} \begin{cases} [A][X] = [B] \\ |f_{t(i)}| \le \left(f^{+}_{n(i)} + f^{-}_{n(i)}\right) \cdot \mu \\ 0 \le f^{-}_{n(i)}, f^{+}_{n(i)} \\ -\frac{s}{2} + \frac{f_{n(i)}}{2 \cdot \sigma_c \cdot t} \le d_i \le \frac{s}{2} - \frac{f_{n(i)}}{2 \cdot \sigma_c \cdot t} \end{cases} \quad (8)$$

where $d_i = \frac{\left(f^{+}_{n(i)} - f^{-}_{n(i)}\right) \cdot s}{2 f_{n(i)}}$ is the moment arm of the resultant compression force $f_{n(i)} = \left(f^{+}_{n(i)} + f^{-}_{n(i)}\right)$ at interface i (see Fig. 5 and Fig. 12). In accordance with the settings described in Section 2, $[B]$ is null except for the vertical contribution to external forces Y_j.

The second constraint represents the friction model according to Coulomb's law. The third one imposes null tensile strength (assuming compression positive, according to the notation in Figure 12), the latter one imposes a finite compressive strength σ_c = 45 MPa, accounting for the bending moment and a rectangular stress block, with $t \times s$ representing the cross-section of the blocks (Fig. 5). The formulation has been implemented in Visual Studio using the Gurobi Optimizer solver.

The solver converges to a solution for an extremely low value of friction coefficient μ = 0.110. This value is slightly larger than $\tan(\alpha)$, where α is the angle of the joints separating the blocks to the vertical. The resultant forces, expressed in kN and approximated to the integer, are visualized in Figure 12b. Plotting the thrust line associated with the found components of internal forces, Figure 12c, reveals that the three central blocks tend to act as an arch resting on the free blocks at the end. This configuration is deemed stable assuming that an uplifting tangential force $f_{t(2)} = f_{n(2)} \cdot \tan(\mu)$, with $\mu \to \tan(\alpha)$, can be developed. Such

Mis en forme ... [138]
Mis en forme ... [139]
Mis en forme : Non Surlignage
Mis en forme ... [140]
Mis en forme : Non Surlignage
Mis en forme : Non Surlignage
Mis en forme ... [141]
Mis en forme ... [142]
Mis en forme ... [143]
Mis en forme : Non Surlignage
Mis en forme ... [144]
Mis en forme ... [145]
Mis en forme : Non Surlignage
Mis en forme : Non Surlignage
Mis en forme ... [146]
Mis en forme ... [147]

a force $f_{i(2)}$ could only be obtained if the central blocks were pre-compressed by the free end blocks. Note that for this low value of the friction coefficient, $\mu = 0.110$, the value of the horizontal thrust, provided by $f_{n(i)}^{+} + f_{n(i)}^{-}$, is considerably greater compared to the value of $f_2^{sl-} = f_3^{sl-}$ obtained in Section 3.2 for $\mu =$ 0.4389.

It is worth observing that, when the friction angle tends to the inclination of the joints, i.e., $\mu \to \tan(\alpha)$, the horizontal thrust diverges, and equilibrium is not possible, as already observed in Section 3.1 with reference to the peculiar inclination of joint $i = 2$: as noted, equilibrium conditions are possible only if $\psi > \alpha$.

Therefore, not accounting for the kinematic aspects corresponding to the equilibrium solutions, the procedure overestimates the safety level, by determining the minimum friction coefficient compatible with the possibility of equilibrium under the assumption that a precompression force is present. Thus, a purely static procedure cannot identify the limit value of the friction coefficient when such a precompression force is absent (or is removed), as is the case of $\mu = 0.4389$ (see Sect. 3.2 and Sect. 4).

The results obtained by means of the lower bound approach just described can be read in light of the in-depth discussion by Ting-Chun Kao (2022) on the issues arising when a pure equilibrium approach is adopted: such an approach can provide prestressing forces while maintaining the static admissibility of the equilibrium formulation.

Mis en forme : Non Surlignage
Mis en forme : Non Surlignage
Mis en forme : Non Surlignage
Mis en forme : Anglais (Royaume-Uni)
Mis en forme : Non Surlignage
Mis en forme : Non Surlignage
Mis en forme : Couleur de police : Rouge
Mis en forme : Non Surlignage

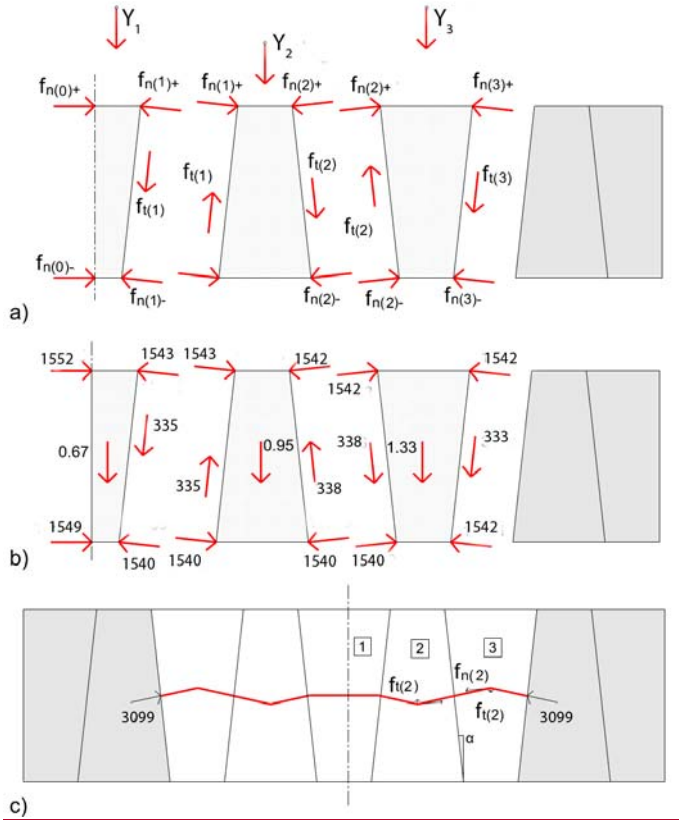


Figure 12. The blocks and notations used in the mathematical programming problem, imposing equilibrium (*a*) and resulting forces, expressed in kN (*b*). The corresponding thrust line (*c*).

Finally, it is remarked that both the Durand-Claye method and the optimization problem described here are based on the static theorem of limit analysis, without considerations of the flow rule. This is the reason why there is a large difference between the value of the friction coefficient just obtained (μ = 0.110) and that derived by the integrated approach presented in Section 3.2 by assuming a non-associated flow rule (μ = 0.4389). Static methods, if not complemented by kinematic analyses, as those performed in Section 3.2,

Mis en forme : Non Surlignage

provide an unsafe value of the limit friction coefficient. Further insights into the assumptions on dilatancy with reference to the unconventional joints will be the subject of future research.

6. A NSCD formulation accounting for mild associative friction

To gain a clear understanding of the equilibrium problem, notable cases identified in Section 3.2 are illustrated using a NSCD masonry formulation within the ChronoEngine simulation platform. The model requires inputs such as boundary conditions, geometry, material density, friction coefficients, and cohesion. Characteristic of Discrete Element Modeling (DEM), it visualizes the mechanical interactions among numerous blocks in complex geometrical arrangements. The NSCD approach assumes infinite compression strength, and the contact forces are regulated by set-valued force laws that accept discontinuities in speeds typical of hard contacts. As verified already in Section 3, the influence of the limited value of the compressive strength on the collapse response of the flat arch is not evident, therefore the infinite compressive strength can be assumed.

The formulation is particularly relevant as it can replicate the mild associative nature of contacts observed in experimental tests (Casapulla and Portioli, 2015; van Zijl, 2004) as demonstrated in (Beatini et al., 2018) by reproducing the classic scenario of potentially sliding blocks noted in Drucker (Drucker, 1954). Specifically, an associative friction model is assumed at the time-step level, but a regularization procedure prevents further dilatation, resulting in a non-associative outcome over time. As detailed by Beatini et al. (2017), this is expressed as a Differential Variational Inequality, which leads to a time-stepping numerical scheme that computes associative contact forces while ensuring unique velocities by solving multiple Cone Complementarity Problems. The ratio between the time-step and the friction coefficient is crucial in transitioning between an associative and a non-associative friction model, with a maximum dilatation of the order of $\mu \Delta t v^T$, where v^T is the tangential velocity, μ is the friction coefficient, and Δt is the time step. Increasing the time step highlights a more non-associative friction model. In the context of this research, the approach seeks the most realistic or "stable" frictional failure, less susceptible to slight variations in the friction coefficient.

Mis en forme : Police :Anglais (Royaume-Uni)

Mis en forme : Normal, Interligne : simple

Supprimé: As mentioned in the Introduction, advances in computational capabilities, have led to the development of various approaches to address equilibrium conditions of blocky structures (Baggio and Trovalusci, 2000; Orduña and Lourenço, 2005; Portioli et al., 2014) through mathematical programming. ¶
The results presented here aim to clarify the meaning of limit solutions obtained by means of the lower bound approach for the flat arch with non-conventional voussoirs. A multi-objective optimization procedure is adopted to find the minimum friction coefficient compatible with the equilibrium of the flat arch. As will be clarified below, the non-standard behaviour of the system strongly affects the limit analysis of such type of structure, showing that static methods must be used with caution when assessing the stability of unconventional block structures.¶
To visualize the interaction between the values of the friction coefficient and internal forces, a verification is conducted limited to the equilibrium conditions. Following the original proposal by Livesley (1978), the method imposes the equilibrium of each block against translations and rotation, and the related equations, expressed in matrix formulation, are then composed for the whole structure as: $[A][X] = [B]$, where $[A]$ is the coefficient matrix of the vector of unknown internal force components $[X]$, and $[B]$ is the vector c ... [148]

Mis en forme ... [149]

Mis en forme ... [150]

Supprimé: ~~Rigid body dynamics analysis~~

Mis en forme ... [151]

Mis en forme ... [152]

Mis en forme : Couleur de police : Rouge

Mis en forme : Couleur de police : Rouge

Mis en forme ... [153]

Mis en forme ... [154]

Mis en forme ... [155]

Mis en forme : Surlignage

Mis en forme ... [156]

Mis en forme ... [157]

Mis en forme ... [158]

Mis en forme : Couleur de police : Rouge

Supprimé: Non-Smooth Contact Dynamics (…SCD ... [159]

Mis en forme : Non Surlignage

Supprimé: As discussed in Section 3 about FEM analysis, also in this case the influence of the limited value of ... [160]

Mis en forme ... [161]

Supprimé: and G

Mis en forme : Couleur de police : Rouge

Supprimé: ~~, where the velocity vector tends to point away from the direction of dilatancy or shear displacement~~

Mis en forme ... [162]

The replicated models maintain the same geometry, density, and boundary conditions as those in Section 2, with the end couple of blocks on both sides fixed, and the centroids of the blocks subjected to self-weight and the equivalent of a uniformly distributed load due to 1 meter of wall resting on the flat arch. The compliance, representing an elastic connection between the blocks, is set at C = 5e-9 m^2/N. This not extremely low value accounts for the low compression state of the blocks and has been calibrated based on an inversely placed wedged block (like the keystone of the flat arch under consideration), resting between two rigid supports, under time step Δt = 0.001 s and having friction coefficient μ = 0.44, which completely detaches from the supports within 2.5 seconds. Varying the compliance by one order of magnitude (to values of 5e-10 and 5e-8) slightly affected the failure time but not the failure mode and conditions.

Figure 14 (left) displays snapshots from three cases, friction coefficients μ = 0.5 - case (*a*) -, μ = 0.44 - case (*b*) -, and finally μ = 0.4 - case (*c*) -, depicted at a simulation time T = 3 seconds and assuming a timestep of Δt = 0.001 s.

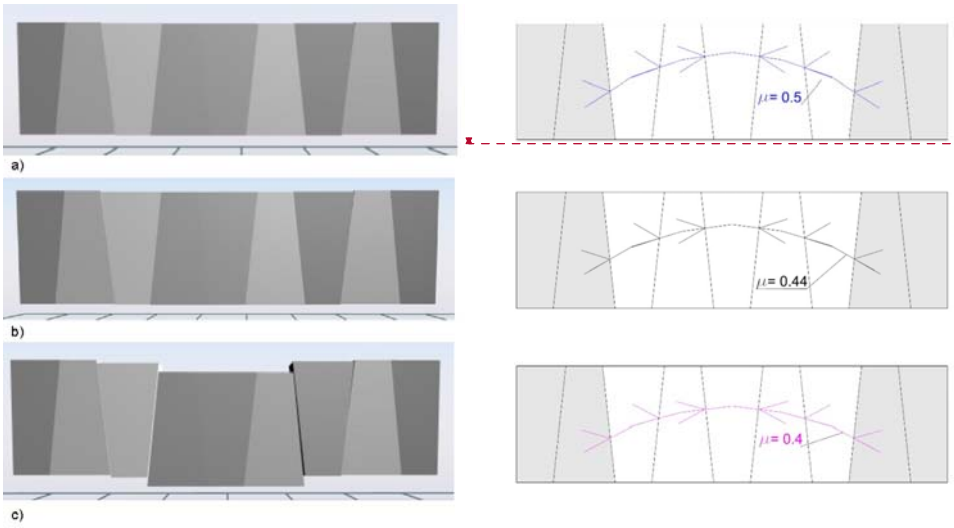


Figure 14. Snapshots from the NSCD simulation at T = 3 s, for Δt = 0.001 s (left); thrust lines obtained from postprocessing the results from the NSCD simulation at T = 0.5 s, for Δt =0.001 s (right). The cases of μ = 0.5 (*a*), μ = 0.44 (*b*) and μ = 0.4 (*c*).

Figure 14 (right) compares the thrust lines obtained from post processing the resultant force of the contact interfaces for the same cases: friction coefficients μ = 0.5 - in blue, case (*a*), μ = 0.44 - in black, case (*b*) -,

Supprimé: 10

Mis en forme : Couleur de police : Rouge

Supprimé: Figure 10 (right) compares the thrust lines obtained from post processing the resultant force of the contact interfaces for the same cases: friction coefficients μ = 0.5 - in blue, case (*a*), μ = 0.44 - in black, case (*b*) -, and finally μ = 0.4 - in purple, case (*c*), plotted alongside their respective friction cones. All friction coefficients led to some displacement, but, notably, the case with μ = 0.4 results in failure. For clarity in presentation, it is important to note that failure mechanisms progress very rapidly. Although the simulations were extended to T = 10 seconds to confirm the observations, the critical behaviours - such as the complete detachment of all blocks - are apparent already for T = 4. No further displacement is observed for $\mu \geq 0.44$. ¶
¶
¶
¶

Mis en forme : Couleur de police : Rouge

Supprimé: ¶

Supprimé: F

Supprimé: 10

Mis en forme : Couleur de police : Rouge

Mis en forme : Espace Après : 0 pt

Mis en forme : Couleur de police : Rouge

Supprimé: .

Supprimé: ¶

and finally μ = 0.4 - in purple, case (*c*), plotted alongside their respective friction cones. All friction coefficients led to some displacement, but, notably, the case with μ = 0.4 results in failure. For clarity in presentation, it is important to note that failure mechanisms progress very rapidly. Although the simulations were extended to T = 10 seconds to confirm the observations, the critical behaviours - such as the complete detachment of all blocks - are apparent already for T = 4. No further displacement is observed for $\mu \geq 0.44$.

From the simulations, it can be deduced that the displacement of the outside blocks, allowing the activation of compression and such frictional contact forces, has a stabilizing effect, provided the friction coefficient is enough. This result is in agreement with the analyses performed in Section 3 and Section 4.

The observation can be more clearly highlighted considering again the case of friction coefficient μ = 0.44, all other parameters being unchanged, but fixing the originally free end blocks (Figure 14). Without sliding, which in the previous cases was possible at the original interface j = 3, now fixed, the central blocks move vertically, with a detachment from the adjacent voussoirs.

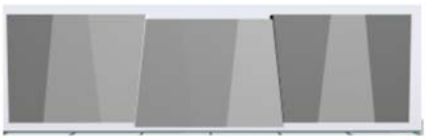


Figure 15. Results from the NSCD simulation at T = 0.5 s, for μ = 0.44 and timestep Δt = 0.001 s, assuming only the three central blocks free to move: snapshot at T = 2 s.

7. Concluding remarks

This contribution provides insights on some sensitive aspects regarding the stability of masonry structures, i.e., the effects of both a non-conventional shape of the voussoirs and a limited friction coefficient on the collapse behaviour. The analysis is developed by considering an interesting case study, an atypical flat arch inspired by the front layer of the flat arch above the transept portal in Prato Cathedral.

For studying the collapse response of the structure, methods from the literature were adopted, which account for both the limited friction coefficient and the unconventional stereotomy of the blocks. Their application to the interesting flat arch, however, was not straightforward and required the extension and modification

Supprimé: 11
Mis en forme : Couleur de police : Rouge
Mis en forme : Couleur de police : Rouge
Supprimé: ~~j+2~~
Mis en forme : Police :Italique, Couleur de police : Rouge
Mis en forme : Couleur de police : Rouge, Barré
Mis en forme : Couleur de police : Rouge, Barré, Surlignage
Supprimé: 11
Mis en forme : Couleur de police : Rouge
Mis en forme : Couleur de police : Rouge
Supprimé: ¶
Mis en forme : Non Surlignage

of such existing procedures. This led not only to a comparison between different approaches, but also to the implementation of appositely developed techniques.

The stability of such a structure is examined at first by an unprecedented semi-analytical integrated approach involving both static and kinematic investigations. The statically admissible solutions are determined through a modern re-visitation of the stability area method originally proposed by Alfred Durand-Claye (1867; 1868). It is assumed that the collapse occurs due to the reaching of a limit condition at the interfaces between the blocks, considering a finite friction coefficient. Furthermore, the model is able to take into account the influence of a limited value of the compressive strength on the structural response, which is not apparent in the current case study.

The possibility of the occurring of a purely sliding mechanism is then analysed by exploiting the virtual work principle, capable of considering the frictional dissipation at the interfaces. The collapse condition is identified as the one that separates equilibrium from initial motion.

This non-standard investigation allows the recognition of potential collapse conditions included in the domain of statically admissible solutions. The limit value of the friction coefficient compatible with an equilibrium condition is thus determined and depends on the value of the compression force guaranteed by the end constraint.

The results obtained by means of the analytical approach are confirmed by the numerical analysis carried out employing the ABAQUS/CAE code. In this case, although the hypotheses on the masonry material are different (isotropic material in the linear elastic range), the voussoirs are modelled independently, and a contact interaction is used to assemble them. Sliding is allowed to occur in the tangential direction by taking into account a frictional contact. Geometric nonlinearity is employed in the analyses to update the nodes' coordinates at each step and simulate variations in the constraints as well as in the precompression force throughout the loading history. The FEA identifies the limit condition as that corresponding to the minimum friction coefficient compatible with the equilibrium of the flat arch removing such pre-compression force. Under such a limit value of the friction coefficient, only the presence of a pre-compression action, provided for example by iron tie-rods within masonry or interlocking voussoirs, could prevent sliding or detachment

Mis en forme : Couleur de police : Rouge

Supprimé: inedited

Mis en forme : Couleur de police : Rouge

Mis en forme : Couleur de police : Rouge

Supprimé: value for the

Mis en forme : Couleur de police : Rouge

Mis en forme : Couleur de police : Rouge

between the blocks. The results obtained by means of the numerical analyses are in excellent agreement with those derived from the non-standard analytical procedure.

In order to better understand the collapse behaviour of the unconventional flat arch, a comparison with the results obtained by means of a lower bound approach is then proposed. To determine the lowest friction coefficient consistent with the flat arch's equilibrium, a multi-objective optimization process is used, by assuming rigid blocks with unilateral constraints, finite friction, and a non-convex formulation for the interfaces (Livesley, 1992). The investigation shows that, due to the non-standard plastic behaviour of the system and the unconventional geometry, the limit analysis conducted by a purely static method may provide unsafe results; indeed, it identifies the lowest friction coefficient compatible with the possibility of equilibrium assuming that a precompression force is applied, without considering if such a force is guaranteed by the unilateral constraints. This result clearly shows the need for caution when assessing the stability of non-conventional blocky structures using static methods.

Finally, a dynamic analysis is conducted by means of the NSCD method, i.e., a discrete element method which shares the assumption of unilateral contacts and normal material. This approach does not require detailed material information (stiff blocks are assumed), but its masonry dedicated formulation is able to track in great details the displacement of the blocks. The contact interfaces are automatically detected (or can be pre-defined) imposing a little perturbation to the mechanical system. While it is the user that shall critically evaluate the kind of failure mode, depicting the failure propagation allows to better consider possible mitigation strategies. In agreement with the non-standard analyses and with the FEA, the simulations show that the displacement of the outer blocks has a stabilizing effect, since the frictional end constraint activate compression.

This research has contributed to develop a critical comparison between different procedures aimed at assessing the collapse behaviour of an atypical flat arch. As derived from the non-standard approach here proposed and from the FEA, not only the limited friction coefficient, but also the unconventional shape of the voussoirs raises stability issues. The collapse mechanisms are re-interpreted and visualized by means

Mis en forme : Couleur de police : Rouge

Supprimé: actually

Supprimé: conventionsl

of the NSCD method, while a purely static method overestimates the safety level unless a pre-compression action is guaranteed.

Insights on the role of dilatancy in the structural response of the flat arch will be the object of further research.

A final remark. Although the modelled unconventional flat arch does not exist, the analyses proposed here can be of crucial importance not only to understand the collapse behaviour of this specific theoretical case study, but also to reflect on the concept of conventional and unconventional voussoirs with reference to other typologies, even masonry arches and domes with ordinary voussoirs. In conventional voussoir structures, conceived as block systems with unilateral constraints at the interfaces, the inclination of the joints ensures that the wedge-shaped voussoirs are held together by compression when gravity loads are considered. Furthermore, when an infinite value of friction is assumed, their collapse behaviour under both gravity and seismic loads can be adequately modelled by classical limit analysis, adopting Heyman's assumptions. However, as is well known, non-standard behaviour may occur in the case of non-associative friction. Furthermore, while for vertical loads the joints are activated as unilateral non-smooth constraints, ensuring compression, seismic loads could lead to situations similar to those foreseen for the unconventional flat arch, involving mutual sliding or detachment between the blocks, since the definition of the concept of conventional or unconventional voussoir depends both on its shape and on the loading conditions. This demonstrates that the critical perspective adopted here for the study of the flat arch can be fundamental for evaluating the collapse response of structures subjected to seismic loads, in order to choose the appropriate limit analysis strategies. This aspect will also be explored further.

Supprimé: Moreover, it is remarked that the critical perspective here adopted can be transferred to the analysis of different case studies, even masonry arches and domes with ordinary voussoirs when such structures are subjected to seismic loads, since the definition of the concept of ordinary or unconventional voussoir depends both on its shape and the loading conditions.

Acknowledgements

The authors express their gratitude to Arch. Francesco Risaliti and to *Piacenti S.p.a. - Centro Restauri - conservazione di beni di interesse storico artistico*, which carried out the restoration of the facades of the Prato Cathedral, for having provided us with the geometric survey as well as photographic material of the flat arch that crowns the transept portal.

Mis en forme : Justifié, Espace Après : 0 pt, Interligne : Double

Supprimé: ¶
¶
Saut de page

References

Aita D, Barsotti R, Bennati S. (2019) Looking at the collapse modes of circular and pointed masonry arches through the lens of Durand-Claye's stability area method. Archive of Applied Mechanics. 89: 1537–1554.

Aita D., Sinopoli A. (2020) Revisiting Monasterio's unpublished manuscript: a critical review of the collapse modes analysis of non-symmetric and symmetric masonry arches. International Journal of Architectural Heritage. 14(5):762–793 (2020), https://doi.org/10.1080/15583058.2019.1648586.

Aita D, Beatini V, Garavaglia E, Paris V, Pizzigoni A, Sgambi L. (2023a) The stone roof of the tholos of Athena Pronaia in Delphi. Structural hyphoteses starting from fragments of marble tiles. The International Archives of the Photogrammetry, Remote Sensing and Spatial Information Sciences. 48:59–66

Aita D., Beatini V., Garavaglia E., Paris V., Pizzigoni A., Sgambi L. (2024a) The Roofing System of the Tholos of Athena Pronaia in Delphi: Archaeological Hypotheses and Structural Suggestions. International Journal of Architectural Heritage. DOI: 10.1080/15583058.2024.2316289

Aita D., Milani G., Taliercio A. (2023) Limit analysis of masonry domes with oculus and lantern: A comparison between different approaches. Mathematics and Mechanics of Solids. doi: 10.1177/10812865231205814

Aita D., Bruggi M., Garavaglia E. (2024) Collapse analysis of masonry arches and domes considering finite friction and uncertainties in compressive strength. Engineering Failure Analysis.163(A): 108462. https://doi.org/10.1016/j.engfailanal.2024.108462.

Code de champ modifié

Mis en forme : Couleur de police : Rouge

Mis en forme : Couleur de police : Rouge

Code de champ modifié

Mis en forme : Italien (Italie)

Mis en forme : Italien (Italie)

Mis en forme : Italien (Italie)

Andreaus U. and Augusti G. (1991) Meccanica delle colonne e delle costruzioni a blocchi lapidei: stato e prospettive degli studi. PACT 32(7): 67–126

Angelillo M., Fortunato A., Montanino A., Lippiello M. (2014) Singular stress fields in masonry structures: Derand was right. Meccanica 49(5):1243–1262

Baggio C., Trovalusci P. (1998) Limit analysis for no-tension and frictional three-dimensional discrete systems. Mechanics of Structures and Machines. 26:287–304.

Baggio C., Trovalusci P. (2000) Collapse behaviour of three-dimensional brick-block systems using non-linear programming. Structural Engineering and Mechanics. 10(2):181–195.

Bagi K. (2014) When Heyman's Safe Theorem of rigid block systems fails: Non-Heymanian collapse modes of masonry structures. International Journal of Solids and Structures. 51(14):2696–2705. https://doi.org/10.1016/j.ijsolstr.2014.03.041

Beatini V., Royer Carfagni G., Tasora A. (2018) Modeling the shear failure of segmental arches. Int. J. Solids Struct. 158. https://doi.org/10.1016/j.ijsolstr.2018.08.023

Beatini V., Royer Carfagni G., Tasora A. (2017) A regularized non-smooth contact dynamics approach for architectural masonry structures. Comput. Struct. 187, 88–100. https://doi.org/10.1016/j.compstruc.2017.02.002

Beatini, V., Royer-Carfagni, G., & Tasora, A. (2019) A non-smooth-contact-dynamics analysis of Brunelleschi's cupola: An octagonal vault or a circular dome?. Meccanica, 54, 525-547.

Mis en forme : Couleur de police : Rouge
Mis en forme : Police :Non Italique, Couleur de police : Rouge
Mis en forme : Couleur de police : Rouge
Mis en forme : Police :Non Gras, Couleur de police : Rouge, Anglais (Royaume-Uni)
Mis en forme : Couleur de police : Rouge, Anglais (Royaume-Uni)
Mis en forme : Couleur de police : Rouge
Mis en forme : Couleur de police : Rouge, Anglais (Royaume-Uni)
Mis en forme : Couleur de police : Rouge
Code de champ modifié
Supprimé: ,
Supprimé: ,
Supprimé: ,
Code de champ modifié
Supprimé: ,
Supprimé: ,
Supprimé: ,
Code de champ modifié
Supprimé: ,
Supprimé: ,
Supprimé: ,

Block P., Lachauer L. (2014) Three-dimensional funicular analysis of masonry vaults. Mech. Res. Commun. 56:53–60

Casapulla C. (1999) Problematiche relative all'analisi limite di strutture murarie a blocchi in presenza di attrito. Ph.D. Thesis, Dept. of Costruzioni, Univ. of Firenze.

Casapulla C., Jossa P. (2001) A safety method in static analysis of block masonry. In Structural Analysis of Historical Constructions; Proc. III intern. seminar, Guimaraes, 7-9 November 2001.

Casapulla C., Lauro F. (2001) A simple computation tool for the limit-state analysis of masonry arches. In Proceedings of the 5th International Congress on Restoration of Architectural Firenze Heritage 2000, pp 2056–2064. Florence, Italy, 17–24 September 2000.

Casapulla C., Portioli F. (2015) Experimental and analytical investigation on the frictional contact behavior of 3D masonry block assemblages. Constr. Build. Mater. 78, 126–143. https://doi.org/10.1016/j.conbuildmat.2014.12.100

Clemente P., Occhiuzzi A., Raithel A. (1995) Limit Behavior of Stone Arch Bridges. Journal of Structural Engineering 121(7): 1045-1050.

Clemente P., Saitta F., Buffarini G., Ormando C. (2023) Masonry Arch Bridges with Finite Compression Strength Subject to Horizontal Longitudinal Seismic Actions, *Appl. Sci. 13*(13): 7509; https://doi.org/10.3390/app13137509

Supprimé: ,

Mis en forme : Couleur de police : Automatique

Mis en forme : Couleur de police : Rouge

Mis en forme : Police :(Par défaut) Times New Roman, 12 pt, Couleur de police : Rouge, Anglais

Mis en forme : Police :(Par défaut) Times New Roman, 12 pt, Couleur de police : Rouge

Mis en forme : Police :(Par défaut) Times New Roman, 12 pt, Couleur de police : Rouge, Anglais

Mis en forme : Police :(Par défaut) Times New Roman, 12 pt, Couleur de police : Rouge

Mis en forme : Police :(Par défaut) Times New Roman, 12 pt, Non Gras, Couleur de police : Rouge, Anglais (Royaume-Uni)

Mis en forme : Police :(Par défaut) Times New Roman, 12 pt, Non Gras, Couleur de police : Rouge, Anglais (Royaume-Uni)

Mis en forme : Bibliographie, Interligne : Double

Mis en forme : Police :Non Gras, Anglais

Mis en forme : Anglais (Royaume-Uni)

Cocchetti G., Rizzi E. (2020) Nonlinear programming numerical formulation to acquire limit self-standing conditions of circular masonry arches accounting for limited friction. Int. J. Masonry Res. Innov. 5(4):569–617.

Como M. (2016) *Statics of Historic Masonry Constructions*. Springer Series in Solid and Structural Mechanics, vol 5. Cham: Springer.

Coulomb C.A. (1776) Essai sur une application des règles de maximis et minimis à quelques problèmes de statique, relatifs à l'architecture. *Mém Math Phys Acad Roy Sci par divers Savants. Paris*. 7: 343–382.

D'Ayala D., Tomasoni E. (2011) Three-dimensional analysis of masonry vaults using limit state analysis with finite friction. International Journal of Architectural Heritage 5(2):140-171.

D'Ayala D., Smars P. (2003). Architectural and Structural Modelling for the Conservation of Cathedrals. *Journal of Architectural Conservation*, 9(3): 51–72. https://doi.org/10.1080/13556207.2003.10785351

Drucker D.C. (1954) Coulomb Friction, Plasticity and Limit Load. J. of Applied Mechanics. 21(1):71-74.

Durand-Claye A. (1867) Note sur la vérification de la stabilité des voûtes en maçonnerie et sur l'emploi des courbes de pression. Annales des Ponts et Chaussées. 13: 63–93.

Durand-Claye A. (1868) Note sur la vérification de la stabilité des arcs métalliques et sur l'emploi des courbes de pression. Annales des Ponts et Chaussées. 15: 109–144.

Mis en forme : Couleur de police : Rouge

Mis en forme : Couleur de police : Rouge

Mis en forme : Bibliographie, Interligne : Double, Espacement automatique entre les caractères asiatiques et latins, Espacement automatique entre les caractères asiatiques et les chiffres

Mis en forme : Couleur de police : Rouge

Mis en forme : Couleur de police : Rouge, Anglais (États-Unis)

Mis en forme : Couleur de police : Rouge, Anglais (Royaume-Uni)

Mis en forme : Bibliographie, Gauche, Retrait : Gauche : 0 cm, Première ligne : 0 cm, Interligne : Double

Supprimé: ¶

Mis en forme : Police :(Par défaut) +Corps (Calibri), 11 pt, Anglais (États-Unis)

Mis en forme : Police :(Par défaut) +Corps (Calibri), 11 pt

Mis en forme : Normal, Interligne : simple

Mis en forme : Couleur de police : Rouge

Mis en forme : Bibliographie, Gauche, Interligne : Double

Mis en forme : Couleur de police : Rouge

Mis en forme : Couleur de police : Rouge

Supprimé: ¶

Mis en forme : Police :(Par défaut) +Corps (Calibri), 11 pt

Fantin M. (2017) *Étude des rapports entre stéréotomie et résistance des voûtes clavées*, Art et histoire de l'art. Université Paris-Est, 2017. Français. NNT : 2017PESC1077. HAL Id: tel-01834617 https://theses.hal.science/tel-01834617

Fantin M., Ciblac T. (2016) Extension of thrust network analysis with joints consideration and new equilibrium states. *International Journal of Space Structures*. 31(2-4):190–202. doi:10.1177/0266351116661814

Ferris M.C, Tin-Loi F. (2001) Limit analysis of frictional block assemblies as a mathematical program with complementarity constraints. International Journal of Mechanical Sciences 43:209–224.

Gilbert M., Melbourne C. (1994) Rigid block analysis of masonry structures. The Structural Engineer. 72(21), 356–361.

Gilbert M., Casapulla C., Ahmed H.M. (2006) Limit analysis of masonry block structures with non-associative frictional joints using linear programming. Computer & Structures. 84:873–887.

Grillanda N., Chiozzi A., Milani G., Tralli A. (2019) Collapse behavior of masonry domes under seismic loads: An adaptive NURBS kinematic limit analysis approach. Engineering Structures. 200: 109517. https://doi.org/10.1016/j.engstruct.2019.109517

Heyman J. (1966) The stone skeleton. International Journal of Solids and Structures. 2(2): 249–279.

Heyman J. (1969) The safety of masonry arches. Int. J. Mech. Sci., Pergamon Press. 11:363–385.

Code de champ modifié

Supprimé: -

Code de champ modifié

Mis en forme : Couleur de police : Rouge

Mis en forme : Interligne : Double

Mis en forme : Police :Soulignement , Couleur de police : Rouge, Motif : Transparente (Blanc)

Supprimé: ¶

Mis en forme : Non souligné, Couleur de police :

Huerta Fernández S. (2012) Wedges and plate-bandes: mechanical theories after De la Hire. In *L'architrave, le plancher, la plate forme : Nouvelle histoire de la construction*, PPUR, p. 405–435.

Hua Y., Milani G. (2023) Simple modeling of reinforced masonry arches for associated and non-associated heterogeneous limit analysis, Computers & Structures, 280:106987 https://doi.org/10.1016/j.compstruc.2023.106987.

Kooharian A. (1952) Limit analysis of voussoirs (segmental) and concrete arches. J. Am. Concr. Inst. 24(4):317–328.

Lampariello, B. (2012) Le système de la plate-bande en Italie. In: Gargiani, R., *L'architrave, le plancher, la plate-forme. Nouvelle histoire de la construction*, Lausanne: PPUR, 101–109.

Livesley H.G. (1978) Limit analysis of structures formed from rigid blocks. International Journal of numerical methods in engineering. 12:1853–1871.

Lo Bianco M. and Mazzarella C. (1983) Limit load of masonry structures. In Final Report IABSE symp., Venezia, 187–194.

Lourenço P.B., Ramos L.F. (2004) Characterization of Cyclic Behavior of Dry Masonry Joints. *ASCE Journal of Structural Engineering*. 130(5):779–786.

Marmo F., Rosati L. (2017) Reformulation and extension of the thrust network analysis. Comput. Struct. 182:104–118.

Mis en forme : Italien (Italie)

Mis en forme : Italien (Italie)

Mis en forme : Couleur de police : Rouge

Mis en forme : Police :Non Italique, Couleur de police : Rouge

Mis en forme : Couleur de police : Rouge

Mis en forme : Couleur de police : Rouge, Anglais (Royaume-Uni)

Supprimé: ¶

Mis en forme : Couleur de police : Rouge, Anglais (Royaume-Uni)

Mis en forme : Couleur de police : Rouge

Mis en forme : Couleur de police : Rouge

Mis en forme : Couleur de police : Rouge

Mis en forme : Couleur de police : Rouge, Anglais (Royaume-Uni)

Mis en forme : Couleur de police : Rouge

Mis en forme : Police :(Par défaut) Times New Roman, 12 pt, Couleur de police : Rouge

Mis en forme : Normal, Retrait : Première ligne : 0 cm, Interligne : Double, Ne pas ajuster l'espace entre le texte latin et asiatique, Ne pas ajuster l'espace entre le texte et les nombres asiatiques

Mis en forme : Police :Times New Roman

Mis en forme : Police :(Par défaut) Times New Roman, 12 pt, Couleur de police : Rouge

Mis en forme : Police :12 pt, Couleur de police : Rouge

Supprimé: ¶

Milani G. (in press) Closed form solutions in Limit Analysis for masonry cloister vaults and domes subjected to concentrated vertical loads applied at the top crown. International Journal of Masonry Research and Innovation. doi: 10.1504/IJMRI.2023.10058815

Motro, R. (2009), An approach to structural morphology, in Motro, R. (Ed.), *An anthology of structural morphology*, World Scientific Publishing, Singapore, 15–32.

Mousavian, E., Bagi, K., Casapulla, C. (2022) Interlocking joint shape optimization for structurally informed design of block assemblages. Journal of Computational Design and Engineering 9, 1279–1297. https://doi.org/10.1093/jcde/qwac054

Orduña A., Lourenço P.B. (2005) Three-dimensional limit analysis of rigid blocks assemblages. Part I: Torsion failure on frictional interfaces and limit analysis formulation. Int. J. Solids Struct. 42, 5140–5160. https://doi.org/10.1016/j.ijsolstr.2005.02.010

Palmer A. C. (1966) A limit theorem for materials with non-associated flow laws. Journal de Mécanique. 5(2):217-222.

Pepe M., Pingaro M., Trovalusci P. (2021) Limit analysis approach for the in-plane collapse of masonry arches, Proceedings of the Institution of Civil Engineers - Engineering and Computational Mechanics, 174:2, 66-81.

Petracca M., Pelà L., Rossi R., Zaghi S., Camata G., Spacone E. (2017) Micro-scale continuous and discrete numerical models for nonlinear analysis of masonry shear walls. Construction and Building Materials, 149, 296-314. https://doi.org/10.1016/j.conbuildmat.2017.05.130

Mis en forme : Couleur de police : Rouge, Anglais (Royaume-Uni)
Mis en forme : Couleur de police : Rouge
Mis en forme : Couleur de police : Rouge, Anglais (Royaume-Uni)
Mis en forme : Couleur de police : Rouge
Mis en forme : Couleur de police : Rouge, Anglais (Royaume-Uni)
Mis en forme : Couleur de police : Rouge
Mis en forme : Couleur de police : Rouge, Anglais (Royaume-Uni)
Mis en forme : Couleur de police : Rouge
Mis en forme : Couleur de police : Rouge, Anglais (Royaume-Uni)
Mis en forme : Couleur de police : Rouge
Mis en forme : Police :(Par défaut) Times New Roman, 12 pt, Couleur de police : Rouge, Anglais
Mis en forme : Normal, Interligne : Double, Ne pas ajuster l'espace entre le texte latin et asiatique, Ne pas ajuster l'espace entre le texte et les nombres asiatiques
Mis en forme : Police :(Par défaut) Times New Roman, 12 pt, Couleur de police : Rouge
Mis en forme ... [163]
Mis en forme ... [164]
Mis en forme ... [165]
Supprimé: ¶ ... [166]
Mis en forme : Couleur de police : Rouge
Supprimé: ,
Supprimé: ,
Code de champ modifié
Supprimé: ¶
Mis en forme : Couleur de police : Rouge
Mis en forme : Espace Après : 0 pt
Mis en forme : Non Surlignage
Mis en forme ... [167]
Mis en forme ... [168]
Mis en forme ... [169]
Mis en forme ... [170]
Mis en forme ... [171]
Mis en forme ... [172]
Mis en forme ... [173]
Mis en forme ... [174]
Mis en forme : Couleur de police : Rouge
Mis en forme : Couleur de police : Rouge

Pizzigoni A, Beatini V, Paris V. (2022) The Stone Roof Marble Tholos Tiles in the Sanctuary of Athena Pronaia at Delphi. Stereotomy and compression resistant forms in the domed roof structures of ancient Greece. STRUCTURAL. 240(8):1–30.

Pizzigoni A, Beatini V, Beghini A, Paris, V, Cocchetti G, Ferrari R and Rizzi E. (2024) Fornix: the circular platform-frame. Proc. International Association for Shell and Spatial Structures (IASS). 1-10

Portioli F., Casapulla C., Gilbert M., Cascini L. (2014) Limit analysis of 3D masonry block structures with non-associative frictional joints using cone programming. Comput. Struct. 143, 108–121. https://doi.org/10.1016/j.compstruc.2014.07.010

Radenkovic D. (1968) Théorémes limites pour un matériau de Coulomb à dilatation non standardisée. Comptes Rendus de l'Académie des Sciences. 4103–4104.

Rossi M., Calderini C., Di Napoli B., Cascini L., Portioli F. (2020) Structural analysis of masonry vaulted staircases through rigid block limit analysis. Structures 23: 180–190, https://doi.org/10.1016/j.istruc.2019.10.015

Ruskin J. (1849) [1880] *The seven lamps of architecture*. New York: Crowell.

Sinopoli A., Corradi M., Foce F. (1997) A modern formulation for pre-elastic theories on masonry arches. Journal of Engineering Mechanics. 2:204-213.

Sinopoli A., Aita D., Foce F. (2007) Further remarks on the collapse of masonry arches with Coulomb friction. In Proc., 5th Int. Conf. on Arch Bridges, edited by P. B. Lourenço, D. V. Oliveira, and A. Portela, 649–657. Guimarães, Portugal: Multicomp.

Supprimé: ¶

Supprimé: -

Supprimé: ¶

Mis en forme : Police :(Par défaut) Times New Roman, 12 pt

Mis en forme : Espace Après : 0 pt, Interligne : Double, Ne pas ajuster l'espace entre le texte latin et asiatique, Ne pas ajuster l'espace entre le texte et les nombres asiatiques

Mis en forme : Couleur de police : Rouge

Mis en forme : Police :(Par défaut) Times New Roman, 12 pt

Smars P. (2000) Etudes sur la stabilité des arcs et voûtes, confrontation des méthodes de l'analyse limite aux voûtes gothiques en brabant (studies on the stability of arches and vaults). Ph.D thesis, K.U. Leuven.

Smars P. (2023) Safety analysis of masonry arch and vaults, with a note on the kinematic safety of arches. In: Aita, D., Benvenuto, G., Corradi, M., Pedemonte, O. (eds) Edoardo Benvenuto Prize. Collection of papers. Studia Ligustica 16, Biblioteca Franzoniana, Genova (Italy), 23–50.

Ting-Chun Kao G., Iannuzzo A., Thomaszewski B., Coros S., Van Mele T., Block P. (2022) Coupled Rigid-Block Analysis: Stability-Aware Design of Complex Discrete-Element Assemblies, Computer-Aided Design, 146: 103216

Trentadue F., De Tommasi D., Marasciuolo N., Vitucci G. (2024) Thrust in a symmetric masonry arch with frictional joints on spreading supports. Acta Mech 235: 659–670.

van Zijl, G.G.P.A. (2004) Modeling Masonry Shear-Compression: Role of Dilatancy Highlighted. J. Eng. Mech. 130, 1289–1296. https://doi.org/10.1061/(ASCE)0733-9399(2004)130:11(1289)

You M. (2011) Strength and damage of marble in ductile failure. Journal of Rock Mechanics and Geotechnical Engineering. 3(2):161–166.

Mis en forme : Couleur de police : Rouge

Supprimé: D'Ayala, D., & Smars, P. (2003). Architectural and Structural Modelling for the Conservation of Cathedrals. *Journal of Architectural Conservation*, 9(3), 51–72. ¶

Mis en forme : Couleur de police : Rouge, Anglais (États-Unis)

Mis en forme : Couleur de police : Rouge

Mis en forme : Couleur de police : Rouge, Anglais (Royaume-Uni)

Mis en forme : Police :Non Italique, Couleur de police : Rouge, Anglais (Royaume-Uni)

Mis en forme : Couleur de police : Rouge, Anglais (Royaume-Uni)

Mis en forme : Couleur de police : Rouge

Supprimé: ¶
Zijl, V., G, G.P.A. (2004) Modeling Masonry Shear-Compression: Role of Dilatancy Highlighted. J. Eng. Mech. 130, 1289–1296. https://doi.org/10.1061/(ASCE)0733-9399(2004)130:11(1289)…¶
¶

Mis en forme : Couleur de police : Rouge

Mis en forme : Non souligné, Couleur de police :

Mis en forme : Anglais (Royaume-Uni)

Mis en forme : Anglais (Royaume-Uni)

Mis en forme : Anglais (Royaume-Uni)

Mis en forme : Anglais (Royaume-Uni)

Supprimé: ¶

Mis en forme : Soulignement , Couleur de police : Bleu, Anglais (Royaume-Uni)

Mis en forme : Anglais (Royaume-Uni)

Captions

Figure 1. The front layer of the flat arch crowning the transept portal in the Prato Cathedral (*a*); sketch of the flat arch and detail of the interlocking blocks, drawn from (Ruskin, 1849) (*b*); the interlocking system (*c*, *d*) (Photo: courtesy of Piacenti S.p.a.).

Figure 2. A PLA model of the flat arch used as a case study, kept in place by the application of a restraining force at supports (*a*). Front layer of the flat arch of the Prato Cathedral: geometric parameters (*b*).

Figure 3. Pure sliding collapse mechanism (*a*); collapse mechanism when blocks (*B*) are fixed (*b*).

Figure 4. Portion of the flat arch comprised between the midspan vertical joint and any joint *i*: notation adopted and positive convention for the stress resultants (*a*); equilibrium: internal forces (in blue) and applied loads (in red); friction cone of amplitude ψ (*c*).

Figure 5. Geometry of the joint (*a*) and generic cross-section I_iE_i (*b*); limit condition by assuming a no-tension material with a compressive strength σ_c (*c*); rotational domain in the (N_i, M_i) plane (*d*).

Figure 6. Stability area (left) and thrust line (right) for $H = 1$ m, and: $\mu = 1.7772$ (*a*); $\mu = 0.5$ (*b*); $\mu = 0.4389$ (*c*); $\mu = 0.3$ (*d*). Joints where the limit sliding condition is attained are coloured blue.

Figure 7. The sliding domain related to any joint *i* in the plane (N_i, T_i) (*a*) and in the plane $(R_{i,n}, R_{i,t})$ (*b*). Internal force at joint *i* and notation adopted (*c*); mutual sliding at joint *i* (*d*).

Figure 8. Pure sliding collapse mechanism retrieved for $\mu = 0.4389$ (*a*); geometric construction in order to determine the virtual displacements (*b*).

Figure 9. Geometry of the flat arch with highlighting the joints between the parts and the constraints (*a*); deformed configuration in the equilibrium situation after all precompression action has been removed (*b*).

Figure 10. Contour plot of contact force values (CNORMF variable).

Mis en forme : Justifié

Commenté [EG9]: Nella didascalia mancava il riferimento (b), ma a parte quello io girerei il riferimento (b) così come l'ho messo e non lo lascerei alla fine, altrimenti non si capisce.

Supprimé: Figure 1. The front layer of the flat arch crowning the transept portal in the Prato Cathedral, left; detail of the interlocking blocks, right (Photo: courtesy of Piacenti S.p.a.).¶

Commenté [EG10]: La sposterei qui come figura ancora n.2

Mis en forme : Non Surlignage

Mis en forme : Non Surlignage
Mis en forme : Non Surlignage
Mis en forme : Non Surlignage
Mis en forme : Non Surlignage
Mis en forme : Non Surlignage
Mis en forme : Non Surlignage
Mis en forme : Non Surlignage
Mis en forme : Non Surlignage
Mis en forme : Non Surlignage
Mis en forme : Non Surlignage
Mis en forme : Non Surlignage
Mis en forme : Non Surlignage
Mis en forme : Non Surlignage
Mis en forme : Non Surlignage
Mis en forme : Non Surlignage
Mis en forme : Non Surlignage
Mis en forme : Non Surlignage
Mis en forme : Non Surlignage
Mis en forme : Non Surlignage
Mis en forme : Non Surlignage
Mis en forme : Justifié
Mis en forme : Non Surlignage
Mis en forme : Non Surlignage

Figure 11. Influence of the friction coefficient on the vertical displacement.

Figure 12. Equilibrium configurations depending on the load (1-3). Collapse mechanism that occurs during load step 4 for a load higher than the reference load (4).

Figure 13. The blocks and notations used in the mathematical programming problem, imposing equilibrium (*a*) and resulting forces, expressed in kN (*b*). The corresponding thrust line (*c*).

Figure 14. Snapshots from the NSCD simulation at $T = 3$ s, for $\Delta t = 0.001$ s (left); thrust lines obtained from postprocessing the results from the NSCD simulation at $T = 0.5$ s, for $\Delta t = 0.001$ s (right). The cases of $\mu = 0.5$ (*a*), $\mu = 0.44$ (*b*) and $\mu = 0.4$ (*c*).

Figure 15. Results from the NSCD simulation at $T = 0.5$ s, for $\mu = 0.44$ and timestep. $\Delta t = 0.001$ s, assuming only the three central blocks free to move: snapshot at $T = 2$ s.

Mis en forme : Gauche

Mis en forme : Justifié

Mis en forme : Police :(Par défaut) +Corps (Calibri), 11 pt, Italique

Mis en forme : Normal, Gauche, Interligne : simple

Mis en forme : Police :(Par défaut) +Corps (Calibri), 11 pt, Italique

Mis en forme : Normal, Gauche, Interligne : simple

Mis en forme : Justifié, Espace Après : 0 pt

Mis en forme : Police :(Par défaut) +Corps (Calibri), 11 pt

Mis en forme : Normal, Gauche

Mis en forme : Police :(Par défaut) +Corps (Calibri), 11 pt, Italique

Mis en forme : Justifié

Mis en forme : Gauche

Mis en forme : Normal, Justifié, Paragraphes solidaires

Supprimé: Figure 2. A PLA model of the flat arch used as a case study, kept in place by the application of a restraining force at supports (*a*). Front layer of the flat arch of the Prato Cathedral: geometric parameters (*b*).¶

Mis en forme : Espace Après : 0 pt, Interligne : Double

Supprimé: Figure 3. Equilibrium of the portion of the structure comprised between the ideal vertical joint at the midspan and any joint *i*: stress resultants (left); friction cone of amplitude ψ (right).¶
¶
Figure 4. Stability area (left) and thrust line (right) for $H = 1$ m, and: $\mu = 1.7772$ (*a*); $\mu = 0.5$ (*b*); $\mu = 0.4389$ (*c*); $\mu = 0.3$ (*d*). Joints where the limit condition is attained are coloured blue.¶
¶
Figure 5. Pure sliding collapse mechanism ($H = 1$ m, $\mu = 0.4389$) (left); collapse mechanism when blocks (*b*) are fixed (right).¶
¶
Figure 6. Geometry of the flat arch with highlighting the joints between the parts and the constraints (left); deformed configuration in the equilibrium situation after all precompression action has been removed (right).¶
¶
Figure 7. Contour plot of contact force values (CNORMF variable).¶
¶
Figure 8. Equilibrium configurations depending on the load (1-3). Collapse mechanism that occurs during load step 4 for a load higher than the reference load (4).¶
¶
Figure 9. The blocks and notations used in the mathematical programming problem, imposing equilibrium (*a*) and resulting forces, expressed in kN (*b*). The corresponding thrust line (*c*).¶
¶
... [175]

Mis en forme : Espacement automatique entre les caractères asiatiques et latins, Espacement automatique entre les caractères asiatiques et les chiffres

Page 4 : [1] Supprimé	Danila Aita	25-11-24 19:28:00

Actually, high friction levels ensure that the static (or safe or lower bound) and kinematic (or unsafe or upper bound) theorems of Limit Analysis - derived from the normality law between statically admissible stress states and the corresponding flow rule for the displacement field - are valid.

Page 8 : [2] Mis en forme	Elsa Garavaglia	25-11-24 10:07:00

Police :(Par défaut) Times New Roman, 12 pt, Couleur de police : Rouge

Page 8 : [2] Mis en forme	Elsa Garavaglia	25-11-24 10:07:00

Police :(Par défaut) Times New Roman, 12 pt, Couleur de police : Rouge

Page 8 : [3] Mis en forme	Danila Aita	25-11-24 20:11:00

Police :Italique

Page 8 : [3] Mis en forme	Danila Aita	25-11-24 20:11:00

Police :Italique

Page 8 : [4] Mis en forme	Elsa Garavaglia	25-11-24 10:07:00

Non Surlignage

Page 8 : [4] Mis en forme	Elsa Garavaglia	25-11-24 10:07:00

Non Surlignage

Page 8 : [4] Mis en forme	Elsa Garavaglia	25-11-24 10:07:00

Non Surlignage

Page 8 : [4] Mis en forme	Elsa Garavaglia	25-11-24 10:07:00

Non Surlignage

Page 8 : [4] Mis en forme	Elsa Garavaglia	25-11-24 10:07:00

Non Surlignage

Page 8 : [4] Mis en forme	Elsa Garavaglia	25-11-24 10:07:00

Non Surlignage

Page 8 : [4] Mis en forme	Elsa Garavaglia	25-11-24 10:07:00

Non Surlignage

Page 8 : [4] Mis en forme	Elsa Garavaglia	25-11-24 10:07:00

Non Surlignage

Page 8 : [4] Mis en forme	Elsa Garavaglia	25-11-24 10:07:00

Non Surlignage

Page 8 : [4] Mis en forme	Elsa Garavaglia	25-11-24 10:07:00

Non Surlignage

Page 8 : [4] Mis en forme	Elsa Garavaglia	25-11-24 10:07:00

Non Surlignage

Page 8 : [4] Mis en forme	Elsa Garavaglia	25-11-24 10:07:00

Non Surlignage

Page 8 : [4] Mis en forme	Elsa Garavaglia	25-11-24 10:07:00

Non Surlignage

Page 8 : [4] Mis en forme	Elsa Garavaglia	25-11-24 10:07:00

Non Surlignage

Page 8 : [4] Mis en forme	Elsa Garavaglia	25-11-24 10:07:00

Non Surlignage

Page 8 : [4] Mis en forme	Elsa Garavaglia	25-11-24 10:07:00

Non Surlignage

Page 8 : [4] Mis en forme	Elsa Garavaglia	25-11-24 10:07:00

Non Surlignage

Page 8 : [5] Mis en forme	Elsa Garavaglia	25-11-24 10:07:00

Couleur de police : Rouge

Page 8 : [5] Mis en forme	Elsa Garavaglia	25-11-24 10:07:00

Couleur de police : Rouge

Page 8 : [5] Mis en forme	Elsa Garavaglia	25-11-24 10:07:00

Couleur de police : Rouge

Page 8 : [5] Mis en forme	Elsa Garavaglia	25-11-24 10:07:00

Couleur de police : Rouge

Page 8 : [5] Mis en forme	Elsa Garavaglia	25-11-24 10:07:00

Couleur de police : Rouge

Page 8 : [5] Mis en forme	Elsa Garavaglia	25-11-24 10:07:00

Couleur de police : Rouge

Page 8 : [6] Mis en forme	Danila Aita	26-11-24 08:21:00

Police :Italique

Page 8 : [6] Mis en forme	Danila Aita	26-11-24 08:21:00

Police :Italique

Page 8 : [6] Mis en forme	Danila Aita	26-11-24 08:21:00

Police :Italique

Page 8 : [6] Mis en forme	Danila Aita	26-11-24 08:21:00

Police :Italique

Page 8 : [7] Mis en forme	Elsa Garavaglia	25-11-24 10:07:00

Non Surlignage

Page 8 : [7] Mis en forme	Elsa Garavaglia	25-11-24 10:07:00

Non Surlignage

Page 8 : [7] Mis en forme	Elsa Garavaglia	25-11-24 10:07:00

Non Surlignage

Page 8 : [7] Mis en forme	Elsa Garavaglia	25-11-24 10:07:00

Non Surlignage

Page 8 : [7] Mis en forme	Elsa Garavaglia	25-11-24 10:07:00

Non Surlignage

Page 8 : [7] Mis en forme	Elsa Garavaglia	25-11-24 10:07:00

Non Surlignage

Page 8 : [7] Mis en forme	Elsa Garavaglia	25-11-24 10:07:00

Non Surlignage

Page 8 : [7] Mis en forme	Elsa Garavaglia	25-11-24 10:07:00

Non Surlignage

Page 8 : [7] Mis en forme	Elsa Garavaglia	25-11-24 10:07:00

Non Surlignage

Page 8 : [7] Mis en forme	Elsa Garavaglia	25-11-24 10:07:00

Non Surlignage

Page 8 : [7] Mis en forme	Elsa Garavaglia	25-11-24 10:07:00

Non Surlignage

Page 8 : [7] Mis en forme	Elsa Garavaglia	25-11-24 10:07:00

Non Surlignage

Page 8 : [7] Mis en forme	Elsa Garavaglia	25-11-24 10:07:00

Non Surlignage

Page 8 : [7] Mis en forme	Elsa Garavaglia	25-11-24 10:07:00

Non Surlignage

Page 8 : [7] Mis en forme	Elsa Garavaglia	25-11-24 10:07:00

Non Surlignage

Page 8 : [8] Mis en forme	Elsa Garavaglia	25-11-24 10:07:00

Couleur de police : Rouge

Page 8 : [8] Mis en forme	Elsa Garavaglia	25-11-24 10:07:00

Couleur de police : Rouge

Page 8 : [9] Mis en forme	Danila Aita	14-11-24 19:50:00

Couleur de police : Rouge

Page 8 : [9] Mis en forme	Danila Aita	14-11-24 19:50:00

Couleur de police : Rouge

Page 8 : [9] Mis en forme	Danila Aita	14-11-24 19:50:00

Couleur de police : Rouge

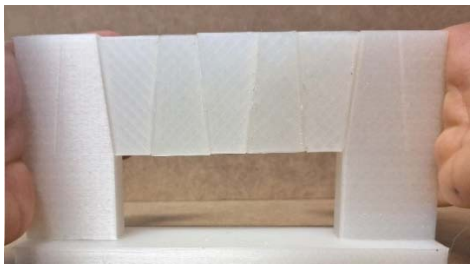
Page 8 : [9] Mis en forme	Danila Aita	14-11-24 19:50:00

Couleur de police : Rouge

Page 9 : [10] Supprimé	Danila Aita	13-11-24 11:14:00

focus will be made on some techniques based on different approaches, i.e., static methods exploiting graphic statics coupled with kinematic approaches based on the virtual work theorem, Finite Element micro-modelling, and DEM within a Non-Smooth Contact Dynamics (NSCD) formulation.

Page 10 : [11] Supprimé	Danila Aita	20-11-24 09:32:00



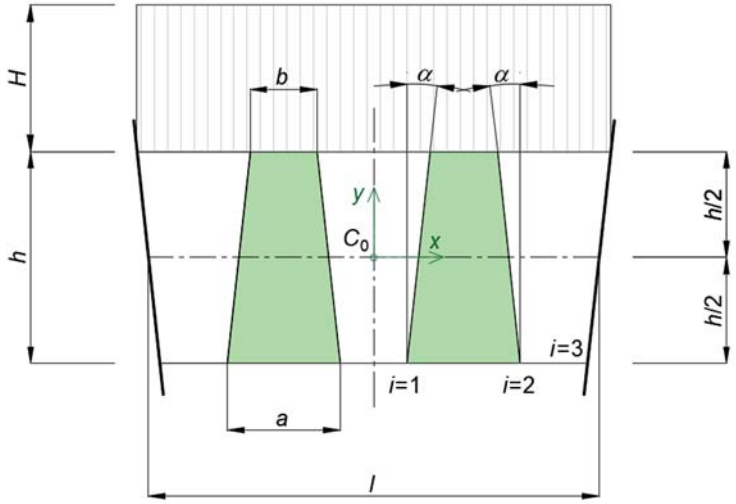


Figure 2. A PLA model of the flat arch used as a case study, kept in place by the application of a restraining force at supports (*a*). Front layer of the flat arch of the Prato Cathedral: geometric parameters (*b*).

Page 10 : [12] Supprimé	Danila Aita	13-11-24 11:45:00

an unedited non-standard analytical approach. By starting from the modified Durand-Claye graphic method (Durand-Claye A.,1867; 1868; Aita, Barsotti and Bennati, 2019; Aita, Milani and Taliercio, 2023),

Page 12 : [13] Mis en forme	Elsa Garavaglia	25-11-24 10:08:00

Non Surlignage

Page 12 : [13] Mis en forme	Elsa Garavaglia	25-11-24 10:08:00

Non Surlignage

Page 12 : [14] Supprimé	Danila Aita	22-11-24 15:38:00

Equilibrium of the portion

Page 12 : [14] Supprimé	Danila Aita	22-11-24 15:38:00

Equilibrium of the portion

Page 12 : [14] Supprimé	Danila Aita	22-11-24 15:38:00

Equilibrium of the portion

Page 12 : [15] Mis en forme	Elsa Garavaglia	25-11-24 10:08:00

Non Surlignage

Page 12 : [15] Mis en forme	Elsa Garavaglia	25-11-24 10:08:00

Non Surlignage

Page 12 : [16] Mis en forme	Elsa Garavaglia	25-11-24 10:08:00

Non Surlignage

Page 12 : [16] Mis en forme	Elsa Garavaglia	25-11-24 10:08:00

Non Surlignage

Page 12 : [16] Mis en forme	Elsa Garavaglia	25-11-24 10:08:00

Non Surlignage

Page 12 : [16] Mis en forme	Elsa Garavaglia	25-11-24 10:08:00

Non Surlignage

Page 12 : [17] Mis en forme	Elsa Garavaglia	25-11-24 10:08:00

Non Surlignage

Page 12 : [17] Mis en forme	Elsa Garavaglia	25-11-24 10:08:00

Non Surlignage

Page 12 : [17] Mis en forme	Elsa Garavaglia	25-11-24 10:08:00

Non Surlignage

Page 12 : [17] Mis en forme	Elsa Garavaglia	25-11-24 10:08:00

Non Surlignage

Page 12 : [18] Mis en forme	Elsa Garavaglia	25-11-24 10:08:00

Police :Italique, Couleur de police : Rouge

Page 12 : [18] Mis en forme	Elsa Garavaglia	25-11-24 10:08:00

Police :Italique, Couleur de police : Rouge

Page 12 : [19] Mis en forme	Elsa Garavaglia	25-11-24 10:08:00

Police :Italique, Couleur de police : Rouge

Page 12 : [19] Mis en forme	Elsa Garavaglia	25-11-24 10:08:00

Police :Italique, Couleur de police : Rouge

Page 12 : [19] Mis en forme	Elsa Garavaglia	25-11-24 10:08:00

Police :Italique, Couleur de police : Rouge

Page 12 : [20] Mis en forme	Elsa Garavaglia	25-11-24 10:10:00

Non Surlignage

Page 12 : [20] Mis en forme	Elsa Garavaglia	25-11-24 10:10:00

Non Surlignage

Page 12 : [20] Mis en forme	Elsa Garavaglia	25-11-24 10:10:00

Non Surlignage

Page 12 : [21] Mis en forme	Elsa Garavaglia	25-11-24 10:10:00

Non Surlignage

Page 12 : [21] Mis en forme	Elsa Garavaglia	25-11-24 10:10:00

Non Surlignage

Page 12 : [21] Mis en forme	Elsa Garavaglia	25-11-24 10:10:00

Non Surlignage

Page 12 : [22] Mis en forme	Elsa Garavaglia	25-11-24 10:10:00

Non Surlignage

Page 12 : [22] Mis en forme	Elsa Garavaglia	25-11-24 10:10:00

Non Surlignage

Page 12 : [22] Mis en forme	Elsa Garavaglia	25-11-24 10:10:00

Non Surlignage

Page 12 : [23] Mis en forme	Elsa Garavaglia	25-11-24 10:10:00

Non Surlignage

Page 12 : [23] Mis en forme	Elsa Garavaglia	25-11-24 10:10:00

Non Surlignage

Page 12 : [23] Mis en forme **Elsa Garavaglia** **25-11-24 10:10:00**

Non Surlignage

Page 12 : [23] Mis en forme **Elsa Garavaglia** **25-11-24 10:10:00**

Non Surlignage

Page 12 : [24] Mis en forme **Elsa Garavaglia** **25-11-24 10:10:00**

Non Surlignage

Page 12 : [24] Mis en forme **Elsa Garavaglia** **25-11-24 10:10:00**

Non Surlignage

Page 12 : [24] Mis en forme **Elsa Garavaglia** **25-11-24 10:10:00**

Non Surlignage

Page 12 : [25] Mis en forme **Elsa Garavaglia** **25-11-24 10:10:00**

Non Surlignage

Page 12 : [25] Mis en forme **Elsa Garavaglia** **25-11-24 10:10:00**

Non Surlignage

Page 12 : [25] Mis en forme **Elsa Garavaglia** **25-11-24 10:10:00**

Non Surlignage

Page 12 : [26] Mis en forme **Danila Aita** **21-11-24 12:24:00**

Police :Ligatures : Standard + Contextuelles

Page 12 : [27] Supprimé **Danila Aita** **15-11-24 21:38:00**

As will be shown below, this static, semi-analytical graphical method can be used to draw the so-called 'stability area'. The method is usually applied to symmetric arches subjected to symmetric gravitational loads but can be extended to the assessment of other types of symmetric structures. The statically admissible solutions are determined by taking into account strength and friction requirements pertaining to any cross-section *i*, as well as the equilibrium conditions related to the portion of the structure between the ideal vertical midspan section, belonging to the *y*-axis, and generic joint *i* (Figure 3).

Page 12 : [28] Mis en forme **Elsa Garavaglia** **25-11-24 10:10:00**

Non Surlignage

Page 12 : [28] Mis en forme **Elsa Garavaglia** **25-11-24 10:10:00**

Non Surlignage

Page 12 : [28] Mis en forme **Elsa Garavaglia** **25-11-24 10:10:00**

Non Surlignage

Page 12 : [29] Supprimé **Danila Aita** **15-11-24 21:37:00**

A

Page 13 : [30] Mis en forme **Elsa Garavaglia** **25-11-24 10:10:00**

Couleur de police : Rouge

Page 13 : [30] Mis en forme **Elsa Garavaglia** **25-11-24 10:10:00**

Couleur de police : Rouge

Page 13 : [31] Mis en forme **Danila Aita** **21-11-24 12:13:00**

Couleur de police : Rouge

Page 13 : [31] Mis en forme **Danila Aita** **21-11-24 12:13:00**

Couleur de police : Rouge

Page 13 : [31] Mis en forme **Danila Aita** **21-11-24 12:13:00**

Couleur de police : Rouge

Page 13 : [31] Mis en forme **Danila Aita** **21-11-24 12:13:00**

Couleur de police : Rouge

Page 13 : [31] Mis en forme **Danila Aita** **21-11-24 12:13:00**

Couleur de police : Rouge

Page 13 : [31] Mis en forme **Danila Aita** **21-11-24 12:13:00**

Couleur de police : Rouge

Page 13 : [31] Mis en forme **Danila Aita** **21-11-24 12:13:00**

Couleur de police : Rouge

Page 13 : [32] Mis en forme **Danila Aita** **21-11-24 12:13:00**

Couleur de police : Rouge

Page 13 : [32] Mis en forme	**Danila Aita**	**21-11-24 12:13:00**

Couleur de police : Rouge

Page 13 : [32] Mis en forme	**Danila Aita**	**21-11-24 12:13:00**

Couleur de police : Rouge

Page 13 : [32] Mis en forme	**Danila Aita**	**21-11-24 12:13:00**

Couleur de police : Rouge

Page 13 : [32] Mis en forme	**Danila Aita**	**21-11-24 12:13:00**

Couleur de police : Rouge

Page 13 : [32] Mis en forme	**Danila Aita**	**21-11-24 12:13:00**

Couleur de police : Rouge

Page 13 : [32] Mis en forme	**Danila Aita**	**21-11-24 12:13:00**

Couleur de police : Rouge

Page 13 : [32] Mis en forme	**Danila Aita**	**21-11-24 12:13:00**

Couleur de police : Rouge

Page 13 : [32] Mis en forme	**Danila Aita**	**21-11-24 12:13:00**

Couleur de police : Rouge

Page 13 : [33] Mis en forme	**Danila Aita**	**21-11-24 12:13:00**

Couleur de police : Rouge

Page 13 : [33] Mis en forme	**Danila Aita**	**21-11-24 12:13:00**

Couleur de police : Rouge

Page 13 : [33] Mis en forme	**Danila Aita**	**21-11-24 12:13:00**

Couleur de police : Rouge

Page 13 : [33] Mis en forme	**Danila Aita**	**21-11-24 12:13:00**

Couleur de police : Rouge

Page 13 : [33] Mis en forme	**Danila Aita**	**21-11-24 12:13:00**

Couleur de police : Rouge

Page 13 : [33] Mis en forme	**Danila Aita**	**21-11-24 12:13:00**

Couleur de police : Rouge

Page 13 : [34] Mis en forme	Danila Aita	21-11-24 12:13:00

Couleur de police : Rouge

Page 13 : [34] Mis en forme	Danila Aita	21-11-24 12:13:00

Couleur de police : Rouge

Page 13 : [34] Mis en forme	Danila Aita	21-11-24 12:13:00

Couleur de police : Rouge

Page 13 : [35] Mis en forme	Danila Aita	15-11-24 21:59:00

Couleur de police : Rouge

Page 13 : [35] Mis en forme	Danila Aita	15-11-24 21:59:00

Couleur de police : Rouge

Page 13 : [36] Mis en forme	Danila Aita	13-11-24 12:14:00

Couleur de police : Rouge

Page 13 : [36] Mis en forme	Danila Aita	13-11-24 12:14:00

Couleur de police : Rouge

Page 13 : [37] Mis en forme	Danila Aita	13-11-24 12:12:00

Couleur de police : Rouge

Page 13 : [37] Mis en forme	Danila Aita	13-11-24 12:12:00

Couleur de police : Rouge

Page 13 : [37] Mis en forme	Danila Aita	13-11-24 12:12:00

Couleur de police : Rouge

Page 13 : [37] Mis en forme	Danila Aita	13-11-24 12:12:00

Couleur de police : Rouge

Page 13 : [38] Mis en forme	Danila Aita	13-11-24 12:12:00

Couleur de police : Rouge

Page 13 : [38] Mis en forme	Danila Aita	13-11-24 12:12:00

Couleur de police : Rouge

Page 13 : [38] Mis en forme	Danila Aita	13-11-24 12:12:00

Couleur de police : Rouge

Page 13 : [38] Mis en forme	Danila Aita	13-11-24 12:12:00

Couleur de police : Rouge

Page 13 : [38] Mis en forme	**Danila Aita**	**13-11-24 12:12:00**

Couleur de police : Rouge

Page 13 : [38] Mis en forme	**Danila Aita**	**13-11-24 12:12:00**

Couleur de police : Rouge

Page 13 : [38] Mis en forme	**Danila Aita**	**13-11-24 12:12:00**

Couleur de police : Rouge

Page 13 : [38] Mis en forme	**Danila Aita**	**13-11-24 12:12:00**

Couleur de police : Rouge

Page 13 : [38] Mis en forme	**Danila Aita**	**13-11-24 12:12:00**

Couleur de police : Rouge

Page 13 : [39] Mis en forme	**Danila Aita**	**13-11-24 12:12:00**

Couleur de police : Rouge

Page 13 : [39] Mis en forme	**Danila Aita**	**13-11-24 12:12:00**

Couleur de police : Rouge

Page 13 : [39] Mis en forme	**Danila Aita**	**13-11-24 12:12:00**

Couleur de police : Rouge

Page 13 : [39] Mis en forme	**Danila Aita**	**13-11-24 12:12:00**

Couleur de police : Rouge

Page 13 : [39] Mis en forme	**Danila Aita**	**13-11-24 12:12:00**

Couleur de police : Rouge

Page 13 : [39] Mis en forme	**Danila Aita**	**13-11-24 12:12:00**

Couleur de police : Rouge

Page 13 : [39] Mis en forme	**Danila Aita**	**13-11-24 12:12:00**

Couleur de police : Rouge

Page 13 : [39] Mis en forme	**Danila Aita**	**13-11-24 12:12:00**

Couleur de police : Rouge

Page 14 : [40] Mis en forme	Danila Aita	13-11-24 12:12:00

Couleur de police : Rouge

Page 14 : [40] Mis en forme	Danila Aita	13-11-24 12:12:00

Couleur de police : Rouge

Page 14 : [40] Mis en forme	Danila Aita	13-11-24 12:12:00

Couleur de police : Rouge

Page 14 : [40] Mis en forme	Danila Aita	13-11-24 12:12:00

Couleur de police : Rouge

Page 14 : [40] Mis en forme	Danila Aita	13-11-24 12:12:00

Couleur de police : Rouge

Page 14 : [40] Mis en forme	Danila Aita	13-11-24 12:12:00

Couleur de police : Rouge

Page 14 : [40] Mis en forme	Danila Aita	13-11-24 12:12:00

Couleur de police : Rouge

Page 14 : [40] Mis en forme	Danila Aita	13-11-24 12:12:00

Couleur de police : Rouge

Page 14 : [40] Mis en forme	Danila Aita	13-11-24 12:12:00

Couleur de police : Rouge

Page 14 : [40] Mis en forme	Danila Aita	13-11-24 12:12:00

Couleur de police : Rouge

Page 14 : [40] Mis en forme	Danila Aita	13-11-24 12:12:00

Couleur de police : Rouge

Page 14 : [40] Mis en forme	Danila Aita	13-11-24 12:12:00

Couleur de police : Rouge

Page 14 : [40] Mis en forme	Danila Aita	13-11-24 12:12:00

Couleur de police : Rouge

Page 14 : [40] Mis en forme	Danila Aita	13-11-24 12:12:00

Couleur de police : Rouge

Page 14 : [40] Mis en forme	Danila Aita	13-11-24 12:12:00

Couleur de police : Rouge

Page 14 : [40] Mis en forme	Danila Aita	13-11-24 12:12:00

Couleur de police : Rouge

Page 14 : [40] Mis en forme	Danila Aita	13-11-24 12:12:00

Couleur de police : Rouge

Page 14 : [40] Mis en forme	Danila Aita	13-11-24 12:12:00

Couleur de police : Rouge

Page 14 : [41] Mis en forme	Danila Aita	13-11-24 12:12:00

Couleur de police : Rouge

Page 14 : [41] Mis en forme	Danila Aita	13-11-24 12:12:00

Couleur de police : Rouge

Page 14 : [41] Mis en forme	Danila Aita	13-11-24 12:12:00

Couleur de police : Rouge

Page 14 : [42] Mis en forme	Elsa Garavaglia	25-11-24 10:10:00

Police :10 pt, Couleur de police : Rouge

Page 14 : [42] Mis en forme	Elsa Garavaglia	25-11-24 10:10:00

Police :10 pt, Couleur de police : Rouge

Page 14 : [42] Mis en forme	Elsa Garavaglia	25-11-24 10:10:00

Police :10 pt, Couleur de police : Rouge

Page 14 : [42] Mis en forme	Elsa Garavaglia	25-11-24 10:10:00

Police :10 pt, Couleur de police : Rouge

Page 14 : [42] Mis en forme	Elsa Garavaglia	25-11-24 10:10:00

Police :10 pt, Couleur de police : Rouge

Page 14 : [42] Mis en forme	Elsa Garavaglia	25-11-24 10:10:00

Police :10 pt, Couleur de police : Rouge

Page 14 : [43] Mis en forme	Danila Aita	13-11-24 12:12:00

Couleur de police : Rouge

Page 14 : [43] Mis en forme	Danila Aita	13-11-24 12:12:00

Couleur de police : Rouge

Page 14 : [43] Mis en forme	**Danila Aita**	**13-11-24 12:12:00**

Couleur de police : Rouge

Page 14 : [43] Mis en forme	**Danila Aita**	**13-11-24 12:12:00**

Couleur de police : Rouge

Page 14 : [43] Mis en forme	**Danila Aita**	**13-11-24 12:12:00**

Couleur de police : Rouge

Page 14 : [44] Mis en forme	**Danila Aita**	**13-11-24 12:12:00**

Couleur de police : Rouge

Page 14 : [44] Mis en forme	**Danila Aita**	**13-11-24 12:12:00**

Couleur de police : Rouge

Page 14 : [44] Mis en forme	**Danila Aita**	**13-11-24 12:12:00**

Couleur de police : Rouge

Page 14 : [44] Mis en forme	**Danila Aita**	**13-11-24 12:12:00**

Couleur de police : Rouge

Page 14 : [44] Mis en forme	**Danila Aita**	**13-11-24 12:12:00**

Couleur de police : Rouge

Page 14 : [44] Mis en forme	**Danila Aita**	**13-11-24 12:12:00**

Couleur de police : Rouge

Page 14 : [44] Mis en forme	**Danila Aita**	**13-11-24 12:12:00**

Couleur de police : Rouge

Page 14 : [44] Mis en forme	**Danila Aita**	**13-11-24 12:12:00**

Couleur de police : Rouge

Page 14 : [44] Mis en forme	**Danila Aita**	**13-11-24 12:12:00**

Couleur de police : Rouge

Page 14 : [44] Mis en forme	**Danila Aita**	**13-11-24 12:12:00**

Couleur de police : Rouge

Page 14 : [45] Mis en forme	**Danila Aita**	**13-11-24 12:12:00**

Couleur de police : Rouge

Page 14 : [45] Mis en forme	**Danila Aita**	**13-11-24 12:12:00**

Couleur de police : Rouge

Page 14 : [45] Mis en forme **Danila Aita** **13-11-24 12:12:00**

Couleur de police : Rouge

Page 14 : [46] Mis en forme **Danila Aita** **13-11-24 12:12:00**

Couleur de police : Rouge

Page 14 : [46] Mis en forme **Danila Aita** **13-11-24 12:12:00**

Couleur de police : Rouge

Page 14 : [46] Mis en forme **Danila Aita** **13-11-24 12:12:00**

Couleur de police : Rouge

Page 14 : [47] Supprimé **Danila Aita** **15-11-24 22:09:00**

,

Page 14 : [47] Supprimé **Danila Aita** **15-11-24 22:09:00**

,

Page 14 : [48] Mis en forme **Danila Aita** **21-11-24 12:58:00**

Couleur de police : Rouge

Page 14 : [48] Mis en forme **Danila Aita** **21-11-24 12:58:00**

Couleur de police : Rouge

Page 14 : [48] Mis en forme **Danila Aita** **21-11-24 12:58:00**

Couleur de police : Rouge

Page 14 : [48] Mis en forme **Danila Aita** **21-11-24 12:58:00**

Couleur de police : Rouge

Page 14 : [49] Mis en forme **Danila Aita** **21-11-24 12:58:00**

Couleur de police : Rouge

Page 14 : [49] Mis en forme **Danila Aita** **21-11-24 12:58:00**

Couleur de police : Rouge

Page 14 : [49] Mis en forme **Danila Aita** **21-11-24 12:58:00**

Couleur de police : Rouge

Page 14 : [49] Mis en forme **Danila Aita** **21-11-24 12:58:00**

Couleur de police : Rouge

Page 14 : [50] Mis en forme	Elsa Garavaglia	25-11-24 10:10:00

Couleur de police : Rouge

Page 14 : [50] Mis en forme	Elsa Garavaglia	25-11-24 10:10:00

Couleur de police : Rouge

Page 14 : [50] Mis en forme	Elsa Garavaglia	25-11-24 10:10:00

Couleur de police : Rouge

Page 14 : [50] Mis en forme	Elsa Garavaglia	25-11-24 10:10:00

Couleur de police : Rouge

Page 14 : [50] Mis en forme	Elsa Garavaglia	25-11-24 10:10:00

Couleur de police : Rouge

Page 14 : [51] Mis en forme	Elsa Garavaglia	25-11-24 10:10:00

Anglais (Royaume-Uni), Non Surlignage

Page 14 : [51] Mis en forme	Elsa Garavaglia	25-11-24 10:10:00

Anglais (Royaume-Uni), Non Surlignage

Page 14 : [51] Mis en forme	Elsa Garavaglia	25-11-24 10:10:00

Anglais (Royaume-Uni), Non Surlignage

Page 14 : [51] Mis en forme	Elsa Garavaglia	25-11-24 10:10:00

Anglais (Royaume-Uni), Non Surlignage

Page 16 : [52] Mis en forme	Elsa Garavaglia	25-11-24 10:11:00

Non Surlignage

Page 16 : [52] Mis en forme	Elsa Garavaglia	25-11-24 10:11:00

Non Surlignage

Page 16 : [52] Mis en forme	Elsa Garavaglia	25-11-24 10:11:00

Non Surlignage

Page 16 : [52] Mis en forme	Elsa Garavaglia	25-11-24 10:11:00

Non Surlignage

Page 16 : [52] Mis en forme	Elsa Garavaglia	25-11-24 10:11:00

Non Surlignage

Page 16 : [52] Mis en forme	Elsa Garavaglia	25-11-24 10:11:00

Non Surlignage

Page 16 : [52] Mis en forme	Elsa Garavaglia	25-11-24 10:11:00

Non Surlignage

Page 16 : [52] Mis en forme	Elsa Garavaglia	25-11-24 10:11:00

Non Surlignage

Page 16 : [52] Mis en forme	Elsa Garavaglia	25-11-24 10:11:00

Non Surlignage

Page 16 : [53] Mis en forme	Elsa Garavaglia	25-11-24 10:11:00

Non Surlignage

Page 16 : [53] Mis en forme	Elsa Garavaglia	25-11-24 10:11:00

Non Surlignage

Page 16 : [53] Mis en forme	Elsa Garavaglia	25-11-24 10:11:00

Non Surlignage

Page 16 : [53] Mis en forme	Elsa Garavaglia	25-11-24 10:11:00

Non Surlignage

Page 16 : [53] Mis en forme	Elsa Garavaglia	25-11-24 10:11:00

Non Surlignage

Page 16 : [53] Mis en forme	Elsa Garavaglia	25-11-24 10:11:00

Non Surlignage

Page 16 : [53] Mis en forme	Elsa Garavaglia	25-11-24 10:11:00

Non Surlignage

Page 16 : [53] Mis en forme	Elsa Garavaglia	25-11-24 10:11:00

Non Surlignage

Page 16 : [53] Mis en forme	Elsa Garavaglia	25-11-24 10:11:00

Non Surlignage

Page 16 : [54] Mis en forme	Elsa Garavaglia	25-11-24 10:11:00

Non Surlignage

Page 16 : [54] Mis en forme	Elsa Garavaglia	25-11-24 10:11:00

Non Surlignage

Page 16 : [54] Mis en forme	Elsa Garavaglia	25-11-24 10:11:00

Non Surlignage

Page 16 : [54] Mis en forme	Elsa Garavaglia	25-11-24 10:11:00

Non Surlignage

Page 16 : [54] Mis en forme	Elsa Garavaglia	25-11-24 10:11:00

Non Surlignage

Page 16 : [55] Mis en forme	Danila Aita	21-11-24 12:33:00

Police :(Par défaut) Times New Roman, Non Italique

Page 16 : [56] Mis en forme	Elsa Garavaglia	25-11-24 10:11:00

Couleur de police : Rouge

Page 16 : [56] Mis en forme	Elsa Garavaglia	25-11-24 10:11:00

Couleur de police : Rouge

Page 16 : [56] Mis en forme	Elsa Garavaglia	25-11-24 10:11:00

Couleur de police : Rouge

Page 16 : [56] Mis en forme	Elsa Garavaglia	25-11-24 10:11:00

Couleur de police : Rouge

Page 16 : [56] Mis en forme	Elsa Garavaglia	25-11-24 10:11:00

Couleur de police : Rouge

Page 16 : [56] Mis en forme	Elsa Garavaglia	25-11-24 10:11:00

Couleur de police : Rouge

Page 16 : [56] Mis en forme	Elsa Garavaglia	25-11-24 10:11:00

Couleur de police : Rouge

Page 16 : [57] Mis en forme	Elsa Garavaglia	25-11-24 10:11:00

Police :10 pt, Non Surlignage

Page 16 : [57] Mis en forme	Elsa Garavaglia	25-11-24 10:11:00

Police :10 pt, Non Surlignage

Page 16 : [57] Mis en forme	Elsa Garavaglia	25-11-24 10:11:00

Police :10 pt, Non Surlignage

Page 16 : [57] Mis en forme	Elsa Garavaglia	25-11-24 10:11:00

Police :10 pt, Non Surlignage

Page 16 : [57] Mis en forme	Elsa Garavaglia	25-11-24 10:11:00

Police :10 pt, Non Surlignage

Page 16 : [57] Mis en forme	Elsa Garavaglia	25-11-24 10:11:00

Police :10 pt, Non Surlignage

Page 16 : [57] Mis en forme	Elsa Garavaglia	25-11-24 10:11:00

Police :10 pt, Non Surlignage

Page 16 : [57] Mis en forme	Elsa Garavaglia	25-11-24 10:11:00

Police :10 pt, Non Surlignage

Page 16 : [57] Mis en forme	Elsa Garavaglia	25-11-24 10:11:00

Police :10 pt, Non Surlignage

Page 16 : [57] Mis en forme	Elsa Garavaglia	25-11-24 10:11:00

Police :10 pt, Non Surlignage

Page 16 : [57] Mis en forme	Elsa Garavaglia	25-11-24 10:11:00

Police :10 pt, Non Surlignage

Page 16 : [58] Mis en forme	Elsa Garavaglia	25-11-24 10:11:00

Police :10 pt, Non Surlignage

Page 16 : [58] Mis en forme	Elsa Garavaglia	25-11-24 10:11:00

Police :10 pt, Non Surlignage

Page 16 : [58] Mis en forme	Elsa Garavaglia	25-11-24 10:11:00

Police :10 pt, Non Surlignage

Page 16 : [58] Mis en forme	Elsa Garavaglia	25-11-24 10:11:00

Police :10 pt, Non Surlignage

Page 16 : [58] Mis en forme	Elsa Garavaglia	25-11-24 10:11:00

Police :10 pt, Non Surlignage

Page 16 : [58] Mis en forme	Elsa Garavaglia	25-11-24 10:11:00

Police :10 pt, Non Surlignage

Page 16 : [58] Mis en forme	Elsa Garavaglia	25-11-24 10:11:00

Police :10 pt, Non Surlignage

Page 16 : [58] Mis en forme	Elsa Garavaglia	25-11-24 10:11:00

Police :10 pt, Non Surlignage

Page 16 : [58] Mis en forme	Elsa Garavaglia	25-11-24 10:11:00

Police :10 pt, Non Surlignage

Page 16 : [58] Mis en forme	Elsa Garavaglia	25-11-24 10:11:00

Police :10 pt, Non Surlignage

Page 16 : [58] Mis en forme	Elsa Garavaglia	25-11-24 10:11:00

Police :10 pt, Non Surlignage

Page 16 : [58] Mis en forme	Elsa Garavaglia	25-11-24 10:11:00

Police :10 pt, Non Surlignage

Page 16 : [58] Mis en forme	Elsa Garavaglia	25-11-24 10:11:00

Police :10 pt, Non Surlignage

Page 16 : [58] Mis en forme	Elsa Garavaglia	25-11-24 10:11:00

Police :10 pt, Non Surlignage

Page 16 : [58] Mis en forme	Elsa Garavaglia	25-11-24 10:11:00

Police :10 pt, Non Surlignage

Page 16 : [58] Mis en forme	Elsa Garavaglia	25-11-24 10:11:00

Police :10 pt, Non Surlignage

Page 16 : [58] Mis en forme	Elsa Garavaglia	25-11-24 10:11:00

Police :10 pt, Non Surlignage

Page 16 : [59] Mis en forme	Danila Aita	21-11-24 16:39:00

Couleur de police : Rouge

Page 16 : [60] Mis en forme	Elsa Garavaglia	25-11-24 10:11:00

Non Surlignage

Page 16 : [60] Mis en forme	Elsa Garavaglia	25-11-24 10:11:00

Non Surlignage

Page 16 : [60] Mis en forme	Elsa Garavaglia	25-11-24 10:11:00

Non Surlignage

Page 16 : [61] Mis en forme	Elsa Garavaglia	25-11-24 10:11:00

Non Surlignage

Page 16 : [61] Mis en forme	Elsa Garavaglia	25-11-24 10:11:00

Non Surlignage

Page 16 : [61] Mis en forme	Elsa Garavaglia	25-11-24 10:11:00

Non Surlignage

Page 16 : [61] Mis en forme	Elsa Garavaglia	25-11-24 10:11:00

Non Surlignage

Page 16 : [62] Mis en forme	Elsa Garavaglia	25-11-24 10:11:00

Couleur de police : Rouge

Page 16 : [62] Mis en forme	Elsa Garavaglia	25-11-24 10:11:00

Couleur de police : Rouge

Page 16 : [63] Mis en forme	Elsa Garavaglia	25-11-24 10:11:00

Non Surlignage

Page 16 : [64] Mis en forme	Elsa Garavaglia	25-11-24 10:11:00

Non Surlignage

Page 16 : [64] Mis en forme	Elsa Garavaglia	25-11-24 10:11:00

Non Surlignage

Page 16 : [65] Mis en forme	Elsa Garavaglia	25-11-24 10:11:00

Couleur de police : Rouge

Page 16 : [65] Mis en forme	Elsa Garavaglia	25-11-24 10:11:00

Couleur de police : Rouge

Page 16 : [65] Mis en forme	Elsa Garavaglia	25-11-24 10:11:00

Couleur de police : Rouge

Page 16 : [66] Mis en forme	Elsa Garavaglia	25-11-24 10:12:00

Non Surlignage

Page 16 : [66] Mis en forme	Elsa Garavaglia	25-11-24 10:12:00

Non Surlignage

Page 16 : [66] Mis en forme	Elsa Garavaglia	25-11-24 10:12:00

Non Surlignage

Page 16 : [66] Mis en forme	Elsa Garavaglia	25-11-24 10:12:00

Non Surlignage

Page 16 : [66] Mis en forme	Elsa Garavaglia	25-11-24 10:12:00

Non Surlignage

Page 16 : [66] Mis en forme	Elsa Garavaglia	25-11-24 10:12:00

Non Surlignage

Page 16 : [66] Mis en forme	Elsa Garavaglia	25-11-24 10:12:00

Non Surlignage

Page 16 : [66] Mis en forme	Elsa Garavaglia	25-11-24 10:12:00

Non Surlignage

Page 16 : [66] Mis en forme	Elsa Garavaglia	25-11-24 10:12:00

Non Surlignage

Page 16 : [67] Mis en forme	Elsa Garavaglia	25-11-24 10:12:00

Non Surlignage

Page 16 : [67] Mis en forme	Elsa Garavaglia	25-11-24 10:12:00

Non Surlignage

Page 16 : [67] Mis en forme	Elsa Garavaglia	25-11-24 10:12:00

Non Surlignage

Page 16 : [67] Mis en forme	Elsa Garavaglia	25-11-24 10:12:00

Non Surlignage

Page 16 : [67] Mis en forme	Elsa Garavaglia	25-11-24 10:12:00

Non Surlignage

Page 16 : [67] Mis en forme	Elsa Garavaglia	25-11-24 10:12:00

Non Surlignage

Page 16 : [67] Mis en forme **Elsa Garavaglia** **25-11-24 10:12:00**

Non Surlignage

Page 16 : [68] Supprimé **Danila Aita** **21-11-24 16:25:00**

according to the equilibrium relation:

$$f_i^{sl\pm} = (W_i + Q_i)\tan\left(\frac{\pi}{2} - \theta_i \pm \psi\right). \qquad (6)$$

In Fig. 3 (right), the

Page 16 : [69] Mis en forme **Elsa Garavaglia** **25-11-24 10:12:00**

Couleur de police : Rouge

Page 16 : [70] Mis en forme **Elsa Garavaglia** **25-11-24 10:12:00**

Couleur de police : Rouge

Page 16 : [70] Mis en forme **Elsa Garavaglia** **25-11-24 10:12:00**

Couleur de police : Rouge

Page 16 : [70] Mis en forme **Elsa Garavaglia** **25-11-24 10:12:00**

Couleur de police : Rouge

Page 16 : [70] Mis en forme **Elsa Garavaglia** **25-11-24 10:12:00**

Couleur de police : Rouge

Page 16 : [70] Mis en forme **Elsa Garavaglia** **25-11-24 10:12:00**

Couleur de police : Rouge

Page 16 : [70] Mis en forme **Elsa Garavaglia** **25-11-24 10:12:00**

Couleur de police : Rouge

Page 16 : [70] Mis en forme **Elsa Garavaglia** **25-11-24 10:12:00**

Couleur de police : Rouge

Page 16 : [70] Mis en forme **Elsa Garavaglia** **25-11-24 10:12:00**

Couleur de police : Rouge

Page 16 : [70] Mis en forme **Elsa Garavaglia** **25-11-24 10:12:00**

Couleur de police : Rouge

Page 16 : [70] Mis en forme **Elsa Garavaglia** **25-11-24 10:12:00**

Couleur de police : Rouge

Page 16 : [70] Mis en forme	Elsa Garavaglia	25-11-24 10:12:00

Couleur de police : Rouge

Page 16 : [70] Mis en forme	Elsa Garavaglia	25-11-24 10:12:00

Couleur de police : Rouge

Page 16 : [70] Mis en forme	Elsa Garavaglia	25-11-24 10:12:00

Couleur de police : Rouge

Page 16 : [70] Mis en forme	Elsa Garavaglia	25-11-24 10:12:00

Couleur de police : Rouge

Page 16 : [70] Mis en forme	Elsa Garavaglia	25-11-24 10:12:00

Couleur de police : Rouge

Page 16 : [70] Mis en forme	Elsa Garavaglia	25-11-24 10:12:00

Couleur de police : Rouge

Page 16 : [70] Mis en forme	Elsa Garavaglia	25-11-24 10:12:00

Couleur de police : Rouge

Page 16 : [70] Mis en forme	Elsa Garavaglia	25-11-24 10:12:00

Couleur de police : Rouge

Page 16 : [70] Mis en forme	Elsa Garavaglia	25-11-24 10:12:00

Couleur de police : Rouge

Page 16 : [70] Mis en forme	Elsa Garavaglia	25-11-24 10:12:00

Couleur de police : Rouge

Page 16 : [71] Mis en forme	Elsa Garavaglia	25-11-24 10:12:00

Couleur de police : Rouge

Page 16 : [71] Mis en forme	Elsa Garavaglia	25-11-24 10:12:00

Couleur de police : Rouge

Page 16 : [72] Mis en forme	Elsa Garavaglia	25-11-24 10:12:00

Couleur de police : Rouge

Page 16 : [72] Mis en forme	Elsa Garavaglia	25-11-24 10:12:00

Couleur de police : Rouge

Page 16 : [73] Mis en forme	Elsa Garavaglia	25-11-24 10:12:00

Couleur de police : Rouge

Page 16 : [73] Mis en forme	Elsa Garavaglia	25-11-24 10:12:00

Couleur de police : Rouge

Page 16 : [73] Mis en forme	Elsa Garavaglia	25-11-24 10:12:00

Couleur de police : Rouge

Page 16 : [74] Mis en forme	Elsa Garavaglia	25-11-24 10:12:00

Couleur de police : Rouge

Page 16 : [74] Mis en forme	Elsa Garavaglia	25-11-24 10:12:00

Couleur de police : Rouge

Page 16 : [75] Mis en forme	Elsa Garavaglia	25-11-24 10:12:00

Couleur de police : Rouge

Page 16 : [75] Mis en forme	Elsa Garavaglia	25-11-24 10:12:00

Couleur de police : Rouge

Page 16 : [75] Mis en forme	Elsa Garavaglia	25-11-24 10:12:00

Couleur de police : Rouge

Page 16 : [76] Mis en forme	Elsa Garavaglia	25-11-24 10:12:00

Non Surlignage

Page 16 : [77] Mis en forme	Elsa Garavaglia	25-11-24 10:12:00

Couleur de police : Rouge

Page 16 : [77] Mis en forme	Elsa Garavaglia	25-11-24 10:12:00

Couleur de police : Rouge

Page 16 : [77] Mis en forme	Elsa Garavaglia	25-11-24 10:12:00

Couleur de police : Rouge

Page 16 : [77] Mis en forme	Elsa Garavaglia	25-11-24 10:12:00

Couleur de police : Rouge

Page 16 : [77] Mis en forme	Elsa Garavaglia	25-11-24 10:12:00

Couleur de police : Rouge

Page 16 : [78] Mis en forme	Elsa Garavaglia	25-11-24 10:12:00

Couleur de police : Rouge

Page 16 : [78] Mis en forme	Elsa Garavaglia	25-11-24 10:12:00

Couleur de police : Rouge

Page 16 : [78] Mis en forme	Elsa Garavaglia	25-11-24 10:12:00

Couleur de police : Rouge

Page 16 : [78] Mis en forme	Elsa Garavaglia	25-11-24 10:12:00

Couleur de police : Rouge

Page 16 : [79] Mis en forme	Danila Aita	26-11-24 07:33:00

Police :Italique

Page 16 : [80] Mis en forme	Elsa Garavaglia	25-11-24 10:12:00

Non Surlignage

Page 16 : [81] Mis en forme	Elsa Garavaglia	25-11-24 10:12:00

Couleur de police : Rouge

Page 16 : [82] Mis en forme	Elsa Garavaglia	25-11-24 10:12:00

Non Surlignage

Page 16 : [82] Mis en forme	Elsa Garavaglia	25-11-24 10:12:00

Non Surlignage

Page 16 : [83] Mis en forme	Elsa Garavaglia	25-11-24 10:12:00

Non Surlignage

Page 16 : [84] Mis en forme	Elsa Garavaglia	25-11-24 10:12:00

Couleur de police : Rouge

Page 16 : [84] Mis en forme	Elsa Garavaglia	25-11-24 10:12:00

Couleur de police : Rouge

Page 16 : [84] Mis en forme	Elsa Garavaglia	25-11-24 10:12:00

Couleur de police : Rouge

Page 16 : [84] Mis en forme	Elsa Garavaglia	25-11-24 10:12:00

Couleur de police : Rouge

Page 16 : [85] Mis en forme	Elsa Garavaglia	25-11-24 10:12:00

Non Surlignage

Page 16 : [85] Mis en forme	Elsa Garavaglia	25-11-24 10:12:00

Non Surlignage

Page 16 : [85] Mis en forme	Elsa Garavaglia	25-11-24 10:12:00

Non Surlignage

Page 16 : [85] Mis en forme	Elsa Garavaglia	25-11-24 10:12:00

Non Surlignage

Page 17 : [86] Mis en forme	Danila Aita	26-11-24 07:38:00

Couleur de police : Rouge

Page 17 : [86] Mis en forme	Danila Aita	26-11-24 07:38:00

Couleur de police : Rouge

Page 17 : [87] Mis en forme	Elsa Garavaglia	25-11-24 10:12:00

Couleur de police : Rouge

Page 17 : [87] Mis en forme	Elsa Garavaglia	25-11-24 10:12:00

Couleur de police : Rouge

Page 17 : [87] Mis en forme	Elsa Garavaglia	25-11-24 10:12:00

Couleur de police : Rouge

Page 17 : [88] Mis en forme	Elsa Garavaglia	25-11-24 10:12:00

Couleur de police : Rouge

Page 17 : [88] Mis en forme	Elsa Garavaglia	25-11-24 10:12:00

Couleur de police : Rouge

Page 17 : [88] Mis en forme	Elsa Garavaglia	25-11-24 10:12:00

Couleur de police : Rouge

Page 17 : [88] Mis en forme	Elsa Garavaglia	25-11-24 10:12:00

Couleur de police : Rouge

Page 17 : [88] Mis en forme	Elsa Garavaglia	25-11-24 10:12:00

Couleur de police : Rouge

Page 17 : [89] Mis en forme	Elsa Garavaglia	25-11-24 10:12:00

Non Surlignage

Page 17 : [89] Mis en forme	Elsa Garavaglia	25-11-24 10:12:00

Non Surlignage

Page 17 : [89] Mis en forme	Elsa Garavaglia	25-11-24 10:12:00

Non Surlignage

Page 17 : [89] Mis en forme	Elsa Garavaglia	25-11-24 10:12:00

Non Surlignage

Page 17 : [89] Mis en forme	Elsa Garavaglia	25-11-24 10:12:00

Non Surlignage

Page 17 : [90] Mis en forme	Elsa Garavaglia	25-11-24 10:12:00

Couleur de police : Rouge

Page 17 : [90] Mis en forme	Elsa Garavaglia	25-11-24 10:12:00

Couleur de police : Rouge

Page 17 : [90] Mis en forme	Elsa Garavaglia	25-11-24 10:12:00

Couleur de police : Rouge

Page 17 : [90] Mis en forme	Elsa Garavaglia	25-11-24 10:12:00

Couleur de police : Rouge

Page 17 : [90] Mis en forme	Elsa Garavaglia	25-11-24 10:12:00

Couleur de police : Rouge

Page 17 : [91] Mis en forme	Elsa Garavaglia	25-11-24 10:13:00

Couleur de police : Rouge

Page 17 : [91] Mis en forme	Elsa Garavaglia	25-11-24 10:13:00

Couleur de police : Rouge

Page 17 : [91] Mis en forme	Elsa Garavaglia	25-11-24 10:13:00

Couleur de police : Rouge

Page 17 : [91] Mis en forme	Elsa Garavaglia	25-11-24 10:13:00

Couleur de police : Rouge

Page 17 : [91] Mis en forme	Elsa Garavaglia	25-11-24 10:13:00

Couleur de police : Rouge

Page 17 : [92] Mis en forme	Danila Aita	26-11-24 07:50:00

Couleur de police : Rouge

Page 17 : [92] Mis en forme	Danila Aita	26-11-24 07:50:00

Couleur de police : Rouge

Page 17 : [92] Mis en forme	Danila Aita	26-11-24 07:50:00

Couleur de police : Rouge

Page 17 : [92] Mis en forme	Danila Aita	26-11-24 07:50:00

Couleur de police : Rouge

Page 17 : [92] Mis en forme	Danila Aita	26-11-24 07:50:00

Couleur de police : Rouge

Page 17 : [92] Mis en forme	Danila Aita	26-11-24 07:50:00

Couleur de police : Rouge

Page 17 : [93] Mis en forme	Danila Aita	26-11-24 07:44:00

Non Surlignage

Page 17 : [93] Mis en forme	Danila Aita	26-11-24 07:44:00

Non Surlignage

Page 17 : [93] Mis en forme	Danila Aita	26-11-24 07:44:00

Non Surlignage

Page 19 : [94] Mis en forme	Danila Aita	21-11-24 13:49:00

Non Surlignage

Page 19 : [94] Mis en forme	Danila Aita	21-11-24 13:49:00

Non Surlignage

Page 19 : [94] Mis en forme	Danila Aita	21-11-24 13:49:00

Non Surlignage

Page 19 : [94] Mis en forme	Danila Aita	21-11-24 13:49:00

Non Surlignage

Page 19 : [95] Mis en forme	Danila Aita	26-11-24 08:32:00

Non Surlignage

Page 19 : [95] Mis en forme	Danila Aita	26-11-24 08:32:00

Non Surlignage

Page 19 : [95] Mis en forme	Danila Aita	26-11-24 08:32:00

Non Surlignage

Page 19 : [95] Mis en forme	Danila Aita	26-11-24 08:32:00

Non Surlignage

Page 19 : [96] Mis en forme	Danila Aita	26-11-24 08:32:00

Non Surlignage

Page 19 : [96] Mis en forme	Danila Aita	26-11-24 08:32:00

Non Surlignage

Page 19 : [96] Mis en forme	Danila Aita	26-11-24 08:32:00

Non Surlignage

Page 19 : [96] Mis en forme	Danila Aita	26-11-24 08:32:00

Non Surlignage

Page 19 : [96] Mis en forme	Danila Aita	26-11-24 08:32:00

Non Surlignage

Page 19 : [96] Mis en forme	Danila Aita	26-11-24 08:32:00

Non Surlignage

Page 19 : [96] Mis en forme	Danila Aita	26-11-24 08:32:00

Non Surlignage

Page 19 : [96] Mis en forme	Danila Aita	26-11-24 08:32:00

Non Surlignage

Page 19 : [97] Mis en forme	Danila Aita	26-11-24 08:32:00

Couleur de police : Rouge

Page 19 : [97] Mis en forme	Danila Aita	26-11-24 08:32:00

Couleur de police : Rouge

Page 19 : [97] Mis en forme	Danila Aita	26-11-24 08:32:00

Couleur de police : Rouge

Page 19 : [97] Mis en forme	Danila Aita	26-11-24 08:32:00

Couleur de police : Rouge

Page 19 : [97] Mis en forme	Danila Aita	26-11-24 08:32:00

Couleur de police : Rouge

Page 19 : [98] Supprimé	**Danila Aita**	**21-11-24 13:58:00**

condition identified

Page 19 : [98] Supprimé	**Danila Aita**	**21-11-24 13:58:00**

condition identified

Page 19 : [99] Mis en forme	**Danila Aita**	**26-11-24 08:32:00**

Non Surlignage

Page 19 : [99] Mis en forme	**Danila Aita**	**26-11-24 08:32:00**

Non Surlignage

Page 19 : [99] Mis en forme	**Danila Aita**	**26-11-24 08:32:00**

Non Surlignage

Page 19 : [100] Mis en forme	**Danila Aita**	**26-11-24 08:32:00**

Non Surlignage

Page 19 : [100] Mis en forme	**Danila Aita**	**26-11-24 08:32:00**

Non Surlignage

Page 19 : [100] Mis en forme	**Danila Aita**	**26-11-24 08:32:00**

Non Surlignage

Page 19 : [100] Mis en forme	**Danila Aita**	**26-11-24 08:32:00**

Non Surlignage

Page 19 : [101] Mis en forme	**Danila Aita**	**26-11-24 08:32:00**

Non Surlignage

Page 19 : [101] Mis en forme	**Danila Aita**	**26-11-24 08:32:00**

Non Surlignage

Page 19 : [101] Mis en forme	**Danila Aita**	**26-11-24 08:32:00**

Non Surlignage

Page 19 : [101] Mis en forme	**Danila Aita**	**26-11-24 08:32:00**

Non Surlignage

Page 19 : [101] Mis en forme	**Danila Aita**	**26-11-24 08:32:00**

Non Surlignage

Page 19 : [102] Mis en forme	Danila Aita	26-11-24 08:32:00

Couleur de police : Rouge

Page 19 : [102] Mis en forme	Danila Aita	26-11-24 08:32:00

Couleur de police : Rouge

Page 19 : [103] Mis en forme	Danila Aita	26-11-24 08:32:00

Couleur de police : Rouge

Page 19 : [103] Mis en forme	Danila Aita	26-11-24 08:32:00

Couleur de police : Rouge

Page 19 : [103] Mis en forme	Danila Aita	26-11-24 08:32:00

Couleur de police : Rouge

Page 19 : [103] Mis en forme	Danila Aita	26-11-24 08:32:00

Couleur de police : Rouge

Page 19 : [104] Mis en forme	Danila Aita	26-11-24 08:32:00

Non Surlignage

Page 19 : [104] Mis en forme	Danila Aita	26-11-24 08:32:00

Non Surlignage

Page 19 : [104] Mis en forme	Danila Aita	26-11-24 08:32:00

Non Surlignage

Page 19 : [104] Mis en forme	Danila Aita	26-11-24 08:32:00

Non Surlignage

Page 19 : [104] Mis en forme	Danila Aita	26-11-24 08:32:00

Non Surlignage

Page 19 : [104] Mis en forme	Danila Aita	26-11-24 08:32:00

Non Surlignage

Page 19 : [104] Mis en forme	Danila Aita	26-11-24 08:32:00

Non Surlignage

Page 19 : [104] Mis en forme	Danila Aita	26-11-24 08:32:00

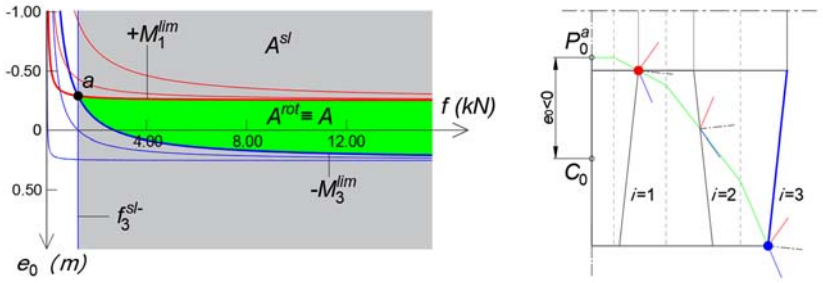
Non Surlignage

Page 19 : [104] Mis en forme	Danila Aita	26-11-24 08:32:00

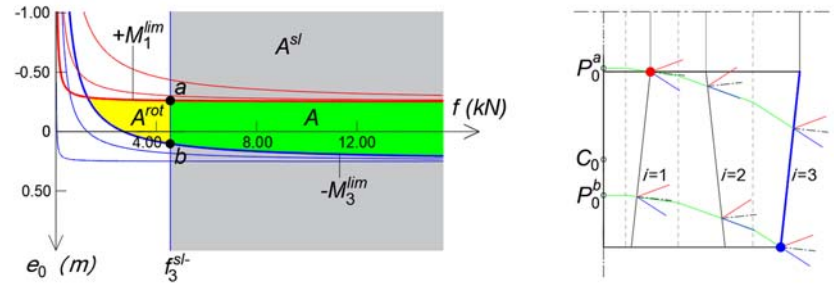
Non Surlignage

Page 20 : [105] Supprimé	Danila Aita	21-11-24 17:15:00

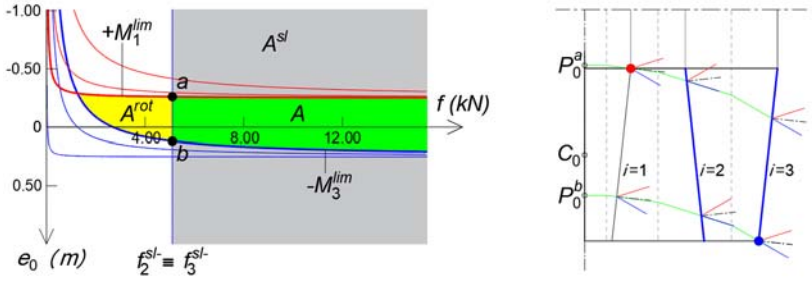
(a)



(b)



(c)



(d)

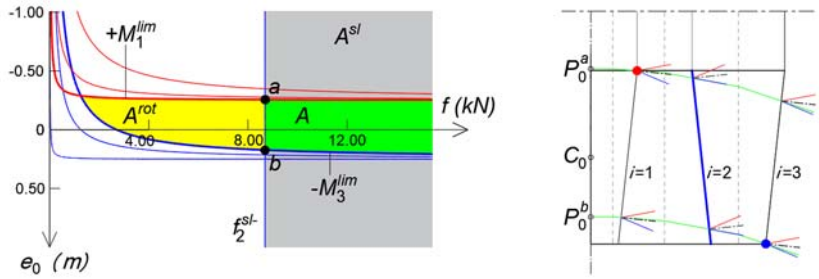


Figure 4. Stability area (left) and thrust line (right) for $H = 1$ m, and: $\mu = 1.7772$ (*a*); $\mu = 0.5$ (*b*); $\mu = 0.4389$ (*c*); $\mu = 0.3$ (*d*). Joints where the limit condition is attained are coloured blue.

Page 22 : [106] Supprimé	Danila Aita	14-11-24 19:41:00

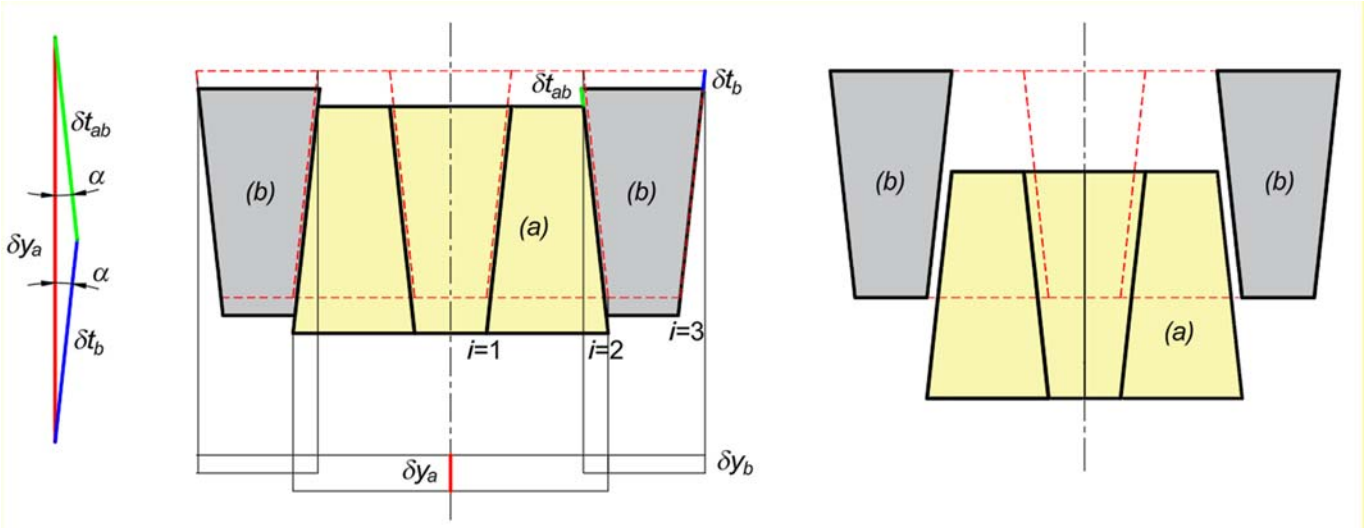


Figure 5. Pure sliding collapse mechanism ($H = 1$ m, $\mu = 0.4389$) (left); collapse mechanism when blocks (*b*) are fixed (right).

Page 22 : [107] Supprimé	Danila Aita	14-11-24 19:41:00

If we now consider for a moment a slightly different case study, imagining that blocks (*b*) are fixed, see Fig. 5, right, it is apparent that block (*a*) could move downwards without a frictional dissipation at the interfaces, unless the structure is subjected to precompression. Indeed, the constraint at joint separating block (*a*) and block (*b*) is non-conventional and the presence of a thrust might not be guaranteed. Concerns regarding the stability of the flat arch are raised by

block (a)'s unusual shape. The above observations are an important point to remember when using static methods on block assemblages. Considering the aforementioned, the case study under consideration can be linked to a few of the instances put forth by Bagi (2014), who focuses on non-Heymanian collapse modes of masonry structures, that is, on the onset of collapse conditions even in situations where statically admissible solutions are found in the hypothesis of an infinite friction. Moereover, it seems interesting to examine this case study in the light of the analysis performed by Ting-Chun Kao et al. (2022), who point out the need of combining both equilibrium and kinematics to assess the stability of rigid blocks assemblages when the shape of the voussoirs is unconventional, and highlight some aspects related both to frictional constraints and detachment between the blocks.

By returning now to the flat arch under examination, for which a finite value of the friction coefficient is assumed, the statically admissible solutions found through the stability area method must be checked also from a kinematic point of view and by considering the global equilibrium of the structure, given the unconventional joint $i = 2$.

Page 23 : [108] Supprimé	Danila Aita	13-11-24 13:17:00

The analytical method just proposed allows for determining the friction coefficient μ_0, above which the rotational domain is fully contained in the sliding domain, by varying the height of the wall, H. By fixing the value of the compressive strength, $\sigma_c = 45$MPa (see Section 2), for $0 \leq H \leq 10$ m, the friction coefficient μ_0 ranges from 1.7158 ($H = 0$) to 1.7991 ($H = 10$ m), while the minimum crown thrust corresponding to a statically admissible solution, i.e., $\max f_i^{sl-}$, increases with H from 0.42456 kN to 8.75852 kN. It is interesting to observe that the value of the friction coefficient μ_0 is affected by the compressive strength σ_c. By fixing now the value of the wall's height, $H = 10$ m, μ_0 increases with σ_c, while the minimum horizontal thrust decreases as the stability area widens. When $\sigma_c = 2.5$ MPa, $\mu_0 = 1.6932$, while $\mu_0 = 1.8049$ is retrieved when the compressive strength is infinite.

Similarly, the semi-analytical approach allows to directly determine the friction coefficient $\boldsymbol{\mu_1}$, which identifies a purely sliding collapse mode (see Fig. 5, left), for different values of the wall height, *H*, by varying the compressive strength. Parametric analyses will be the subject of a forthcoming paper. To the aims of this research, it is interesting to observe that, by fixing $\boldsymbol{\sigma_c = 45\text{MPa}}$, the value of $\boldsymbol{\mu_1}$ increases while decreasing *H*, ranging from $\boldsymbol{\mu_1 = 0.4023}$ (for $\boldsymbol{H = 10\ \text{m}}$) to $\boldsymbol{\mu_1 = 0.5709}$ (for $\boldsymbol{H = 0}$). These values are considerably lower than $\boldsymbol{\mu_0}$.

Page 23 : [109] Mis en forme **Danila Aita** **26-11-24 12:50:00**
Couleur de police : Rouge

Page 23 : [109] Mis en forme **Danila Aita** **26-11-24 12:50:00**
Couleur de police : Rouge

Page 23 : [109] Mis en forme **Danila Aita** **26-11-24 12:50:00**
Couleur de police : Rouge

Page 23 : [110] Mis en forme **Danila Aita** **26-11-24 12:50:00**
Couleur de police : Rouge

Page 23 : [110] Mis en forme **Danila Aita** **26-11-24 12:50:00**
Couleur de police : Rouge

Page 23 : [110] Mis en forme **Danila Aita** **26-11-24 12:50:00**
Couleur de police : Rouge

Page 23 : [111] Mis en forme **Danila Aita** **26-11-24 12:50:00**
Couleur de police : Rouge

Page 23 : [111] Mis en forme **Danila Aita** **26-11-24 12:50:00**
Couleur de police : Rouge

Page 23 : [111] Mis en forme **Danila Aita** **26-11-24 12:50:00**
Couleur de police : Rouge

Page 23 : [112] Mis en forme **Danila Aita** **26-11-24 12:50:00**
Couleur de police : Rouge

Page 23 : [112] Mis en forme **Danila Aita** **26-11-24 12:50:00**
Couleur de police : Rouge

Page 23 : [113] Mis en forme	Danila Aita	26-11-24 12:50:00

Couleur de police : Rouge

Page 23 : [113] Mis en forme	Danila Aita	26-11-24 12:50:00

Couleur de police : Rouge

Page 23 : [114] Mis en forme	Danila Aita	26-11-24 12:50:00

Couleur de police : Rouge

Page 23 : [114] Mis en forme	Danila Aita	26-11-24 12:50:00

Couleur de police : Rouge

Page 23 : [114] Mis en forme	Danila Aita	26-11-24 12:50:00

Couleur de police : Rouge

Page 23 : [114] Mis en forme	Danila Aita	26-11-24 12:50:00

Couleur de police : Rouge

Page 23 : [114] Mis en forme	Danila Aita	26-11-24 12:50:00

Couleur de police : Rouge

Page 23 : [115] Mis en forme	Danila Aita	26-11-24 12:50:00

Couleur de police : Rouge

Page 23 : [115] Mis en forme	Danila Aita	26-11-24 12:50:00

Couleur de police : Rouge

Page 23 : [115] Mis en forme	Danila Aita	26-11-24 12:50:00

Couleur de police : Rouge

Page 23 : [116] Mis en forme	Danila Aita	26-11-24 12:50:00

Couleur de police : Rouge

Page 23 : [116] Mis en forme	Danila Aita	26-11-24 12:50:00

Couleur de police : Rouge

Page 23 : [116] Mis en forme	Danila Aita	26-11-24 12:50:00

Couleur de police : Rouge

Page 23 : [117] Mis en forme	Danila Aita	26-11-24 12:50:00

Couleur de police : Rouge

Page 23 : [117] Mis en forme	Danila Aita	26-11-24 12:50:00

Couleur de police : Rouge

Page 23 : [117] Mis en forme	Danila Aita	26-11-24 12:50:00

Couleur de police : Rouge

Page 23 : [118] Mis en forme	Danila Aita	26-11-24 12:50:00

Couleur de police : Rouge

Page 23 : [118] Mis en forme	Danila Aita	26-11-24 12:50:00

Couleur de police : Rouge

Page 23 : [118] Mis en forme	Danila Aita	26-11-24 12:50:00

Couleur de police : Rouge

Page 23 : [119] Mis en forme	Danila Aita	26-11-24 12:50:00

Couleur de police : Rouge

Page 23 : [119] Mis en forme	Danila Aita	26-11-24 12:50:00

Couleur de police : Rouge

Page 23 : [119] Mis en forme	Danila Aita	26-11-24 12:50:00

Couleur de police : Rouge

Page 23 : [120] Mis en forme	Danila Aita	26-11-24 12:50:00

Couleur de police : Rouge

Page 23 : [120] Mis en forme	Danila Aita	26-11-24 12:50:00

Couleur de police : Rouge

Page 23 : [120] Mis en forme	Danila Aita	26-11-24 12:50:00

Couleur de police : Rouge

Page 23 : [121] Mis en forme	Danila Aita	26-11-24 12:50:00

Couleur de police : Rouge

Page 23 : [121] Mis en forme	Danila Aita	26-11-24 12:50:00

Couleur de police : Rouge

Page 23 : [121] Mis en forme	Danila Aita	26-11-24 12:50:00

Couleur de police : Rouge

Page 23 : [121] Mis en forme	Danila Aita	26-11-24 12:50:00

Couleur de police : Rouge

Page 23 : [122] Mis en forme	Danila Aita	26-11-24 12:50:00

Police :12 pt, Couleur de police : Rouge

Page 23 : [122] Mis en forme	Danila Aita	26-11-24 12:50:00

Police :12 pt, Couleur de police : Rouge

Page 23 : [122] Mis en forme	Danila Aita	26-11-24 12:50:00

Police :12 pt, Couleur de police : Rouge

Page 23 : [123] Mis en forme	Danila Aita	26-11-24 12:50:00

Police :12 pt, Couleur de police : Rouge

Page 23 : [123] Mis en forme	Danila Aita	26-11-24 12:50:00

Police :12 pt, Couleur de police : Rouge

Page 23 : [123] Mis en forme	Danila Aita	26-11-24 12:50:00

Police :12 pt, Couleur de police : Rouge

Page 23 : [123] Mis en forme	Danila Aita	26-11-24 12:50:00

Police :12 pt, Couleur de police : Rouge

Page 23 : [124] Mis en forme	Danila Aita	26-11-24 12:50:00

Police :12 pt, Couleur de police : Rouge

Page 23 : [124] Mis en forme	Danila Aita	26-11-24 12:50:00

Police :12 pt, Couleur de police : Rouge

Page 23 : [124] Mis en forme	Danila Aita	26-11-24 12:50:00

Police :12 pt, Couleur de police : Rouge

Page 23 : [125] Mis en forme	Danila Aita	26-11-24 12:50:00

Police :12 pt, Couleur de police : Rouge

Page 23 : [125] Mis en forme	Danila Aita	26-11-24 12:50:00

Police :12 pt, Couleur de police : Rouge

Page 23 : [125] Mis en forme	Danila Aita	26-11-24 12:50:00

Police :12 pt, Couleur de police : Rouge

Page 23 : [125] Mis en forme	Danila Aita	26-11-24 12:50:00

Police :12 pt, Couleur de police : Rouge

Page 23 : [125] Mis en forme	**Danila Aita**	**26-11-24 12:50:00**

Police :12 pt, Couleur de police : Rouge

Page 23 : [126] Mis en forme	**Danila Aita**	**26-11-24 12:50:00**

Police :(Par défaut) Times New Roman, 12 pt, Couleur de police : Rouge

Page 23 : [127] Mis en forme	**Danila Aita**	**26-11-24 12:50:00**

Police :12 pt, Couleur de police : Rouge

Page 23 : [127] Mis en forme	**Danila Aita**	**26-11-24 12:50:00**

Police :12 pt, Couleur de police : Rouge

Page 23 : [127] Mis en forme	**Danila Aita**	**26-11-24 12:50:00**

Police :12 pt, Couleur de police : Rouge

Page 23 : [127] Mis en forme	**Danila Aita**	**26-11-24 12:50:00**

Police :12 pt, Couleur de police : Rouge

Page 23 : [127] Mis en forme	**Danila Aita**	**26-11-24 12:50:00**

Police :12 pt, Couleur de police : Rouge

Page 23 : [128] Mis en forme	**Danila Aita**	**26-11-24 12:50:00**

Police :(Par défaut) Times New Roman, 12 pt, Couleur de police : Rouge

Page 23 : [129] Mis en forme	**Danila Aita**	**26-11-24 12:50:00**

Police :12 pt, Couleur de police : Rouge

Page 23 : [129] Mis en forme	**Danila Aita**	**26-11-24 12:50:00**

Police :12 pt, Couleur de police : Rouge

Page 23 : [129] Mis en forme	**Danila Aita**	**26-11-24 12:50:00**

Police :12 pt, Couleur de police : Rouge

Page 23 : [129] Mis en forme	**Danila Aita**	**26-11-24 12:50:00**

Police :12 pt, Couleur de police : Rouge

Page 23 : [129] Mis en forme	**Danila Aita**	**26-11-24 12:50:00**

Police :12 pt, Couleur de police : Rouge

Page 23 : [129] Mis en forme	**Danila Aita**	**26-11-24 12:50:00**

Police :12 pt, Couleur de police : Rouge

Page 23 : [130] Mis en forme	Danila Aita	26-11-24 12:50:00

Couleur de police : Rouge

Page 23 : [130] Mis en forme	Danila Aita	26-11-24 12:50:00

Couleur de police : Rouge

Page 23 : [130] Mis en forme	Danila Aita	26-11-24 12:50:00

Couleur de police : Rouge

Page 23 : [131] Mis en forme	Danila Aita	26-11-24 12:54:00

Police :12 pt, Anglais (Royaume-Uni)

Page 23 : [131] Mis en forme	Danila Aita	26-11-24 12:54:00

Police :12 pt, Anglais (Royaume-Uni)

Page 23 : [132] Mis en forme	Danila Aita	26-11-24 12:54:00

Non Surlignage

Page 23 : [132] Mis en forme	Danila Aita	26-11-24 12:54:00

Non Surlignage

Page 23 : [132] Mis en forme	Danila Aita	26-11-24 12:54:00

Non Surlignage

Page 23 : [133] Mis en forme	Danila Aita	26-11-24 12:54:00

Non Surlignage

Page 23 : [133] Mis en forme	Danila Aita	26-11-24 12:54:00

Non Surlignage

Page 23 : [133] Mis en forme	Danila Aita	26-11-24 12:54:00

Non Surlignage

Page 23 : [134] Mis en forme	Danila Aita	26-11-24 12:54:00

Non Surlignage

Page 23 : [134] Mis en forme	Danila Aita	26-11-24 12:54:00

Non Surlignage

Page 23 : [134] Mis en forme	Danila Aita	26-11-24 12:54:00

Non Surlignage

Page 23 : [135] Mis en forme	Danila Aita	26-11-24 12:54:00

Non Surlignage

Page 23 : [135] Mis en forme	Danila Aita	26-11-24 12:54:00

Non Surlignage

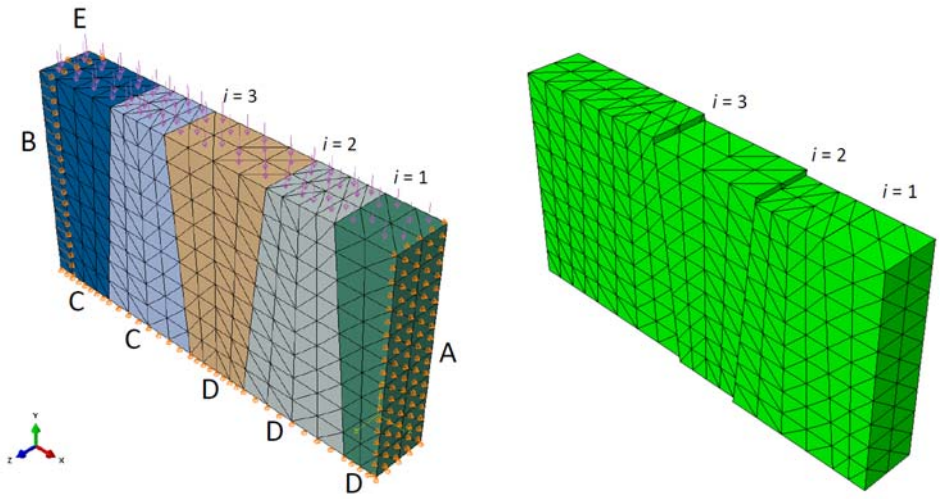
Page 23 : [135] Mis en forme	Danila Aita	26-11-24 12:54:00

Non Surlignage

Page 23 : [136] Supprimé	Danila Aita	26-11-24 12:53:00

[EG1]

Page 26 : [137] Supprimé	Danila Aita	24-11-24 18:09:00



Page 31 : [138] Mis en forme	Danila Aita	28-11-24 08:38:00

Non Surlignage

Page 31 : [138] Mis en forme	Danila Aita	28-11-24 08:38:00

Non Surlignage

Page 31 : [138] Mis en forme	Danila Aita	28-11-24 08:38:00

Non Surlignage

Page 31 : [139] Mis en forme	Danila Aita	28-11-24 08:38:00

Non Surlignage

Page 31 : [139] Mis en forme	Danila Aita	28-11-24 08:38:00

Non Surlignage

Page 31 : [140] Mis en forme	Danila Aita	28-11-24 08:38:00

Non Surlignage

Page 31 : [140] Mis en forme	Danila Aita	28-11-24 08:38:00

Non Surlignage

Page 31 : [140] Mis en forme	Danila Aita	28-11-24 08:38:00

Non Surlignage

Page 31 : [140] Mis en forme	Danila Aita	28-11-24 08:38:00

Non Surlignage

Page 31 : [141] Mis en forme	Danila Aita	28-11-24 08:40:00

Non Surlignage

Page 31 : [141] Mis en forme	Danila Aita	28-11-24 08:40:00

Non Surlignage

Page 31 : [141] Mis en forme	Danila Aita	28-11-24 08:40:00

Non Surlignage

Page 31 : [141] Mis en forme	Danila Aita	28-11-24 08:40:00

Non Surlignage

Page 31 : [141] Mis en forme	Danila Aita	28-11-24 08:40:00

Non Surlignage

Page 31 : [141] Mis en forme	Danila Aita	28-11-24 08:40:00

Non Surlignage

Page 31 : [141] Mis en forme	Danila Aita	28-11-24 08:40:00

Non Surlignage

Page 31 : [141] Mis en forme	Danila Aita	28-11-24 08:40:00

Non Surlignage

Page 31 : [141] Mis en forme	Danila Aita	28-11-24 08:40:00

Non Surlignage

Page 31 : [141] Mis en forme	Danila Aita	28-11-24 08:40:00

Non Surlignage

Page 31 : [141] Mis en forme	Danila Aita	28-11-24 08:40:00

Non Surlignage

Page 31 : [141] Mis en forme	Danila Aita	28-11-24 08:40:00

Non Surlignage

Page 31 : [141] Mis en forme	Danila Aita	28-11-24 08:40:00

Non Surlignage

Page 31 : [141] Mis en forme	Danila Aita	28-11-24 08:40:00

Non Surlignage

Page 31 : [141] Mis en forme	Danila Aita	28-11-24 08:40:00

Non Surlignage

Page 31 : [141] Mis en forme	Danila Aita	28-11-24 08:40:00

Non Surlignage

Page 31 : [141] Mis en forme	Danila Aita	28-11-24 08:40:00

Non Surlignage

Page 31 : [141] Mis en forme	Danila Aita	28-11-24 08:40:00

Non Surlignage

Page 31 : [141] Mis en forme	Danila Aita	28-11-24 08:40:00

Non Surlignage

Page 31 : [141] Mis en forme	Danila Aita	28-11-24 08:40:00

Non Surlignage

Page 31 : [141] Mis en forme	Danila Aita	28-11-24 08:40:00

Non Surlignage

Page 31 : [141] Mis en forme	Danila Aita	28-11-24 08:40:00

Non Surlignage

Page 31 : [141] Mis en forme	Danila Aita	28-11-24 08:40:00

Non Surlignage

Page 31 : [141] Mis en forme	Danila Aita	28-11-24 08:40:00

Non Surlignage

Page 31 : [141] Mis en forme	Danila Aita	28-11-24 08:40:00

Non Surlignage

Page 31 : [141] Mis en forme	Danila Aita	28-11-24 08:40:00

Non Surlignage

Page 31 : [141] Mis en forme	Danila Aita	28-11-24 08:40:00

Non Surlignage

Page 31 : [141] Mis en forme	Danila Aita	28-11-24 08:40:00

Non Surlignage

Page 31 : [141] Mis en forme	Danila Aita	28-11-24 08:40:00

Non Surlignage

Page 31 : [141] Mis en forme	Danila Aita	28-11-24 08:40:00

Non Surlignage

Page 31 : [141] Mis en forme	Danila Aita	28-11-24 08:40:00

Non Surlignage

Page 31 : [141] Mis en forme	Danila Aita	28-11-24 08:40:00

Non Surlignage

Page 31 : [141] Mis en forme	Danila Aita	28-11-24 08:40:00

Non Surlignage

Page 31 : [141] Mis en forme	Danila Aita	28-11-24 08:40:00

Non Surlignage

Page 31 : [141] Mis en forme	Danila Aita	28-11-24 08:40:00

Non Surlignage

Page 31 : [141] Mis en forme	Danila Aita	28-11-24 08:40:00

Non Surlignage

Page 31 : [141] Mis en forme	Danila Aita	28-11-24 08:40:00

Non Surlignage

Page 31 : [141] Mis en forme	Danila Aita	28-11-24 08:40:00

Non Surlignage

Page 31 : [141] Mis en forme	Danila Aita	28-11-24 08:40:00

Non Surlignage

Page 31 : [141] Mis en forme	Danila Aita	28-11-24 08:40:00

Non Surlignage

Page 31 : [141] Mis en forme	Danila Aita	28-11-24 08:40:00

Non Surlignage

Page 31 : [141] Mis en forme	Danila Aita	28-11-24 08:40:00

Non Surlignage

Page 31 : [141] Mis en forme	Danila Aita	28-11-24 08:40:00

Non Surlignage

Page 31 : [141] Mis en forme	Danila Aita	28-11-24 08:40:00

Non Surlignage

Page 31 : [141] Mis en forme	Danila Aita	28-11-24 08:40:00

Non Surlignage

Page 31 : [141] Mis en forme	Danila Aita	28-11-24 08:40:00

Non Surlignage

Page 31 : [142] Mis en forme	Danila Aita	28-11-24 08:40:00

Non Surlignage

Page 31 : [142] Mis en forme	Danila Aita	28-11-24 08:40:00

Non Surlignage

Page 31 : [142] Mis en forme	Danila Aita	28-11-24 08:40:00

Non Surlignage

Page 31 : [142] Mis en forme	Danila Aita	28-11-24 08:40:00

Non Surlignage

Page 31 : [142] Mis en forme	Danila Aita	28-11-24 08:40:00

Non Surlignage

Page 31 : [142] Mis en forme	Danila Aita	28-11-24 08:40:00

Non Surlignage

Page 31 : [142] Mis en forme	Danila Aita	28-11-24 08:40:00

Non Surlignage

Page 31 : [142] Mis en forme	Danila Aita	28-11-24 08:40:00

Non Surlignage

Page 31 : [142] Mis en forme	Danila Aita	28-11-24 08:40:00

Non Surlignage

Page 31 : [142] Mis en forme	Danila Aita	28-11-24 08:40:00

Non Surlignage

Page 31 : [142] Mis en forme	Danila Aita	28-11-24 08:40:00

Non Surlignage

Page 31 : [142] Mis en forme	Danila Aita	28-11-24 08:40:00

Non Surlignage

Page 31 : [142] Mis en forme	Danila Aita	28-11-24 08:40:00

Non Surlignage

Page 31 : [142] Mis en forme	Danila Aita	28-11-24 08:40:00

Non Surlignage

Page 31 : [142] Mis en forme	Danila Aita	28-11-24 08:40:00

Non Surlignage

Page 31 : [142] Mis en forme	Danila Aita	28-11-24 08:40:00

Non Surlignage

Page 31 : [142] Mis en forme	Danila Aita	28-11-24 08:40:00

Non Surlignage

Page 31 : [142] Mis en forme	Danila Aita	28-11-24 08:40:00

Non Surlignage

Page 31 : [142] Mis en forme	Danila Aita	28-11-24 08:40:00

Non Surlignage

Page 31 : [142] Mis en forme	Danila Aita	28-11-24 08:40:00

Non Surlignage

Page 31 : [143] Mis en forme	Danila Aita	28-11-24 08:40:00

Non Surlignage

Page 31 : [143] Mis en forme	Danila Aita	28-11-24 08:40:00

Non Surlignage

Page 31 : [143] Mis en forme	Danila Aita	28-11-24 08:40:00

Non Surlignage

Page 31 : [143] Mis en forme	Danila Aita	28-11-24 08:40:00

Non Surlignage

Page 31 : [143] Mis en forme	Danila Aita	28-11-24 08:40:00

Non Surlignage

Page 31 : [143] Mis en forme	Danila Aita	28-11-24 08:40:00

Non Surlignage

Page 31 : [143] Mis en forme	Danila Aita	28-11-24 08:40:00

Non Surlignage

Page 31 : [143] Mis en forme	Danila Aita	28-11-24 08:40:00

Non Surlignage

Page 31 : [143] Mis en forme	Danila Aita	28-11-24 08:40:00

Non Surlignage

Page 31 : [143] Mis en forme	Danila Aita	28-11-24 08:40:00

Non Surlignage

Page 31 : [143] Mis en forme	Danila Aita	28-11-24 08:40:00

Non Surlignage

Page 31 : [143] Mis en forme	Danila Aita	28-11-24 08:40:00

Non Surlignage

Page 31 : [143] Mis en forme	Danila Aita	28-11-24 08:40:00

Non Surlignage

Page 31 : [144] Mis en forme	Danila Aita	28-11-24 08:44:00

Couleur de police : Rouge, Non Surlignage

Page 31 : [144] Mis en forme	Danila Aita	28-11-24 08:44:00

Couleur de police : Rouge, Non Surlignage

Page 31 : [144] Mis en forme	Danila Aita	28-11-24 08:44:00

Couleur de police : Rouge, Non Surlignage

Page 31 : [144] Mis en forme	Danila Aita	28-11-24 08:44:00

Couleur de police : Rouge, Non Surlignage

Page 31 : [144] Mis en forme	Danila Aita	28-11-24 08:44:00

Couleur de police : Rouge, Non Surlignage

Page 31 : [144] Mis en forme	Danila Aita	28-11-24 08:44:00

Couleur de police : Rouge, Non Surlignage

Page 31 : [145] Mis en forme	Danila Aita	28-11-24 08:45:00

Couleur de police : Rouge, Non Surlignage

Page 31 : [145] Mis en forme	Danila Aita	28-11-24 08:45:00

Couleur de police : Rouge, Non Surlignage

Page 31 : [145] Mis en forme	Danila Aita	28-11-24 08:45:00

Couleur de police : Rouge, Non Surlignage

Page 31 : [145] Mis en forme	Danila Aita	28-11-24 08:45:00

Couleur de police : Rouge, Non Surlignage

Page 31 : [146] Mis en forme	Danila Aita	28-11-24 08:52:00

Non Surlignage

Page 31 : [146] Mis en forme	Danila Aita	28-11-24 08:52:00

Non Surlignage

Page 31 : [146] Mis en forme	Danila Aita	28-11-24 08:52:00

Non Surlignage

Page 31 : [146] Mis en forme	Danila Aita	28-11-24 08:52:00

Non Surlignage

Page 31 : [146] Mis en forme	Danila Aita	28-11-24 08:52:00

Non Surlignage

Page 31 : [146] Mis en forme	Danila Aita	28-11-24 08:52:00

Non Surlignage

Page 31 : [146] Mis en forme **Danila Aita** **28-11-24 08:52:00**

Non Surlignage

Page 31 : [146] Mis en forme **Danila Aita** **28-11-24 08:52:00**

Non Surlignage

Page 31 : [146] Mis en forme **Danila Aita** **28-11-24 08:52:00**

Non Surlignage

Page 31 : [146] Mis en forme **Danila Aita** **28-11-24 08:52:00**

Non Surlignage

Page 31 : [147] Mis en forme **Danila Aita** **28-11-24 08:53:00**

Couleur de police : Rouge

Page 31 : [147] Mis en forme **Danila Aita** **28-11-24 08:53:00**

Couleur de police : Rouge

Page 34 : [148] Supprimé **Danila Aita** **28-11-24 08:57:00**

As mentioned in the Introduction, advances in computational capabilities, have led to the development of various approaches to address equilibrium conditions of blocky structures (Baggio and Trovalusci, 2000; Orduña and Lourenço, 2005; Portioli et al., 2014) through mathematical programming.

The results presented here aim to clarify the meaning of limit solutions obtained by means of the lower bound approach for the flat arch with non-conventional voussoirs. A multi-objective optimization procedure is adopted to find the minimum friction coefficient compatible with the equilibrium of the flat arch. As will be clarified below, the non-standard behaviour of the system strongly affects the limit analysis of such type of structure, showing that static methods must be used with caution when assessing the stability of unconventional block structures.

To visualize the interaction between the values of the friction coefficient and internal forces, a verification is conducted limited to the equilibrium conditions. Following the original proposal by Livesley (1978), the method imposes the equilibrium of each block against translations and

rotation, and the related equations, expressed in matrix formulation, are then composed for the whole structure as: $[A][X]=[B]$, where $[A]$ is the coefficient matrix of the vector of unknown internal force components $[X]$, and $[B]$ is the vector of external forces. Due to the indeterminacy of the problem, the matrix $[A]$ is vertically rectangular. This, along with the linearity of the equations, categorizes the problem as a linear programming or linear optimization problem.

The contact surface can be modelled either with a convex model, in which all forces and moments are assumed concentrated at the centre of convexity of the contact surface, or in a non-convex formulation, where they spread across the contact interface (Livesley, 1992). The latter approach is followed here due to its more straightforward implementation when limit strengths are assumed. With reference to Figure 9a, being the problem 2D, three forces are sufficient to describe each contact interface (j, j+1). Two normal forces, $f^{+}_{n(j,j+1)}$ and $f^{-}_{n(j,j+1)}$, account for non-uniform axial stress distribution and related bending/crushing failure, whereas a tangential force $f_{t(j,j+1)}$ accounts for possible deviations of the thrust line from normal to the contact interface and allows for consideration of potential sliding failure. The external actions are applied at the centers of mass G_j of the j-th blocks subjected to self-weight and the weight of an upper wall of height 1 m, as done in Section 3.2 and in Section 4. Considering half a structure due to symmetry, the resulting matrix $[A]$ is a [9,11] matrix.

Bearing in mind the above, the problem is formulated as a multi-objective optimization aimed at minimizing the friction coefficient μ and the sum of internal normal forces, as follows:

Objective Function:

Minimize μ and $\sum_{j=1}^{n} f_{(j,j+1)}$

$$\textit{subject to} \begin{cases} [A][X]=[B] \\ \left|f_{t(j,j+1)}\right| \le \left(f^{+}_{n(j,j+1)}+f^{-}_{n(j,j+1)}\right)\cdot\mu \\ f^{+}_{n(j,j+1)}+f^{-}_{n(j,j+1)} \le \sigma_{ck}\cdot S \\ 0 \le f^{-}_{n(j,j+1)}, f^{+}_{n(j,j+1)} \end{cases} \quad (8)$$

In accordance with the settings described in Section 2, $[B]$ is null except for the vertical contribution to external forces G_j due to the self-weight and the weight of a superimposed 1 m wall made of the same material. The second constraint represents the friction model according to Coulomb's law. The last constraints refer to the strength limits of the material, considered in a simplified way, and impose respectively null tensile strength (assuming compression positive, according to the notation in Figure 9) and finite compressive strength, being $\sigma_c = 46$ MPa, and S the cross-section of the blocks. The formulation has been implemented in Visual Studio using the Gurobi Optimizer solver.

The solver converges to a solution for an extremely low value of friction coefficient $\mu = 0.111$. This value is slightly larger than $\tan(\alpha)$, where α is the angle of the joints separating the blocks to the vertical. The resultant forces, expressed in kN and approximated to the integer, are visualized in Figure 9b. Plotting the thrust line associated with the found components of internal forces, Figure 9c, reveals that the three central blocks tend to act as an arch resting on the free blocks at the end. This configuration is deemed stable assuming that a compression force $f_{n(3,2)} = f_{n(2,3)}$ can be developed large enough that the tangential force $f_{t(2,3)} = f_{n(2,3)} \cdot \tan(\alpha)$ is resisted by a tangential frictional force $f_{t(3,2)} = f_{n(2,3)} \cdot \mu$. Such a force $f_{n(2,3)}$ could only be obtained if the central blocks were pre-compressed by the free end blocks. Note that for this low value of the friction coefficient, $\mu = 0.111$, the value of the horizontal thrust, provided by $f^{+}_{n(0,1)} + f^{-}_{n(0,1)}$, is considerably greater compared to the value of f_3^{sl-} obtained in Section 3.2 for $\mu = 0.4389$.

It is worth observing that, when the friction angle tends to the inclination of the joints, i.e., $\mu \to \tan(\alpha)$, the horizontal thrust diverges, and equilibrium is not possible. Therefore, not accounting for the kinematic aspects corresponding to the equilibrium solutions, the procedure overestimates the safety level, by determining the minimum friction coefficient compatible with the possibility of equilibrium under the assumption that a precompression force is present. Thus,

a purely static procedure cannot identify the limit value of the friction coefficient compatible with the equilibrium of the structure when such a precompression force is absent (or is removed), as is the case of $\mu = 0.4389$ (see Sect. 3.2 and Sect. 4).

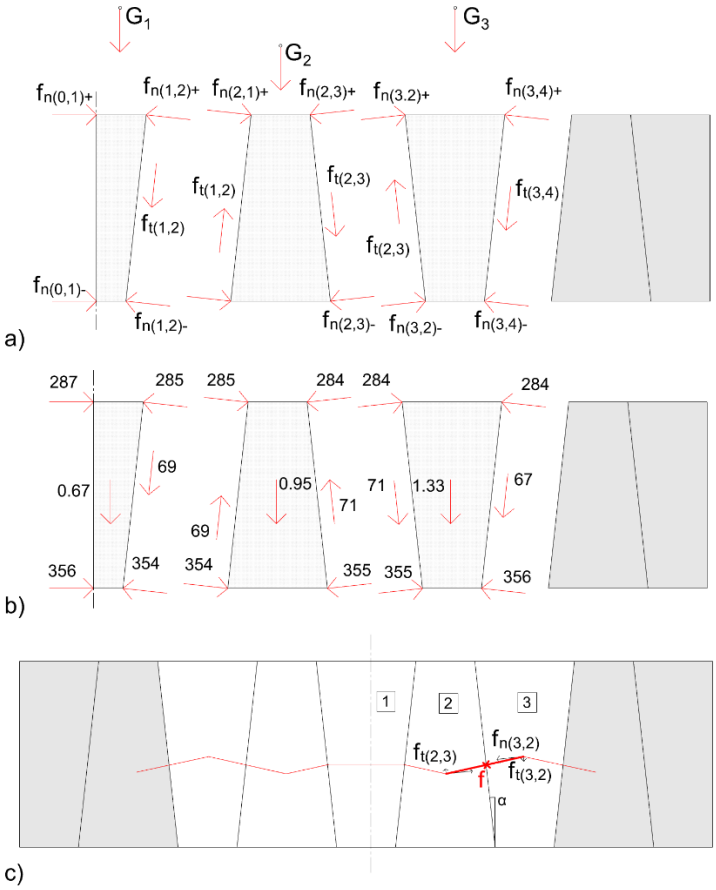


Figure 9. The blocks and notations used in the mathematical programming problem, imposing equilibrium (*a*) and resulting forces, expressed in kN (*b*). The corresponding thrust line (*c*).

The results obtained by means of the lower bound approach just described can be read in light of the observations reported at the end of Section 3.1, related to the stability area method when considering the peculiar inclination of joint $i = 2$. As noted, equilibrium conditions are possible only if $\psi > \alpha$, since if $\psi \leq \alpha$, both f_i^{sl-} and f_i^{sl+} are unbounded, and the stability area vanishes.Finally, it is remarked that both the Durand-Claye method and the optimization problem described here are based on the static theorem of limit analysis, without considerations of the flow rule. This is the reason why there is a large difference between the value of the

friction coefficient just obtained (μ = 0.111) and that derived by the integrated approach presented in Section 3.2 by assuming a non-associated flow rule (μ = 0.4389). Static methods, if not complemented by kinematic analyses, as those performed in Section 3.2, provide an unsafe value of the limit friction coefficient. Further insights into the assumptions on dilatancy with reference to the unconventional joints will be the subject of future research.

Page 34 : [149] Mis en forme	**Danila Aita**	**26-11-24 19:43:00**

Couleur de police : Rouge

Page 34 : [149] Mis en forme	**Danila Aita**	**26-11-24 19:43:00**

Couleur de police : Rouge

Page 34 : [149] Mis en forme	**Danila Aita**	**26-11-24 19:43:00**

Couleur de police : Rouge

Page 34 : [150] Mis en forme	**Danila Aita**	**27-11-24 08:01:00**

Surlignage

Page 34 : [150] Mis en forme	**Danila Aita**	**27-11-24 08:01:00**

Surlignage

Page 34 : [150] Mis en forme	**Danila Aita**	**27-11-24 08:01:00**

Surlignage

Page 34 : [150] Mis en forme	**Danila Aita**	**27-11-24 08:01:00**

Surlignage

Page 34 : [151] Mis en forme	**Danila Aita**	**27-11-24 08:01:00**

Surlignage

Page 34 : [151] Mis en forme	**Danila Aita**	**27-11-24 08:01:00**

Surlignage

Page 34 : [151] Mis en forme	**Danila Aita**	**27-11-24 08:01:00**

Surlignage

Page 34 : [151] Mis en forme	**Danila Aita**	**27-11-24 08:01:00**

Surlignage

Page 34 : [151] Mis en forme	Danila Aita	27-11-24 08:01:00

Surlignage

Page 34 : [152] Mis en forme	Danila Aita	27-11-24 08:01:00

Surlignage

Page 34 : [152] Mis en forme	Danila Aita	27-11-24 08:01:00

Surlignage

Page 34 : [152] Mis en forme	Danila Aita	27-11-24 08:01:00

Surlignage

Page 34 : [152] Mis en forme	Danila Aita	27-11-24 08:01:00

Surlignage

Page 34 : [152] Mis en forme	Danila Aita	27-11-24 08:01:00

Surlignage

Page 34 : [152] Mis en forme	Danila Aita	27-11-24 08:01:00

Surlignage

Page 34 : [152] Mis en forme	Danila Aita	27-11-24 08:01:00

Surlignage

Page 34 : [152] Mis en forme	Danila Aita	27-11-24 08:01:00

Surlignage

Page 34 : [152] Mis en forme	Danila Aita	27-11-24 08:01:00

Surlignage

Page 34 : [152] Mis en forme	Danila Aita	27-11-24 08:01:00

Surlignage

Page 34 : [152] Mis en forme	Danila Aita	27-11-24 08:01:00

Surlignage

Page 34 : [152] Mis en forme	Danila Aita	27-11-24 08:01:00

Surlignage

Page 34 : [152] Mis en forme	Danila Aita	27-11-24 08:01:00

Surlignage

Page 34 : [152] Mis en forme	Danila Aita	27-11-24 08:01:00

Surlignage

Page 34 : [152] Mis en forme	Danila Aita	27-11-24 08:01:00

Surlignage

Page 34 : [152] Mis en forme	Danila Aita	27-11-24 08:01:00

Surlignage

Page 34 : [152] Mis en forme	Danila Aita	27-11-24 08:01:00

Surlignage

Page 34 : [152] Mis en forme	Danila Aita	27-11-24 08:01:00

Surlignage

Page 34 : [152] Mis en forme	Danila Aita	27-11-24 08:01:00

Surlignage

Page 34 : [152] Mis en forme	Danila Aita	27-11-24 08:01:00

Surlignage

Page 34 : [152] Mis en forme	Danila Aita	27-11-24 08:01:00

Surlignage

Page 34 : [152] Mis en forme	Danila Aita	27-11-24 08:01:00

Surlignage

Page 34 : [152] Mis en forme	Danila Aita	27-11-24 08:01:00

Surlignage

Page 34 : [152] Mis en forme	Danila Aita	27-11-24 08:01:00

Surlignage

Page 34 : [152] Mis en forme	Danila Aita	27-11-24 08:01:00

Surlignage

Page 34 : [152] Mis en forme	Danila Aita	27-11-24 08:01:00

Surlignage

Page 34 : [152] Mis en forme	Danila Aita	27-11-24 08:01:00

Surlignage

Page 34 : [152] Mis en forme	Danila Aita	27-11-24 08:01:00

Surlignage

Page 34 : [152] Mis en forme	Danila Aita	27-11-24 08:01:00

Surlignage

Page 34 : [152] Mis en forme	Danila Aita	27-11-24 08:01:00

Surlignage

Page 34 : [152] Mis en forme	Danila Aita	27-11-24 08:01:00

Surlignage

Page 34 : [152] Mis en forme	Danila Aita	27-11-24 08:01:00

Surlignage

Page 34 : [152] Mis en forme	Danila Aita	27-11-24 08:01:00

Surlignage

Page 34 : [152] Mis en forme	Danila Aita	27-11-24 08:01:00

Surlignage

Page 34 : [152] Mis en forme	Danila Aita	27-11-24 08:01:00

Surlignage

Page 34 : [152] Mis en forme	Danila Aita	27-11-24 08:01:00

Surlignage

Page 34 : [152] Mis en forme	Danila Aita	27-11-24 08:01:00

Surlignage

Page 34 : [152] Mis en forme	Danila Aita	27-11-24 08:01:00

Surlignage

Page 34 : [152] Mis en forme	Danila Aita	27-11-24 08:01:00

Surlignage

Page 34 : [152] Mis en forme	Danila Aita	27-11-24 08:01:00

Surlignage

Page 34 : [152] Mis en forme	Danila Aita	27-11-24 08:01:00

Surlignage

Page 34 : [152] Mis en forme	Danila Aita	27-11-24 08:01:00

Surlignage

Page 34 : [153] Mis en forme	Danila Aita	24-11-24 16:54:00

Couleur de police : Rouge

Page 34 : [153] Mis en forme	Danila Aita	24-11-24 16:54:00

Couleur de police : Rouge

Page 34 : [154] Mis en forme	Danila Aita	26-11-24 17:34:00

Couleur de police : Rouge

Page 34 : [154] Mis en forme	Danila Aita	26-11-24 17:34:00

Couleur de police : Rouge

Page 34 : [155] Mis en forme	Danila Aita	24-11-24 16:58:00

Couleur de police : Rouge, Surlignage

Page 34 : [155] Mis en forme	Danila Aita	24-11-24 16:58:00

Couleur de police : Rouge, Surlignage

Page 34 : [156] Mis en forme	Elsa Garavaglia	25-11-24 10:28:00

Surlignage

Page 34 : [156] Mis en forme	Elsa Garavaglia	25-11-24 10:28:00

Surlignage

Page 34 : [156] Mis en forme	Elsa Garavaglia	25-11-24 10:28:00

Surlignage

Page 34 : [156] Mis en forme	Elsa Garavaglia	25-11-24 10:28:00

Surlignage

Page 34 : [157] Mis en forme	Elsa Garavaglia	25-11-24 10:28:00

Surlignage

Page 34 : [157] Mis en forme	Elsa Garavaglia	25-11-24 10:28:00

Surlignage

Page 34 : [157] Mis en forme	Elsa Garavaglia	25-11-24 10:28:00

Surlignage

Page 34 : [157] Mis en forme	Elsa Garavaglia	25-11-24 10:28:00

Surlignage

Page 34 : [158] Mis en forme	Danila Aita	26-11-24 17:35:00

Couleur de police : Rouge, Barré

Page 34 : [158] Mis en forme	Danila Aita	26-11-24 17:35:00

Couleur de police : Rouge, Barré

Page 34 : [158] Mis en forme **Danila Aita** **26-11-24 17:35:00**

Couleur de police : Rouge, Barré

Page 34 : [159] Supprimé **Danila Aita** **26-11-24 19:45:00**

Non-Smooth Contact Dynamics (

Page 34 : [159] Supprimé **Danila Aita** **26-11-24 19:45:00**

Non-Smooth Contact Dynamics (

Page 34 : [160] Supprimé **Danila Aita** **26-11-24 17:36:00**

As discussed in Section 3 about FEM analysis, also in this case the influence of the limited value of the compressive strength on the collapse response of the flat arch is not evident, therefore the infinite compressive strength can be assumed. See also Section 4.

Page 34 : [161] Mis en forme **Elsa Garavaglia** **25-11-24 09:52:00**

Couleur de police : Rouge, Surlignage

Page 34 : [161] Mis en forme **Elsa Garavaglia** **25-11-24 09:52:00**

Couleur de police : Rouge, Surlignage

Page 34 : [162] Mis en forme **Danila Aita** **28-11-24 12:32:00**

Couleur de police : Rouge, Barré, Surlignage

Page 34 : [162] Mis en forme **Danila Aita** **28-11-24 12:32:00**

Couleur de police : Rouge, Barré, Surlignage

Page 47 : [163] Mis en forme **Danila Aita** **15-11-24 06:55:00**

Police :(Par défaut) Times New Roman, 12 pt, Couleur de police : Rouge, Anglais (Royaume-Uni)

Page 47 : [164] Mis en forme **Danila Aita** **15-11-24 06:55:00**

Police :(Par défaut) Times New Roman, 12 pt, Couleur de police : Rouge

Page 47 : [165] Mis en forme **Danila Aita** **15-11-24 06:55:00**

Police :(Par défaut) Times New Roman, 12 pt, Couleur de police : Rouge, Anglais (Royaume-Uni)

Page 47 : [166] Supprimé **Danila Aita** **15-11-24 06:54:00**

Page 47 : [167] Mis en forme	Danila Aita	24-11-24 17:34:00

Couleur de police : Rouge, Non Surlignage

Page 47 : [168] Mis en forme	Danila Aita	24-11-24 17:34:00

Police :(Par défaut) Times New Roman, 12 pt, Couleur de police : Rouge, Non Surlignage

Page 47 : [169] Mis en forme	Danila Aita	24-11-24 17:34:00

Couleur de police : Rouge, Non Surlignage

Page 47 : [170] Mis en forme	Danila Aita	24-11-24 17:34:00

Police :(Par défaut) Times New Roman, 12 pt, Couleur de police : Rouge, Non Surlignage

Page 47 : [171] Mis en forme	Danila Aita	24-11-24 17:34:00

Couleur de police : Rouge, Non Surlignage

Page 47 : [172] Mis en forme	Danila Aita	24-11-24 17:34:00

Police :(Par défaut) Times New Roman, 12 pt, Couleur de police : Rouge, Non Surlignage

Page 47 : [173] Mis en forme	Danila Aita	24-11-24 17:34:00

Couleur de police : Rouge, Non Surlignage

Page 47 : [174] Mis en forme	Danila Aita	24-11-24 17:34:00

Couleur de police : Rouge, Non Surlignage

Page 51 : [175] Supprimé	Danila Aita	24-11-24 18:00:00

Figure 3. Equilibrium of the portion of the structure comprised between the ideal vertical joint at the midspan and any joint *i*: stress resultants (left); friction cone of amplitude ψ (right).

Figure 4. Stability area (left) and thrust line (right) for $H = 1$ m, and: $\mu = 1.7772$ (*a*); $\mu = 0.5$ (*b*); $\mu = 0.4389$ (*c*); $\mu = 0.3$ (*d*). Joints where the limit condition is attained are coloured blue.

Figure 5. Pure sliding collapse mechanism ($H = 1$ m, $\mu = 0.4389$) (left); collapse mechanism when blocks (*b*) are fixed (right).

Figure 6. Geometry of the flat arch with highlighting the joints between the parts and the constraints (left); deformed configuration in the equilibrium situation after all precompression action has been removed (right).

Figure 7. Contour plot of contact force values (CNORMF variable).

Figure 8. Equilibrium configurations depending on the load (1-3). Collapse mechanism that occurs during load step 4 for a load higher than the reference load (4).

Figure 9. The blocks and notations used in the mathematical programming problem, imposing equilibrium (*a*) and resulting forces, expressed in kN (*b*). The corresponding thrust line (*c*).

Figure 10. Snapshots from the NSCD simulation at $T = 3$ s, for $\Delta t = 0.001$ s (left); thrust lines obtained from postprocessing the results from the NSCD simulation at $T = 0.5$ s, for $\Delta t = 0.001$ s. The cases of $\mu = 0.5$ (*a*), $\mu = 0.44$ (*b*) and $\mu = 0.4$ (*c*).

Figure 11. Results from the NSCD simulation at $T = 0.5$ s, for $\mu = 0.44$ and timestep. $\Delta t = 0.001$ s, assuming only the three central blocks free to move: snapshot at $T = 2$ s.